

8-20-2015

Targeted Transplantation of Mitochondria to Liver Cells

Nidhi Gupta

University of Connecticut - Storrs, nidhi_in84@yahoo.com

Follow this and additional works at: <https://opencommons.uconn.edu/dissertations>

Recommended Citation

Gupta, Nidhi, "Targeted Transplantation of Mitochondria to Liver Cells" (2015). *Doctoral Dissertations*. 899.
<https://opencommons.uconn.edu/dissertations/899>

Targeted Transplantation of Mitochondria to Liver Cells

Nidhi Gupta, PhD

University of Connecticut (2015)

Abstract

Hepatocyte damage caused by genetic and acquired defects in mitochondria can result in severe liver dysfunction causing disease and death. Mammalian hepatocytes possess specific receptors on their surfaces called asialoglycoprotein receptors (AsGRs), which can recognize and bind asialoglycoproteins (AsGs). After binding, AsGs are internalized by receptor-mediated endocytosis within membrane-limited vesicles, endosomes, which ultimately fuse with lysosomes resulting in degradation. This pathway represents a natural mechanism by which substances outside cells can gain access to the interior of liver cells. In the past, small molecules have been bound to AsGs to deliver them specifically to the liver. The aim of this study was to determine whether AsGs could serve as targetable carriers for mitochondria to permit targeting specifically to hepatocytes by the AsGR pathway. We describe here, a method by which mitochondria can be coated with AsGs by a non-damaging interaction. We converted an AsG into a highly positively charged molecule, and took advantage of the fact that the surface of mitochondria is negatively charged. By mixing a positively charged AsG protein conjugate with mitochondria, the conjugate could bind to mitochondria in a strong, but non-damaging electrostatic (charge-charge) interaction forming protein-mitochondrial complexes. This results in recognition and internalization of mitochondria

Nidhi Gupta, University of Connecticut (2015)

specifically by hepatocytes. We have also developed a method by which AsGs—mitochondria complexes can be released from endosomes. This allows escape from endosomes before lysosomal digestion and cytoplasmic delivery of healthy mitochondria to the cells. The system can result in rescue of cells rendered mitochondria-free by drug toxicity, and proliferation of both host cells and transplanted mitochondria. Currently, there is no treatment for mitochondrial dysfunction, and no means to repair or replace damaged mitochondria. Targeting healthy mitochondria to hepatocytes with defective or damaged mitochondria by the AsGR pathway would be expected to confer on those cells a selective survival advantage. As a result, those cells would be expected to proliferate, eventually replace defective cells reversing hepatotoxicity.

Targeted Transplantation of Mitochondria to Liver Cells

Nidhi Gupta

B.S., Panjab University, India (2008)

A Dissertation

Submitted in Partial Fulfillment of the

Requirements for the Degree of

Doctor of Philosophy

at the

University of Connecticut

(2015)

Copyright by
Nidhi Gupta

(2015)

APPROVAL PAGE

Doctor of Philosophy Dissertation

Targeted Transplantation of Mitochondria to Liver Cells

Presented by

Nidhi Gupta, B.S.

Major Advisor _____

Dr. George Y. Wu

Associate Advisor _____

Dr. Blanka Rogina

Associate Advisor _____

Dr. Catherine H. Wu

Associate Advisor _____

Dr. Gordon Carmichael

Associate Advisor _____

Dr. Peter Maye

University of Connecticut

(2015)

ACKNOWLEDGMENTS

I would like to thank my advisor, Dr. George Y Wu for supervising my research during my PhD training. I am also grateful to my committee, Dr. Blanka Rogina, Dr. Catherine Wu, Dr. Gordon Carmichael and Dr. Peter Maye for their suggestive comments and insightful questions.

I want to thank my mother, Surekha Rani and father, Navtej K Goyal for supporting me, listening to me when frustrated and encouraging me to do my best. I am also thankful to my sister, Milky; my brother, Deepak; sister-in-law, Leena, and last but not least my nieces Relisha and Akshi whose conversations would always cheer me up. Without their support it would have been very hard.

I especially thank my husband, Sushil, who supported me to finish my PhD training before I could move with him on the other end of the country. He patiently listened to me every day, advised to help manage the problems and encouraged whenever I hit a roadblock.

I also would like to thank many people who helped me behind the scenes, including my uncle, Dr. Rajesh K. Garg and aunt, Dr. Neeta Garg who always supported and encouraged me. I always felt relieved after sharing my troubles with them.

I hope I will always have everyone's love and support in future as well.

Table of Contents

Approval Page	III
Acknowledgments.....	IV
Table of Contents	V
List of Tables	X
List of Figures.....	XI
Chapter 1: Introduction.....	1
Mitochondria	1
Mitochondrial structure	1
Morphological Dynamics of Mitochondria.....	2
The Mitochondrial Genome	3
Mitochondrial Regulation of Cell Apoptosis	5
Mitochondrial Dysfunctional Diseases.....	5
Diagnosis and Treatment of Mitochondrial Dysfunctional Disorders	8
Mitochondrial Hepatopathies	14
The Liver	19
Metabolic Detoxification By The Liver	21
Liver Damage	23
Receptor-Mediated Endocytosis	25

Endosomes.....	25
Lysosomal Degradation.....	27
Asialoglycoprotein Receptors (AsGR) Pathway	28
Endosomal Escape.....	30
Hypotheses	34
Aims	35
Cells And Cell Culture	36
Model System for Evaluating Uptake by Human Hepatocytes	36
Source of Mitochondria for Uptake Assays	37
Source of GFP-Labeled Mitochondria	37
Mitochondria-Depleted Cells	38
Figures	40
Chapter 2: Formation of Stable Complexes of Mitochondria with AsG.	43
Asialo-orosomucoid Protein Carrier	44
Formation of Stable Complexes of FI-AsOR-PL and Mitochondria.....	45
Methods	46
Cells and Cell Culture	46
Mitochondria Preparation	46
Carrier Preparation	47
Mass Spectrometry.....	48

Complex Formation and Stability.....	48
Particle Size Analysis	49
Uptake Assay by Fluorescence Microscopy	49
Results and Discussion	50
Figures	53
Chapter 3: Assessment of Binding and Uptake of AsG–mitochondrial Complexes by Model Cells	60
Methods	62
Uptake Assay	62
Quantitative PCR (qPCR).....	62
Results and Discussion	65
Figures and Tables	67
Chapter 4: Effects of Endosomal Disruption Agents on Intracellular Localization of Targeted Mitochondria	71
Listeriolysin O (LLO) Facilitated Endosomal Escape.....	71
AsOR-LLO Conjugates	72
Effects of Colchicine Treatment	74
Effects of Low Temperatures on Cell Membranes.....	74
Methods	76
Preparation of Targetable LLO	76

Cytochrome C Oxidase Assay	77
Hemolysis	77
Cell Culture	78
Uptake Assay	78
Confocal Microscopy	79
Results and Discussion	81
Figures and Tables	86
Chapter 5: Assessment of Function and Stability of Mitochondria Targeted to Hepatocytes Lacking Mitochondria	98
Mitochondrial Respiration	100
Methods	103
Preparation of Mitochondria (-) Cells	103
Cell Proliferation Assay	103
Mitochondria Respiration Assays	104
Mitochondria (-) Cell Uptake Assay	104
Results and Discussion	106
Figures and Tables	111
Chapter 6: Conclusions and Significance	120
Chapter 7: Future Directions	122

Enhanced Escape of AsG-Mitochondria Complexes from Endosomes After	
Internalization.....	122
Cryopreservation of Mitochondria	124
AsGR-mediated Healthy and Functional Mitochondria Delivery to Hepatocytes in	
animals.....	126
Appendices	129
Appendix A: Determination of change in size of AsOR after adding fluorescence tags	
and poly-lysine chains by SDS-PAGE	129
Appendix B: Fluorescence of GFP-labeled mitochondria while determining stability of	
FI-AsOR-PL- mitochondria complexes.....	130
Appendix C: Determination of stability of FI-AsOR-PL–mitochondria complex by	
electron microscopy	131
Appendix D: Determination of uptake of proteins by using radioactive tag (¹²⁵ I).....	132
Appendix E: Determination of uptake of proteins by fluorescence	133
Appendix F: Effects of amantadine on mitochondrial DNA levels after uptake of FI-	
AsOR-PL–mitochondria complex.....	134
Appendix G: Fate of fluorescence in cells after uptake	136
Appendix H: Fate of mitochondrial DNA in cells after uptake.....	138
Appendix I: Fate of mitochondrial DNA in mitochondria free cells after uptake for	
extended periods of time.....	140
References	141

LIST OF TABLES

Table 3.1. Sequences of Primers Used For Quantification	67
Table 4.1. Hemolytic Activity of LLO and AsOR-LLO Conjugate	89

LIST OF FIGURES

Figure 1.1. Mitochondrial Genotypic Mutations Associated with Human Mitochondrial Disorders.	40
Figure 1.2. A schematic representation of AsGR-mediated endocytosis of AsGs by hepatocytes.	41
Figure 1.3. A representation of targeted LLO-mediated endosomal rupture	42
Figure 2.1. A representation of electrostatic binding of an FI-AsOR-PL conjugate to mitochondria.	53
Figure 2.2. Fluorescence of proteins tagged with Dylight 650 dye.....	54
Figure 2.3. Gel electrophoresis showing the direction of migration of FI-AsOR and FI-AsOR-PL.	55
Figure 2.4. Mass spectrometric data.....	56
Figure 2.5. FI-AsOR-PL uptake analysis by fluorescence microscopy.....	57
Figure 2.6. Particle size analysis by light scattering.....	58
Figure 2.7. Stability of FI-AsOR-PL–mitochondria complexes.	59
Figure 3.1. Primer specificity for mitochondrial DNA by amplification.	68
Figure 3.2. Uptake of FI-AsOR-PL–mitochondria complexes as measured by fluorescence.....	69
Figure 3.3. Uptake of FI-AsOR-PL–mitochondria complexes as measured by qPCR. .	70
Figure 4.1. A diagram of a targetable AsG–LLO conjugate cleavable under reducing conditions.	86
Figure 4.2. SDS-PAGE of AsOR-LLO conjugate and components stained with Coomassie Brilliant Blue.	87

Figure 4.3. Cytochrome C oxidase assay.	88
Figure 4.4. Changes in fluorescence after co-administration of complexed mitochondria and AsOR-LLO conjugates in cells.	90
Figure 4.5. HTC mitochondrial DNA levels in cells after exposure to complexed mitochondria and AsOR-LLO conjugates.	91
Figure 4.6. HTC mitochondrial DNA levels in colchicine-treated Huh 7 cells after exposure to complexed mitochondria and AsOR-LLO conjugates.	92
Figure 4.7. HTC mitochondrial DNA levels in Huh 7 cells at 4°C after exposure to complexed mitochondria and AsOR-LLO conjugates.	93
Figure 4.8. Isolation of an HTC mito-GFP cell line by fluorescence-activated cell sorting (FACS).	94
Figure 4.9. HTC Mito-GFP cells stained with Mito-Tracker Red.	95
Figure 4.10. Localization of early endosomes and GFP-labeled HTC mitochondria by confocal fluorescence microscopy.	96
Figure 4.11. A plot of fluorescence intensities of confocal microscopic images versus stack number.	97
Figure 5.1. Mitochondrial DNA levels in Huh 7 and SK Hep1 cells treated with ddC.	111
Figure 5.2. Cellular DNA levels (ng/well) of cells in wells after change to supplement-free media.	112
Figure 5.3. Determination of FI-AsOR uptake in mito (-) cells.	113
Figure 5.4. Fluorescence in Huh 7-mito (-) cells after co-administration of complexed mitochondria and controls.	114

Figure 5.5. Fluorescence in SK Hep1-mito (-) cells after co-administration of complexed mitochondria and controls.	115
Figure 5.6. Mitochondrial DNA levels in mito (-) cells after co-administration of complexed mitochondria and AsOR-LLO, and controls.....	116
Figure 5.7. Cellular DNA levels in mito (-) cells after co-administration of complexed mitochondria and controls.	117
Figure 5.8. Characterization of mitochondrial respiration.	118
Figure 5.9. Oxygen consumption rates in Huh 7-mito (-) cells after co-administration of complexed mitochondria and controls.	119

CHAPTER 1: INTRODUCTION

MITOCHONDRIA

Mitochondria are intracellular organelles that are involved in energy generation [1], signaling [2, 3], cellular differentiation [4-6] and cell death [7-10]. Because they are primary source of generating ATP, mitochondria are considered the metabolic powerhouses of mammalian cells [1]. Mitochondria also play an essential role in maintaining the high energy needs of certain organs such as the liver, which has more mitochondria per cell than most other cell types like small lymphocytes [11].

MITOCHONDRIAL STRUCTURE

Mitochondria are unique among intracellular organelles in that their surface consists of an outer and inner membrane. The membranes differ from each other in composition, properties, and function [1]. However, one essential characteristic that they have in common is that the integrity of inner and outer membranes must be maintained for their proper functions. This membrane integrity is strictly regulated through interactions between various cellular proteins [12]. The basic structure of the mitochondrial membranes is similar to the cell membranes. It consists of a lipid bilayer with two sheets of phospholipids such that hydrophilic phosphate heads point out on either side of the bilayer and the hydrophobic tails point in towards the core of the bilayer. Several integral proteins and cholesterol [13] are associated with these lipid bilayers to act as receptors or transporters and to ensure that the membrane stays fluid and flexible. The

phospholipid composition of outer membrane of mitochondria differs from that of other membranes [14]. It also contains porins, which are integral membrane proteins, that allow large molecules to freely diffuse across the membrane [15]. Proteins such as translocase on the outer membrane are involved in the active transport of larger proteins across the membrane [16]. Some essential mitochondrial outer membrane proteins like TOM20 and TOM22 result in a negatively charged outer membrane of mitochondria [17, 18]. The inner mitochondrial membrane is extensively folded into cristae, which increase the total membrane surface area compared to outer membrane [19]. The lipid composition of inner membrane is similar to bacterial membranes characterized by low levels of triglycerides causing increased unsaturation [20]. It is freely permeable to oxygen, carbon dioxide, and water and is associated with several essential proteins and enzymes, which are involved with aerobic respiration [21]. Together these proteins constitute the respiratory complex of mitochondria, which takes part in synthesis of ATP by mitochondria [22]. The inner and outer membranes result in the creation of 2 compartments in the mitochondria called inter-membrane space and inner matrix.

MORPHOLOGICAL DYNAMICS OF MITOCHONDRIA

In spite of their size and complexity, mitochondria are highly dynamic and change size and shape frequently by processes of fusion, fission and movement across the cytoskeletal structure [23]. Frequent fusion and fission of mitochondria in cells provide an efficient means of homeostasis and inter-mitochondrial DNA complementation

through exchange of mitochondrial genomes between fusing mitochondria. As a result, mitochondria morphologically can be highly polymorphic [24] and function independently within cells [25]. A group of proteins play a role in regulating morphological remodeling of mitochondria [26]. Some proteins like Drp1/Dnm1 [27, 28] or Fis1/Mdv2 [29] localized on outer membrane of mitochondria regulate fission of mitochondria. Once initiated, fission of mitochondria takes place in approximately 3 hours [30]. Other proteins like Mgm1/OPA1 [31, 32] and Fzo1p/Mfn 1&2 [33] localized on inner or outer membrane of mitochondria regulate fusion of mitochondria.

THE MITOCHONDRIAL GENOME

Human mitochondrial DNA is approximately 16,600 base pairs long, and codes for 37 genes [34, 35] which includes 13 genes for subunits of respiratory complexes, 22 for mitochondrial tRNA, and 2 for rRNA [36]. Most of the essential structural and functional proteins of mitochondria are expressed from the cell nucleus, and are transported to mitochondria. Therefore, mitochondrial proteins are encoded from genomes that originate from two distinct sources, the nucleus and the mitochondria itself. Each mitochondrion contains 5-12 copies of DNA, which is circular and double-stranded [37]. Mitochondria have their own DNA replication machinery enclosed in inner membrane compartment, which allows them to replicate independent of cell nuclear DNA division. Unlike cell nuclear DNA polymerase which has a proof-reading exonuclease mechanism [38], mitochondrial DNA polymerase lack these nucleotide excision repair mechanisms [39] which repair errors or mis-matches that take place during the DNA

replication process or damage by radiation or chemicals [40]. Although other types of mitochondrial DNA repair pathways, such as base excision repair [41], have been reported, increased damage to mitochondrial DNA due to close proximity to reactive oxygen species generated by electron transport chain on inner membrane of mitochondria and lack of other proof reading and editing pathways leads to accumulations of mutations in mitochondrial DNA, and give rise to heteroplasmic (a mixture of non-uniform collection of mitochondrial DNA with normal or mutated DNA sequences) mitochondrial DNA [42]. Severe mutations can lead to cell, organ, and organism death. However, milder mutations can permit survival, but abnormalities are defined by possible mitochondrial dysfunction [43]. The proportion of mutations accumulated in mitochondrial DNA molecules determines both the penetrance and severity of expression of some mitochondrial diseases. Mitochondria divide during cell division, and also independent of cell division primarily in response to the energy needs of the cell [1, 44]. Introduction of normal mitochondrial DNA to mitochondria containing mutated DNA by dynamic networking provides an efficient mechanism of mitochondrial repair [45]. Since mitochondria are sorted randomly among daughter cells during cell division, each daughter cell can receive different proportions of mitochondria carrying normal and mutant mitochondrial DNA. Mitochondrial DNA sequence heteroplasmy can also be used to determine lineages [46].

Despite the rearrangement of genes, comparison of mitochondrial DNA sequences in different species show high levels of homology. Mitochondrial DNA sequences from different species can be distinguished from each other based on non-homologous and rearranged regions of mitochondrial DNA [47].

MITOCHONDRIAL REGULATION OF CELL APOPTOSIS

Apoptosis, programmed cell death, provides a defense mechanism by which unwanted and potentially dangerous cells are eliminated and cell number regulated [48].

Apoptosis is under tight control of several protein families and signaling cascades.

Proteolytic activity of the caspase protein family plays a major role in apoptosis [49].

Biochemical studies have identified numerous mitochondrial proteins that have a complex role in activating cellular apoptotic programs directly [50, 51]. Permeabilization of the outer membrane of mitochondria triggers the activation of the caspase proteases. Release of various pro-apoptotic proteins from inter-membrane space of mitochondria, such as cytochrome c, promotes caspase activation [52]. Consequently, the integrity of the outer membranes of mitochondria is highly regulated through interactions between several pro- and anti-apoptotic proteins in cells [7, 53]. Damage to the outer membranes of mitochondria also leads to mitochondrial dysfunction and usually causes cell death regardless of the activity of caspase proteases.

MITOCHONDRIAL DYSFUNCTIONAL DISEASES

Dysfunction of mitochondria has been recognized as an important contributor to an array of human diseases including hepatic mitochondrial disorders [54, 55], cardiac dysfunction [56] and autism [57]. Mutations in both nuclear and mitochondrial genomes encoding mitochondrial proteins can cause mitochondrial dysfunction [58]. Many factors including a threshold effect, and segregation and clonal expansion govern the manifestation of mitochondrial disease. Although the accumulation of mutations

increases with aging, normal mitochondrial DNA in cells allow mitochondria to function properly until a threshold level is reached where the ratio of mutated mitochondrial DNA increases significantly compared to normal mitochondrial DNA. At this point, clinical symptoms of mitochondrial dysfunction start to appear [59]. While the segregation of mitochondria into two daughter cells is usually random, if a mutant load in a specific cell type exceeds the pathogenic threshold, clinical indicators of mitochondrial disorders can appear [60]. In addition, clonal expansion of specific mutated mitochondrial DNA molecules in cells can cause increased risk for the development of mitochondrial disorders [61, 62].

Many types of mutations are possible in mitochondrial DNA. Point mutations may occur in protein-coding genes during mitochondrial DNA replication, and can cause major mitochondrial functional defects. Although mitochondria are heteroplasmic, these mutations tend to be recessive. However, if levels of mutations increase beyond threshold levels, these mutations can have a deleterious effect on mitochondrial functions [63-65]. Another type of mitochondrial DNA mutation is large-scale deletions and rearrangements of DNA [66]. An exponential accumulation of such deletions has been reported in aged tissues and in individuals with neurodegenerative diseases [67, 68]. Because mitochondria are sorted randomly among daughter cells during cell division, each daughter cell can receive different proportions of mitochondria carrying normal and mutant mitochondrial DNA. A database compiling the description of all known pathogenic mitochondrial DNA mutations is under construction [58].

Population-based studies have shown that mitochondrial disorders are relatively common [69]. Population genetic bottlenecks and founder effects can cause under- or

over-representation of specific mitochondrial DNA disorders [70]. Studies on childhood and adult mitochondrial disorders suggests that prevalence is at least 1 in 5000, and could be much higher [71]. Genetic and clinical manifestations of mitochondrial disorders increase with aging because of accumulation of mitochondrial mutations [72]. However, the age of onset depends on levels of mutations accumulated and the severity of the biochemical defect caused by mutations [73, 74]. Other nuclear genetic or environmental factors also play a role in expression of disease. The clinical symptoms associated with mitochondrial DNA mutations are extremely variable and can occur at any stage in life [75]. There is clear evidence supporting the involvement of mitochondrial DNA mutations in aging, neurodegeneration, and tumorigenesis [76]. Figure 1.1 shows some of the mitochondrial DNA mutations that are associated with human mitochondrial disorders. Some mitochondrial diseases have an early onset starting in infants or young children, example Leigh syndrome [77], Kearns–Sayre syndrome (KSS) [78], and Depletion syndrome (found in various organs depending on tissues which have mitochondrial DNA depletion, resulting in muscle weakness, progressive encephalopathy or liver failure [79]. Organ transplantation can be an effective therapeutic approach in these patients if suffering from a specific tissue defect. Mitochondrial disorders affecting the central nervous system usually manifest in late childhood or adult life with clinical syndromes including mitochondrial encephalopathy, lactic acidosis, stroke-like episodes [80, 81], chronic progressive external ophthalmoplegia [59], neuropathy, ataxia, retinitis pigmentosa [82], Leber's hereditary optic neuropathy [83, 84], myoclonic epilepsy and ragged red fibers [85]. Mitochondrial genetic liver diseases are introduced in a later section. As mentioned above, besides

inheritance of mitochondrial DNA defects, damage to the mitochondria can also be caused by environmental factors [86]. Several toxic substances internalized by cells can cause direct damage to mitochondria and result in cell death.

Instead of size and location of deletions, the levels and tissue distribution of deleted mitochondrial DNA are more important factors in determining clinical syndromes [87]. In most cases, mutations in mitochondrial DNA impair mitochondrial function, depriving the cell its main source of energy required for its optimal function. As a result, cell function is impaired or it causes cell death, which compromises tissue or organ function and leads to disease.

DIAGNOSIS AND TREATMENT OF MITOCHONDRIAL DYSFUNCTIONAL DISORDERS

Lack of clear correlation between mitochondrial DNA genotype and disorder phenotype makes the diagnosis of mitochondrial DNA disorders complicated. Clinically, family history and histological changes are helpful to diagnose mitochondrial disease, but these are not always clear. Development of rational diagnostic algorithms has improved over time with help of molecular testing supported by histochemical, and biochemical testing [88].

A few key histochemical and molecular approaches currently are being used to diagnose mitochondrial genetic disorders are as follows:

Histochemical and biochemical testing: Some patients show specific histological and histochemical alterations in affected tissue indicating mitochondrial respiratory complex

dysfunction. Appearance of ragged-fiber like structures in tissues reflects the accumulation of defective mitochondria with cytochrome c oxidase abnormalities.

Cytochrome c oxidase is an essential enzyme found on inner membrane of mitochondria which takes part in the synthesis of ATP by mitochondria [89].

Abnormalities in cytochrome c oxidase can cause severe metabolic disorders.

Cytochrome c oxidase contains subunits encoded by both nuclear and mitochondrial genomes, and the appearance of ragged-fiber like structures in tissues suggests mitochondrial DNA involvement. However, this histological finding is of limited use because tissue biopsies from patients with known mitochondrial DNA mutations, for example a MELAS phenotype, have shown no distinct fiber-like structures [90].

Determination of enzyme activities involved in respiratory function of mitochondria from clinically affected tissue [91] is often used to diagnose mitochondrial disorders. Oxygen consumption and ATP synthesis by intact organelles from affected tissue also helps to determine the type of mitochondrial dysfunction [92]. The identification of specific mitochondrial enzyme abnormalities can help to identify the specific molecular genetic defect.

Molecular genetic testing: Mitochondrial DNA point mutations, deletions and rearrangements can be assayed by Southern blotting [93, 94], PCR or sequencing [95, 96]. Determination of quantitative loss of normal mitochondrial DNA or accumulation of defective mitochondrial DNA by real-time PCR has been a good indicator of mitochondrial disorders. Several known genes have been implicated in myopathic or hepatocerebral disorders. Because of its small size, screening the entire mitochondrial DNA for rare or novel mutations is relatively easy. Denaturing gradient gel

electrophoresis [97] and denaturing high-performance liquid chromatography [98] and several new emerging technologies such as microarrays [99] have proven very useful. Given the highly heteroplasmic nature of mitochondrial DNA, careful assessment of newly identified mutations and variations is required to establish the association with human diseases.

Although several guidelines to establish a novel mitochondrial DNA variant as pathogenic have been proposed [58] and some have been applied in clinical studies [100], more canonical criteria are required to accurately identify new variations associated with human mitochondrial disorders.

Treatment Strategies: Despite an increased understanding of mitochondrial genetics and function, and pathogenesis of mitochondrial DNA variations, currently no effective treatment options are available, except cases where transplant surgery might be helpful. Treatments with vitamins, cofactors, metabolites or electron acceptors to bypass respiratory complex defects have been attempted, but have not been very successful (227). Currently more focused and disease-specific treatments are under investigation.

Exercise therapy: Exercise therapy aims to improve physical capacity and quality of life in patients who have myopathy caused by mitochondrial DNA variations. Although it does not cause any significant change in mutations in mitochondrial DNA, clinical studies have shown improved mitochondrial function [101]. Muscle training studies in mice have shown enhanced ATP levels, delayed disease onset, and increased life expectancy [102]. Effects of long-term training on mitochondrial DNA mutation load are still under investigation. Stimulation of muscle regeneration by proliferating

undifferentiated myogenic cells in response to injury caused by resistance exercise is also under study. Activation of undifferentiated myogenic cells containing normal mitochondria into muscle tissue of patients with high levels of sporadically mutated mitochondrial DNA in mature muscle could shift heteroplasmy levels towards healthy mitochondrial genome, and may help to recover muscular function [103]. Although further studies are required to determine the optimal parameters for an exercise regime, this method has been found to be clinically useful to some extent [104].

Gene therapy: Shifting the balance of mutant to normal mitochondrial genome can help in manipulating heteroplasmy levels in mitochondria and may prove to be useful for treatment of mitochondrial disorders. Genetic-based strategies to inhibit the replication of mutated mitochondrial DNA and hence allowing normal mitochondrial genome to propagate are under investigation [105]. This can be accomplished by transferring interfering molecules into the mitochondria. A major obstacle in these strategies is transport of molecules across the two mitochondrial membranes. However, investigations are under way to establish the ability of such molecules to enter mitochondria to inhibit mutated mitochondria DNA replication and their effectiveness *in vivo*.

Alternatively restriction endonucleases capable of distinguishing between mutated and normal mitochondrial genomes have also been used. This approach may be limited to such mutations that would give rise to additional restriction sites [106]. Selective targeting of mutated mitochondrial DNA can also be attempted with targeted zinc finger DNA methylases and nucleases, which can bind and modify or cleave mutant genomes

in cells, in a sequence-specific manner [107]. This strategy may also be limited by targeted transfection and successful expression in defective tissues.

The expression of mitochondrial genes in the nucleus to compensate for mutated genes in mitochondrial DNA causing functional defects in mitochondria can also be helpful to recover respiratory defects of mitochondria [108]. Studies of mitochondrial localization of such expressions from nucleus are under investigation [109]. Recently a mechanism to import cytosolic tRNA to mitochondria has been demonstrated [110] which can help in the development of future therapies for mitochondrial DNA mutations causing defects in genes expressing mitochondrial tRNAs. Overall, current investigations towards the development of successful gene therapies for the treatment of mitochondrial dysfunctional disorders are encouraging.

Implantation of reprogrammed cells derived from patients with heteroplasmic mutations in mitochondrial DNA is another potential treatment under investigation [111]. Induced pluripotent stem cells (iPSC) displaying normal mitochondrial functions can be screened from a population of iPSCs derived from affected patients. Generation of pluripotent cells by replacing nuclear DNA of the egg with nuclear DNA of the diseases somatic cells (somatic cell nuclear transfer) and thus, containing healthy mitochondria and nucleus, is another method to obtain potential cells that can be used to correct mitochondrial disorders.

The rates of transmission of mitochondrial DNA mutations from mother to offspring vary considerably [112]. This makes genetic counseling extremely challenging. Though prenatal genetic diagnosis can help in detecting mitochondrial DNA mutation load, the

major clinical concern is whether heteroplasmy levels would reflect phenotypic outcomes at other fetal tissue levels [113]. Studies in heteroplasmic mice have shown that transfer of the pronuclei from a fertilized zygote of a female mouse with mitochondrial DNA disease to an enucleated zygote from a healthy donor female has successfully produced healthy offspring [114]. In addition, the United Kingdom has approved a gene-therapy technique, which involves transferring the nucleus from a human female egg to a donor enucleated egg with healthy mitochondria and then fertilizing the donor egg [115-117].

Moreover, in spite of significant progress in understanding and documenting mitochondrial DNA defects responsible for the development of mitochondrial dysfunction, the diagnosis of disorders is challenging due to increasing numbers of reported pathogenic mutations and constantly evolving rules of pathogenicity. Although implementation of high-throughput screening approaches has improved the situation, the lack of effective treatments has been disappointing. New experimental approaches under investigation are promising for mitochondrial DNA disease treatment. In addition to this, recent research strategies focused on elucidating the molecular mechanisms of disease and complex relationships between mitochondrial DNA variations and their diverse clinical phenotypes have been helpful in developing therapies for these disorders. Further progress in understanding the pathogenesis of specific mitochondrial disorders will be necessary to uncover novel targets or molecular pathways that may be exploited for developing therapies. In the meantime, approaches to develop generic treatments for mitochondrial DNA disorders need to be actively pursued.

MITOCHONDRIAL HEPATOPATHIES

Because of their high metabolic activity, hepatocytes require, and contain the highest density of mitochondria of all human cell types [37]. Consequently, hepatocytes are also more susceptible to disorders that affect mitochondria [118]. Mitochondrial hepatopathies can be inherited as a mitochondrial genetic defect or acquired due to alcohol or drug injury to cells.

Disorders affecting mitochondrial function would directly affect hepatocellular metabolism resulting in impaired liver function, steatosis and cell death. Clinically, genetic and more commonly drug- and alcohol-induced mitochondrial damage has been shown to cause severe liver disease, which ultimately leads to liver failure and death [119, 120]. Current medical treatments available for mitochondrial hepatopathies are largely ineffective, and their diagnosis is difficult because of lack of distinct clinical symptoms. However, several specific molecular defects (including mutations, deletion or rearrangement of mitochondrial DNA) have been identified in recent years.

GENETIC MITOCHONDRIAL DISORDERS OF LIVER

Clinically, mitochondrial hepatopathies have varied manifestations that include acute or chronic liver failure, lactic acidosis, and cholestasis. Below are few examples of primary hepatopathies caused by mitochondrial defects:

Neonatal Liver Failure: Acute liver failure that occurs in infants who are only a few weeks to a few months old is due to respiratory chain defects [121]. This is caused by defective mitochondrial genes encoded by the nuclear genome. This disease progresses rapidly and typically causes death within months of manifestation.

Mitochondrial DNA depletion syndrome: This syndrome is due to decreased mitochondrial DNA copy number resulting into insufficient expression of mitochondrial genes from mitochondrial DNA [122]. Patients present with myopathy, hepatomegaly and progressive liver failure causes death at an early age.

Alpers-Huttenlocher Syndrome (Delayed-Onset Liver Disease): This is caused by defective expression of mitochondrial genes in nuclear DNA. Disease is characterized by hepatomegaly, jaundice, and progressive coagulopathy and hypoglycemia [123]. Onset of symptoms occurs between 2 months to 8 years of life.

Pearson's Syndrome: In this syndrome, multi organ system failure (hematopoietic system, exocrine pancreas, liver, and kidneys) occurs due to mitochondrial DNA depletion and rearrangement defects. Liver failure and death has been reported before the age of 4 years [124].

Villous Atrophy Syndrome: Caused by deletion in mitochondrial DNA resulting in respiratory dysfunction [125]. Symptoms are severe anorexia, vomiting, chronic diarrhea, and villus atrophy in the first year of life. Hepatic involvement is characterized by mild elevation of aminotransferases, hepatomegaly, and steatosis.

Navajo Neurohepatopathy: Caused by rearrangement in mitochondrial DNA resulting in intra-cellular respiratory dysfunction [126]. Clinical symptoms are cholestasis and cirrhosis. Liver failure may occur in infancy or childhood.

Currently various vitamins, cofactors, respiratory substrates, or antioxidant compounds are being used to by-pass the damage to the respiratory function of cells [127-129]. Such clinical management has very limited success [130] and is largely supportive.

Because of involvement of other organ systems, advantages of liver transplantation are also speculative [131, 132]. Despite extensive research on genetic mitochondrial hepatopathies in recent years, much remains to be learned about these disorders.

ACQUIRED MITOCHONDRIAL DISORDERS OF LIVER

Besides genetic mitochondrial hepatopathies, mitochondrial injuries in liver cells can also be acquired by exposure to alcohol and drugs. [120]. Since detoxification of most drugs takes place in the liver, hepatocytes are susceptible to adverse effects of these drugs. This poses a major issue for pharmaceutical companies because it causes failure of a drug during development phase or withdrawal of an already marketed medicine [119]. Although hepatotoxicity can be induced in different ways [133], mitochondrial dysfunction is a common mechanism of injury [134]. Deleterious effects of drugs on hepatic mitochondria can disturb mitochondrial respiratory functions or affect mitochondrial DNA. By blocking mitochondrial respiratory function, damaging mitochondrial membranes and causing pro-apoptotic proteins to leak into the cytoplasm or triggering mitochondrial DNA mutations, drugs can cause necrosis or apoptosis of hepatocytes, which can lead to liver cirrhosis or failure [134]. Depending on susceptibility, various hepatic conditions as microvesicular steatosis, lesions, hypoglycaemia hyperlactataemia, lactic acidosis, myopathy, rhabdomyolysis, pancreatitis, peripheral neuropathy or lipoatrophy can occur [135, 136]. Severe liver injury caused by mitochondrial dysfunction in clinical trials can be avoided by careful studies of newly developed drugs during the preclinical safety studies.

The following are a few mechanisms by which drugs/metabolites are thought to induce mitochondrial dysfunction:

Induction of mitochondrial outer membrane damage and release of pro-apoptotic proteins: Several drugs cause damage to outer membrane of mitochondria, which leads to release of pro-apoptotic proteins, such as cytochrome c, into cytoplasm, initiating apoptosis pathways resulting in cell death. Extensive liver cell death can lead to liver failure. For example, acetaminophen, valproic acid, salicylic acid and others have been shown to cause fulminant hepatic failure [137, 138]. The molecular mechanisms of induction of mitochondrial membrane damage by drugs are still poorly understood. Release of pro-apoptotic proteins from mitochondria can also be induced indirectly by translocation of proteins from inter-membrane space to cytoplasm [139].

Impairment of respiration enzymes: Some drugs can act as mitochondrial poisons by directly impairing one or more mitochondrial enzyme involved in respiration process to produce ATP [140]. Higher intra-mitochondrial accumulation of drugs like amiodarone, perhexiline or tamoxifen causes progressive decrease in mitochondrial respiration [140, 141]. This leads to a decrease in ATP production in cells [142].

Several drugs can impair other function of mitochondria, such as fatty acid oxidation impairment [143]. Others can cause more than one kind of damage to mitochondria in cells [134].

Mitochondrial DNA depletion or mutation: Nucleoside based anti-viral drugs have shown to either inhibit mitochondrial DNA replication directly by inhibiting mitochondrial DNA polymerase as in case of fialuridine (FIAU) [144]) or by incorporation into growing chain of mitochondria and immediately terminating the replication as in case of stavudine (d4T), zidovudine (AZT) or didanosine (ddI)) [145]. Some toxins can manipulate

mitochondrial DNA replication resulting in point mutations or deletions/rearrangements in mitochondrial DNA.

Environmental factors can also enhance the risk of drug-induced mitochondrial dysfunction [146, 147]. Alcohol abuse have shown to induce underlying mitochondrial dysfunctions, which may render the liver more susceptible to drug-induced mitochondrial disorder [148]. Some microsomal enzyme inducers or viral infections may also act as predisposing factor to drug-induced mitochondrial dysfunction in the liver [149, 150]. Release of viral proteins, cytokines and interferons can affect mitochondrial function and disturb intracellular homeostasis that can have additive effects to drug induced mitochondrial dysfunction [135].

Although exercise therapies and gene therapies are extensively being studied, effective treatment strategies for hepatic mitochondrial dysfunction disorders are still lacking.

THE LIVER

The liver is the largest and one of most important organs of human body and is located on upper-right portion of the abdominal cavity [151]. In humans, the liver consists of four lobes. Because of its complexity, no other organ or artificial device can reproduce all the functions of the liver [152]. The liver is a highly specialized organ consisting of four major cell types; parenchymal hepatocytes, stellate cells, sinusoidal endothelial cells and Kupffer cells [153]. Among these, hepatocytes form 80% of liver cytoplasmic mass, and are responsible for the majority of physiological functions of liver.

The liver has rich blood supply, receiving blood from the hepatic portal vein and hepatic arteries. Seventy-five percent of the blood supply to the liver is delivered by hepatic portal vein which carries venous blood drained from the spleen, gastrointestinal tract, and its associated organs [154]. Unlike most veins, the hepatic portal vein does not drain into the heart [155]. Instead it delivers venous blood into another liver microvascular system, namely the hepatic sinusoids of the liver [156]. Blood from the gastrointestinal tract reaching liver by hepatic portal vein supplies the liver with absorbed nutrients and toxins from intestines and allows the liver to process nutrients and detoxify ingested toxins or drugs [157]. The hepatic arteries supply arterial blood to the liver, which accounts for rest of 25% of liver blood flow. Oxygen demands of the liver are met by both sources of blood supply, but mostly from the hepatic artery. Blood from hepatic artery and portal vein flows into low-pressure vascular channels called sinusoids [158, 159]. Sinusoids are lined with highly fenestrated endothelial cells which allow free flow of plasma from sinusoidal blood into the space between hepatocytes and endothelial cells [160]. Hepatocytes absorb nutrients and other substances from this

plasma brought by blood and excretes waste or detoxified materials into it [161].

Hepatocytes are involved in a wide variety of biochemical reactions, including the synthesis and breakdown of molecules. Hepatocytes are also involved in other functions, including detoxification of various metabolites and drugs (modification, and excretion of exogenous and endogenous toxic substances) [162], protein synthesis, nutrient storage and production of several bio-chemicals required for digestion.

Hepatocytes also play a major role in metabolism including regulation of glycogen storage, hormone production and plasma protein synthesis.

Hepatic sinusoids are also populated by numerous Kupffer cells for phagocytosis of harmful particles carried to the liver through blood [163]. Kupffer cells are the resident liver macrophages acting as scavenger cells, responsible for removing unwanted particulate material from the liver circulation [164]. However, studies indicate that Kupffer cells may also be involved in the pathogenesis of various liver diseases [165]. Kupffer cells may cause destruction of hepatocytes by producing harmful soluble mediators [166] or fibrosis by production of cytokines that lead to the transformation of stellate cells into myofibroblasts [167]. Kupffer cells have also been implicated in alcohol-induced injury to liver [168].

Stellate (fat storing cells) in liver have been shown to be the source of fibrosis which occurs in response to chronic liver injury [169]. Activation of these stellate cells converts them to myofibroblasts producing excess extracellular matrix, [170] and reducing the flow of blood through sinusoids [159] which are lined with specialized endothelial cells [160]. These latter cells are involved in determining which solutes are filtered and can reach the hepatocytes that line the sinusoids.

The liver plays a crucial role in detoxification of substances, including alcohol, drugs, pesticides, and heavy metals, that are harmful for body [171]. Exposure to higher levels of these substances can overwhelm the liver, resulting in liver failure [172]. Toxins are primarily delivered to the liver by the portal vein where they are processed and excreted. Toxic byproducts of normal metabolism (e.g. ammonia) and excess hormones (e.g. estrogen) are also processed in liver. Many drugs, including acetaminophen, anti-HIV/HCV drugs, and herbal drugs are also processed by the liver and can cause severe liver damage [120, 145, 172]. Damaged liver may not adequately process these toxic substances, which potentially could lead to dangerously high toxin levels in blood and significant side effects [173, 174].

METABOLIC DETOXIFICATION BY THE LIVER

Detoxification refers to a specific metabolic pathway that processes unwanted substances for elimination. It involves a series of enzymatic reactions that results in neutralization and solubilization of toxins, and recycling or transportation to secretory organs (like kidneys), for excretion from the body [175]. Endogenously-produced substances such as inflammatory molecules, excess hormones, vitamins, and signaling compounds are eliminated by the same detoxification systems that protect the body from environmental toxins or clear drugs and toxins from blood circulation and helps in homeostatic balance in the body. Unprocessed toxins may act as mutagens causing DNA damage or mutations, carcinogens or disrupt other metabolic pathways resulting in dysfunction of other biological systems such as the nervous system or kidneys [176, 177].

Detoxification can be divided into three phases.

Phase I: Enzymatic transformation: The metabolic detoxification systems enzymatically transform lipid-soluble compounds into water soluble compounds by conjugating water-soluble molecules to the lipid-soluble toxins to increase solubilization of toxins for next phase of detoxification [178]. Following the solubilization, some modified toxins can be transported out of the cell and excreted directly.

Phase II: Enzymatic conjugation: Transformed toxin in phase I of detoxification may still be unsuitable for immediate elimination from the cell. This can be because of insufficient water-solubility of molecules even after phase I reactions to complete the entire excretion pathway or products from the phase I reactions are more reactive than the original toxins and that can potentially be more destructive. Activities of the phase II enzymes increase solubility and reduce toxicity of phase I products. Phase II enzymes are also responsible for anti-mutagenic and anti-carcinogenic properties of the metabolic detoxification systems [179, 180].

Phase III: Transport: Phase III transporters actively pump out neutralized toxins that require specific transporters to move in and out of cells through the cell membrane for excretion as water-soluble compounds [181]. These transporters are also known as multidrug resistance proteins, because drug-resistant cancer cells use these proteins to protect themselves against chemotherapy drugs [182].

Balance between Phase I and Phase II Reactions

Although sometimes products of phase I detoxification are potentially more toxic than original substances, they do not impose any threat if phase II enzymes are functioning properly to rapidly neutralize products from phase I detoxification as they are formed.

This delicate balance is upset by factors that can increase the activity of phase I more than phase II which leads to production of harmful metabolites faster than they can be detoxified, and increase the risk of cellular damage. Several factors including diet, smoking, age, disease or genetic composition of cells can cause this imbalance [183]. Several drugs, for example higher doses of acetaminophen [184] and anti-viral drugs have been found to have profound effects on this balance. Increased levels of toxins induce several types of damage to cells including nuclear and mitochondrial DNA damage, increased reactive metabolites, activation of apoptotic proteins, lipid peroxidation, mitochondrial dysfunction and inflammation.

LIVER DAMAGE

Several factors, as described above, can increase the risk of serious liver damage. If the liver is unable to clear toxins, drugs and metabolic by-products from blood, levels of these chemicals may increase in the blood, leading to impaired function of other organs. Sustained liver damage may result in fibrosis, steatosis, cirrhosis or liver cancer [185]. Various complex and interactive mechanisms are involved in liver injury. Hepatotoxicity and drug-induced liver injury has been a major cause of acute liver failure [186, 187]. Biochemical mechanisms of liver injury mostly involve chemicals that are detoxified in the liver [187]. Some toxic metabolites may alter cell membrane [188], mitochondria [145], intracellular ion homeostasis [189, 190] or degradative enzymatic activity [191].

Immune mechanisms mediated by cytokines, nitric oxide, and complement may also be involved on liver injury [166, 192]. Pathologic [193] and chemical [194] apoptosis is potentially another mechanism of acute liver injury. Knowledge of the involved mechanisms in liver injury at the cellular and molecular level may help to develop therapeutic strategies that might prevent liver failure.

Liver injury can be determined by measuring the levels of certain liver enzymes in blood. Under normal circumstances, these enzymes are intracellular, which upon injury are released into blood [195]. Examples include aspartate aminotransferase (AST), alanine aminotransferase (ALT) and alkaline phosphatase [196]. Liver inflammation [197] and change [198, 199] in histological pattern of liver tissue are also useful to determine liver injury.

Unlike most other differentiated cells, hepatocytes are capable of dividing in response to liver injury. Mitochondria in hepatocytes proliferate in response to cell division and energy needs [200]. However, if mitochondria are significantly damaged, mitochondrial division will not occur, and cell death and potentially liver failure will ensue. Aside from liver transplantation, there is currently no way to repair mitochondrial damage, or replace dysfunctional mitochondria [201]. Development of a method that could deliver healthy and functional mitochondria to hepatocytes that can replace the dysfunctional mitochondria could help treat several mitochondrial hepatopathies caused due to direct damage to mitochondria and drug/alcohol induced mitochondrial damage.

RECEPTOR-MEDIATED ENDOCYTOSIS

Many different types of receptors are present on the surface membranes of cells. Some receptors recognize and bind to specific molecules or ligands present in extracellular environment, and internalize the receptor-ligand complex in membrane-limited vesicle, an endosome. Endosomes eventually fuse with lysosomes, which contain degradative enzymes resulting in breakdown of the internalized ligands. This whole process is called receptor-mediated endocytosis [202]. Hence, receptor-mediated endocytosis allows transport of macromolecules into cells through a complex series of intracellular transfers. Some surface receptors such as receptors for hormone, bile acid, and some types of glycoprotein receptors are specific for certain cell types [203].

ENDOSOMES

After receptors on cell surface recognize and bind to specific molecules or ligands, cell membrane invaginates and the whole receptor-ligand complex is internalized by the cell in a membrane-enclosed vacuole called endosomes [204].

EARLY ENDOSOMES

Early endosomes following entry of receptor-ligand complex are found near the periphery of cells. They are highly polymorphic, and can be up to 1 micron in size [205]. The size of endosomes changes with expression of different factors such as p97 ATPases [206], Mon 1 a/b [207] and can lead to increase in size up to 1.5 microns. Early endosomes can be distinguished from other organelles with some specific markers like RAB5A and RAB4 [208], transferrin and its receptor [209] and EEA1

[210]. Early endosomes consist of a dynamic tubular-vesicular network which allows them to mature into late endosomes later [211]. Sorting of early endosomal content determines the subsequent fate of internalized ligands [212], directing them for recycling to the plasma membrane [213], degradation in lysosomes [214] or delivery to the trans-Golgi network [215]. Through recruitment and assembly of the sorting machinery distinct microdomains are formed within early endosomes for sorting [216] followed by morphological changes in the early endosomal membranes.

With help of newly formed tubular membranes recycling cargos and cargos for trans-Golgi network are efficiently transported out of the early endosomes [217]. Remaining microdomains transform into late endosomes, and are directed towards degradation.

Vesicles from the Golgi move towards endosomes with help of adaptors like GGAs and AP-1 clathrin-coated vesicles [218]. Retromer generates vesicles in early endosomes that move towards Golgi [219]. Further, mannose-6-phosphate receptors follow retrograde traffic pathway mediated by Rab9 and TIP47 and carry lysosomal hydrolases to early endosomes [220, 221]. After release of hydrolases in the acidic environment of endosomes, the receptor is retrieved to the Golgi by retromer and Rab9. This cross-talk between the Golgi and endosomes with the help of vesicles helps the early endosome to mature into late endosomes [222].

Molecules like receptors for LDL, EGF, and the iron transport protein transferrin, are concentrated in the tubules of early endosomes for recycling [213, 223, 224]. Other receptors like that for asialoglycoproteins, LDL and transferrin are released in endosomes because of the lower pH, and recycled to the cell surface. This is followed

by maturation of early endosomes to late endosomes. Several additional factors and pathways have been identified to play crucial role in early to late endosome transition [207].

LATE ENDOSOMES

Late endosomes are found closer to nucleus than early endosomes; and are spherical. They lack tubules and have the appearance of multivesicular bodies (MVBs) [225]. They differ from early endosomes by their lower pH, different protein composition and markers. Because of delivery of vesicles containing lysosomal hydrolases from the Golgi, late endosomes become acidic. They have markers including RAB7 [226], RAB9 [227], and mannose 6-phosphate receptors [228]. Time of delivery vary between cell types and between cells in culture and in living tissue from minutes to several hours (half-life 6 hours) [229]. Lysosomal integral membrane glycoproteins are delivered from trans-Golgi network with the help of adaptor AP-3 [229]. Late endosomes can fuse with other late endosomes [230] resulting into morphological remodeling or can fuse with lysosomes [229] leading to degradation of endosomal contents. Certain proteins serve to reform late endosomes and hence are recycled out of late endosomes to the Golgi to avoid degradation [231].

LYSOSOMAL DEGRADATION

Lysosomal proteolysis is one of major protein degradation pathways in cells. Lysosomes contain an array of digestive enzymes that play major role in cell metabolism including digestion of extracellular proteins internalized through endocytosis

and gradual turnover of cytoplasmic proteins and organelles [232]. Lysosomes prevent uncontrolled destruction of cellular contents by containment of digestive enzymes and proteases [233]. Therefore, lysosomal degradation requires fusion of vesicles (autophagosomes or endosomes) to the lysosomes [234].

Autophagosomes are membrane enclosed small regions of cytoplasm or cytoplasmic organelles derived from the endoplasmic reticulum [235]. Fusion and digestion of autophagosomes by lysosomal enzymes allow the cells to maintain homeostasis in cellular environment [236].

Late endosomes formed after maturation of early endosomes contain processed internalized extracellular proteins destined to digestion. Lysosomes are denser than late endosomes and the hybrids have an intermediate density [237]. Transport from late endosomes to lysosomes is also unidirectional, as late endosome are consumed in the process of fusion to a lysosome [238]. Hence, endosomal content end up degraded in lysosomes unless they escape or are retrieved in some way.

Lysosomal degradation helps the cells to degrade and recycle the products of the internalized substances in endosomes or autophagosome. Hence this process is required to maintain homeostasis and growth of cells and tissues [239, 240].

ASIALOGLYCOPROTEIN RECEPTORS (AsGR) PATHWAY

The asialoglycoprotein receptor (AsGR)-mediated endocytosis is one of the most extensively studied models of receptor-mediated endocytosis and found in well

differentiated hepatocytes, providing the cells a membrane bound active site for cell to cell interactions and mediating other activities like uptake of selective agents and viruses. Several factors govern the AsGR activity and distribution in cells, such as sub unit interactions [241] or post-translational modifications [242]. AsGR is composed of two protein sub-units and both are required for its functional binding activity [243] and distribution [244]. Post-translational glycosylation of AsGR also has a major impact on its physiological status [242]. AsGR requires calcium (Ca^{2+}) for ligand binding [241] and has high affinity for the galactose-terminating oligosaccharides of desialylated glycoproteins, facilitating their uptake and degradation by parenchymal hepatocytes [245]. Confluent cells show increased levels of AsGR expression compared to cells that are actively dividing.

Glycoproteins are proteins which have glycan residues, carbohydrate chains, covalently bound to polypeptide side chains of proteins during post-translational modification called glycosylation. Glycoproteins play various essential roles in human body. The glycan residues of human glycoproteins frequently have exposed sialic acid groups at the ends of the chains [246] which helps keeping the protein functional. These sialic acid residues are lost over time with a number of enzymatic and metabolic activities, exposing the penultimate sugar, galactose.

AsGRs present on the surfaces of hepatocytes recognize and bind to exposed galactose residues of asialo-glycoproteins (AsGs) [247]. Binding of AsGs to AsGRs triggers invagination of the cell membrane, and eventually internalizing the AsGR-AsG complexes within endosomes (Figure 1.2) Endosomes are short-lived, and appear to fuse with each other, and vesicles from the Golgi [248]. As the pH of the endosomes

decreases [249], uncoupling of receptor-ligand complex starts [248]. Subsequent to dissociation, AsGR is recycled back to cell surface for re-use [250]. AsGs have been used as a targetable carriers to deliver genetic material or macromolecular drugs specifically to hepatocytes using soluble complexes of DNA/drugs and AsGs both in vitro [251, 252] and in vivo [253]. AsGR-mediated pathway is degradative since after internalization endosomal contents are subjected to degradation by lysosomal fusion (Figure 1.2) into constituent smaller products. This process can be arrested if lysosomal digestion is inhibited, which can be accomplished specifically by increasing the pH of endosomes or increasing the release of endosomal contents into cytoplasm before lysosomal fusion.

ENDOSOMAL ESCAPE

Development of methods for efficient and specific delivery systems is an important issue in success of delivery and application of drugs and gene therapy [254]. Since the major uptake mechanism of cells is endocytic pathway, most drugs and agents are entrapped in endosomes, and subsequently are degraded by lysosomal digestion which limits the effects of delivered agents [255]. Several mechanisms to facilitate the endosomal escape and increase cytoplasmic delivery are under investigation. Bacteria and viruses use several mechanisms such as formation of pores in the endosomal membrane, changes in pH of endosomes/lysosomes and fusion membrane of endosomes to enable the endosomal escape [256]. Chemical agents, synthetic polymers/peptides and photochemical methods are also being developed to serve the purpose [257]. An

optimal agent for endosomal escape is required which should have high efficiency and no toxicity. Understanding the mechanism of escape of endosomal contents with the help of different agents is important to develop the therapeutic agents.

Following are a few known mechanisms of endosomal escape:

PORE FORMATION IN THE ENDOSOMAL MEMBRANE

Some agents or peptides can bind and cause decrease in tension of the membranes resulting in pore formation in endosomal membranes [258]. Some peptides can polymerize to make barrel-stave pore or toroidal pore giving rise to holes in membranes [259].

pH-BUFFERING EFFECT

Some agents can alter the protonation in endosomes which induces influx of water and ions into endosome that subsequently causes rupture of endosomes and release of endosomal contents in cytoplasm [260].

ENDOSOMAL MEMBRANE FUSION

Some fusogenic peptides, commonly found in viruses, undergo conformational changes when triggered by change in pH in endosomes allowing the protein to induce fusion in membrane [261]. This induces fusion of membrane of biologic agent to endosomal membrane and hence releasing the internal contents of biological agent in the cytoplasm

PHOTOCHEMICAL INTERNALIZATION

Several photosensitizers localize in the membrane of the endosomes and lysosomes [262] and induce reactive oxygen formation upon exposure to light, which destroy organelle membrane leading to release of contents in cytoplasm [263].

Several potential agents to enhance endosomal escape are under investigation to improve the drug and gene therapy effects. Following are few examples of types of escape agents being studied:

MEMBRANE-ACTIVE PROTEINS AND PEPTIDES

Usually derived from biological agents like virus, bacteria or plants and made more desirable by recombinant technologies, protein and peptide based agents are most promising group of endosomolytic agents.

Virus derived agents: Examples, haemagglutinin (HA) protein of the influenza virus has fusogenic properties [264], influenza-derived fusogenic peptide diINF-7 [265], fusogenic penton base protein of adenovirus [266], pore forming gp41 transmembrane protein of HIV [267], Tat protein of HIV causes membrane destabilization [268], membrane-disrupting L2 peptide of Papillomavirus [269], fusogenic envelope protein (E) of the West Nile virus [270].

Bacteria derived agents: Examples, pore-forming listeriolysin O (LLO) from *Listeria monocytogenes* [271], pore-forming toxins *Pneumococcal pneumolysin* (PLO) and *Streptococcal streptolysin* O (SLO) [272], fusogenic peptide Diphtheria toxin (DT) secreted by *Corynebacterium diphtheria* [273], fusogenic exotoxin A (ETA) from *Pseudomonas aeruginosa*, [274],

Plant derived agents: Examples, ribosome-inactivating protein, Ricin from *Ricinus communis* (mechanism not known) [275], Saporin and Gelonin (mechanism not known) [276].

Human / animal derived agents: Examples, human calcitonin derived peptide, hCT(9-32) causes lipid raft-mediated endocytosis [277], fibroblast growth factors (FGFs) (mechanism not known) [278], Melittin, bee venom, induces membrane destabilization [279].

Synthetic peptides: Examples, Arginine-rich cell-penetrating peptides called (R-Ahx-R)(4) AhxB, binds to proteoglycans on membranes [280], fusogenic synthetic analogue of glycoprotein H (gpH) [281], small peptide sequences derived from haemagglutinin subunit HA-2 [282] and GALA [283] of influenza virus, penetratin (pAntp), a domain of antennapedia protein [284], R6-penetratin [285], synthetic analog of penetratin EB1 destabilizes the endosomal membrane [286], bovine prion protein (bPrPp) [287], Histidine-rich peptides [288], sweet arrow peptide (SAP) [289].

MEMBRANE-ACTIVE CHEMICAL AGENTS

Several chemical agents with endosome disruptive properties are also being developed. Example, polyethylenimine (PEI) [290] and imidazole-containing polymers [291] cause pH changes, agents such as ammonium chloride, chloroquine, and methylamine penetrate the cell membranes and alter pH [292]

For effective delivery of drugs and agents, to reduce the risk of degradation and increase chances of safe release of therapeutic gene/protein/drug, it would be ideal to have an efficient and safe endosomal escape agent with low immunogenicity.

HYPOTHESES

We hypothesized that: 1) Isolated mitochondria can be coated with positively charged AsGs in a non-damaging electrostatic interaction. 2) These AsG–mitochondria complexes could be targeted to hepatocytes, which would recognize and bind to AsGR on cell surface. Complexes could be internalized by hepatocytes through AsGR-mediated endocytosis. 3) An endosomolytic agent could be used to facilitate the escape of internalized mitochondria from lysosomal digestion. 4) Healthy mitochondria delivered to hepatocytes with defective or damaged mitochondria could substitute for the damaged organelles, and proliferate until the energy requirements of the cell were met resulting in rescue from hepatocyte death, and prevention of liver failure.

AIMS

The aim of the study was to determine whether healthy and functional mitochondria could be targeted to hepatocytes, substitute for the damaged organelles, and proliferate to meet the energy requirements and correct the mitochondrial dysfunctional disorders of the hepatocytes.

CELLS AND CELL CULTURE

Suitable cell culture models are required to study uptake of AsG-coated mitochondria by hepatocytes and for further assays to evaluate stability and function of the mitochondria delivered to the hepatocytes specifically. Cells showing AsGR mediated activity to evaluate internalization and for source of mitochondria to make complexes with AsGs were required.

MODEL SYSTEM FOR EVALUATING UPTAKE BY HUMAN HEPATOCYTES

HUH 7 CELLS

Human hepatoblastoma cells, Huh 7 cells, AsGR (+) are well-differentiated transformed liver cells. These cells express AsGR on cell surface and have been shown to actively internalize AsGs through AsGR mediated endocytosis [293]. Unlike other common AsGR expressing hepatoma cell lines, Huh 7 cells grow in monolayers. Huh 7 cells were used to evaluate binding and internalization of AsGs coated mitochondria and stability and function of delivered mitochondria.

SK HEP1 CELLS

Human hepatoma cells, SK Hep1 cells [AsGR (-)] is a poorly-differentiated, transformed liver cell line. These cells do not exhibit many hepatic-specific features [294]. In particular, SK Hep1 cells express little AsGR on cell surface. These cells were used as negative controls to determine if internalization of AsGs coated mitochondria by Huh 7 [AsGR (+)] cells is mediated through AsGR pathway and not random phagocytosis.

SOURCE OF MITOCHONDRIA FOR UPTAKE ASSAYS

HTC CELLS

HTC is a well-differentiated rat hepatoma cell line [295]. HTC cells were used as source cells to obtain mitochondria for complex formation with AsGs and internalization by human hepatocytes expressing AsGR on cell surface. These cells have mitochondrial DNA sequences different than human mitochondrial DNA sequences that can be distinguished using PCR amplification with specific primers for respective cell mitochondrial DNA sequences. Despite of 70% homology, specific sets of primers have been used to differentiate between human and rat mitochondrial DNA [47]. This helps in differentiating between cellular endogenous mitochondria and internalized mitochondria from extracellular environment in human hepatocytes after uptake of AsG-coated mitochondria.

SOURCE OF GFP-LABELED MITOCHONDRIA

HTC MITO-GFP CELLS

HTC mito-GFP cell line was genetically constructed by transfecting HTC cells with pAcGFP1-Mito plasmids (Clontech Laboratories) expressing green fluorescent protein (GFP) fused to a mitochondria targeting sequence (subunit VIII of human cytochrome c oxidase). When expressed in cells, subunit VIII of cytochrome c oxidase carry fused GFP to inner membranes of mitochondria and labeling the mitochondria with GFP. GFP labeled cells were selectively sorted using fluorescence-activated cell sorter to construct a stable HTC mito-GFP cell line and kept under selective pressure. These cells were used as the source of GFP labeled mitochondria to track the localization of internalized

mitochondria by hepatocytes uptake of AsG-coated mitochondria using fluorescence microscopy.

MITOCHONDRIA-DEPLETED CELLS

HUH 7-MITO (-) AND SK HEP1-MITO (-) CELLS

Huh 7 and SK Hep1 cells have high numbers of mitochondria to meet energy requirement of cells. To eliminate the background human mitochondria so that chances of propagation of newly delivered mitochondria increase, damage to endogenous mitochondria of cells was required. Delivery of external mitochondria to cells with damaged mitochondria would also help to determine stability and function of delivered mitochondria.

Mitochondria in cells can be damaged by treatment with various types of mitochondrial toxins. Continuous damage to mitochondria in cells can result in cells with permanently damaged mitochondria and cell death unless cells are supported artificially by providing required supplement materials externally.

Huh 7 and SK Hep1 cells were treated with 2'-3'-dideoxycytidine (ddC), zalcitabine. ddC is a pyrimidine analog derived from deoxycytidine, by replacing the hydroxyl group in position 3' with a hydrogen terminating the chain elongation during DNA replication [296]. Although both nuclear and mitochondrial DNA replications are susceptible to ddC, mitochondrial DNA replication is more affected in presence of ddC because of significantly smaller size of mitochondrial DNA compared to nuclear DNA [297]. Continuous treatment of cells with ddC results in mitochondrial DNA depletion and

eventually forming mitochondrial DNA free cells [298]. Mitochondrial structures (inner and outer membrane of mitochondria) are still found in cells since structural proteins composing those are expressed by mitochondrial genes in nucleus. However, due to complete loss of mitochondrial DNA, expression of mitochondrial genes from mitochondrial DNA is absent, which causes complete loss of mitochondrial respiration and function.

Huh 7-mito (-) and SK Hep1-mito (-) cells were constructed by treatment with ddC for 2-3 weeks. Complete loss of mitochondrial DNA was determined with real-time PCRs. Cells were supported with L-glutamine, sodium pyruvate and uridine [299] externally to avoid cell death. These mitochondria free cells allowed elimination of background human mitochondria, and served as a model for severe mitochondrial damage.

FIGURES

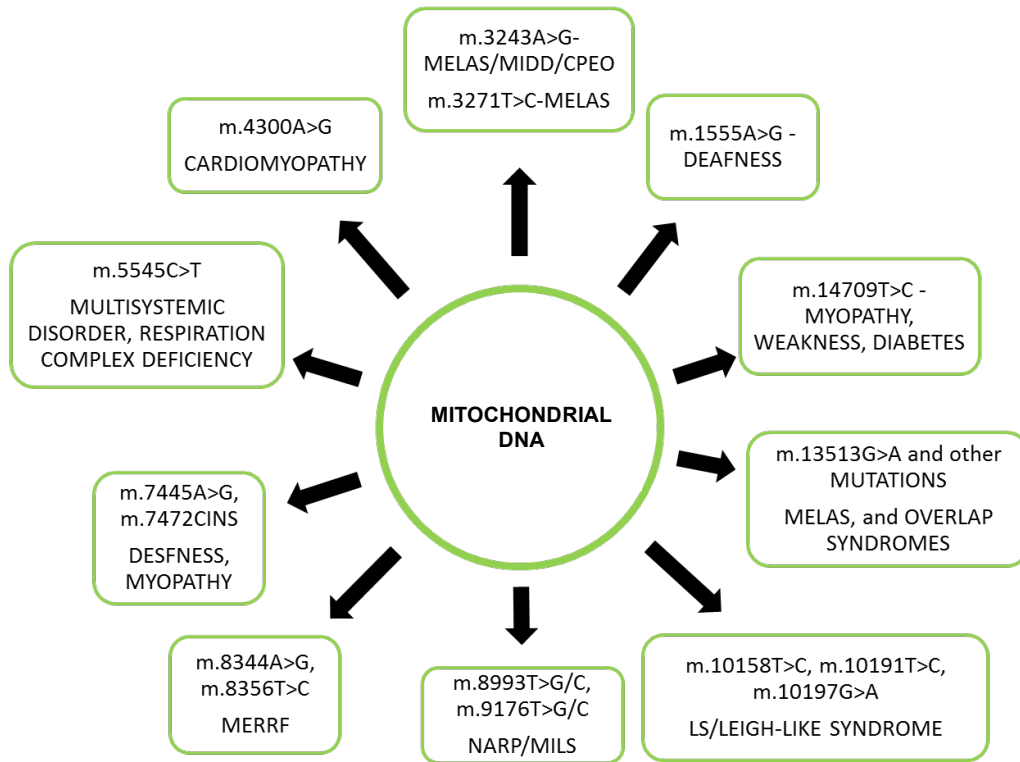


Figure 1.1. Mitochondrial Genotypic Mutations Associated with Human Mitochondrial Disorders.

A list of common primary mitochondrial DNA mutations causing human diseases.

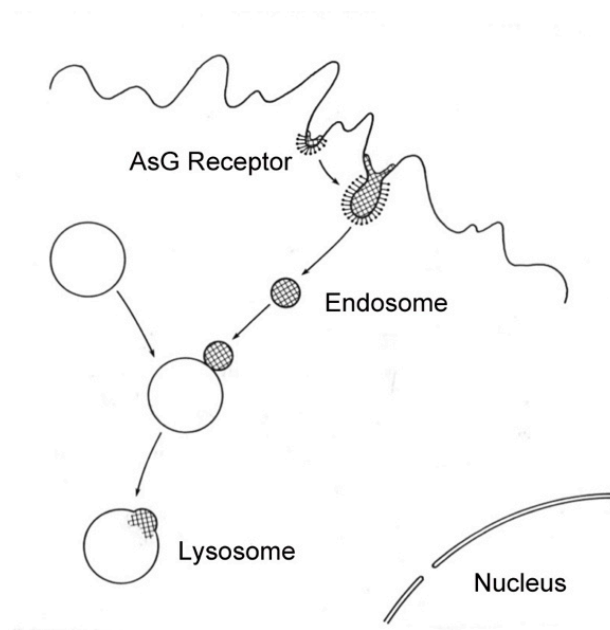


Figure 1.2. A schematic representation of AsGR-mediated endocytosis of AsGs by hepatocytes.

AsGR on cell membrane bind to AsG, followed by internalization of AsGR-AsG complexes in endosomes. These endosomes fuse with lysosomes resulting in degradation of endosomal contents.

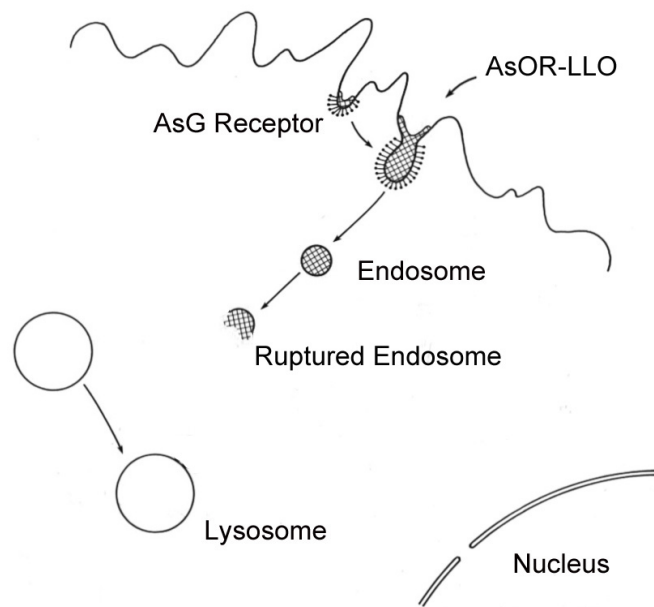


Figure 1.3. A representation of targeted LLO-mediated endosomal rupture

After internalization of LLO conjugates in endosomes, LLO becomes activated in the low pH and reducing environment of endosomes which results in pore formation and rupture of endosomal membranes. This allows the escape of endosomal contents in cytoplasm before lysosomal digestion can occur.

CHAPTER 2: FORMATION OF STABLE COMPLEXES OF MITOCHONDRIA WITH AsG.

In order to evaluate binding and internalization of asialo-glycoprotein (AsGs)-mitochondria complexes with hepatocytes, coating of mitochondria with AsGs is required so that cells could recognize the AsGs and take the whole complex in. However, mitochondrial membranes are delicate and susceptible to damage. In particular, covalent bonding could alter or destroy important membrane structures. Since, the surface of mitochondria is known to be negatively charged (See Chapter 1), preparation of an AsG that was highly positively charged, could result in a non-covalent electrostatic complex formation by mixing of the carrier with mitochondria.

Poly-L-lysine refers to a synthetic polymer composed of a positively charged amino acid, lysine. Coupling of poly-lysine chains to other proteins provides positive charge to those proteins. Poly-lysines can be coupled with other proteins using carbodiimide cross-linkers. Carbodiimides (1-Ethyl-3-(3-dimethylaminopropyl) carbodiimide) are water soluble hydrochloride cross-linkers used as carboxyl activating agents to couple primary amines to yield amide bonds [300]. Hence, carbodiimides help binding two protein molecules covalently. Depending on number of lysine residues, poly-lysine chains can vary in length, which also results in varying amount of additional positive charge added to the coupled protein molecules. Larger size of poly-lysine chains can provide higher amount of positive charges to the desired protein, which can result in formation of aggregates when used to make complexes with negatively charged molecules. Here smaller sized poly-lysine chains (average molecular weight 1000) were

used to stably bind to AsGs using carbodiimides cross-linkers to avoid aggregation of AsGs-mitochondria complexes when added to isolated mitochondria.

ASIALO-OROSOMUCOID PROTEIN CARRIER

Orosomucoid (OR) is an abundant human plasma glycoprotein (normal plasma concentration between 0.6-1.2 mg/mL [301]). OR was de-sialated to remove terminal sialic acid groups enzymatically and form asialoorosomucoid (AsOR) with exposed glycan residues to make complexes with isolated mitochondria. AsOR is an extensively studied AsG that is recognized and internalized by hepatocytes via AsGR mediated endocytosis [302] and has been used for targeted delivery of other drugs/ proteins and genes specifically to hepatocytes [252, 303].

To follow and measure uptake of the carrier by hepatocytes, AsOR was labeled with fluorescence dylight 650 dye to construct fluorescence labeled AsOR (FI-AsOR). FI-AsOR is negatively charged. To convert FI-AsOR to a positively charged molecule, poly-lysine chains were covalently coupled to the protein using carbodiimides cross-linkers to create positively charged poly-lysine tagged FI-AsOR (FI-AsOR-PL). Changes in charges on the protein were determined with gel electrophoresis. Proteins were loaded in the middle of the gel such that positively charged proteins could run towards negative terminal and negatively charged proteins could run towards positive terminal. Average number of fluorescent tags and poly-lysine chains bound per AsOR molecule were calculated. Addition of fluorescent tags and poly-lysine chains could have altered the structure of AsOR such that it could not be recognized by hepatocytes. Hence uptake

assays were performed to determine if after addition of fluorescent tags and poly-lysine chains, FI-AsOR-PL is still being recognized by hepatocytes. FI-AsOR-PL was anticipated to bind to isolated mitochondria by electrostatic interactions.

FORMATION OF STABLE COMPLEXES OF FI-AsOR-PL AND MITOCHONDRIA

FI-AsOR-PL is a positively charged protein, and isolated mitochondria have a negatively charged outer membrane. Isolated mitochondria and FI-AsOR-PL were mixed to form FI-AsOR-PL–mitochondria complexes by an electrostatic interaction (Figure 2.1). To deliver the mitochondria to hepatocytes via AsGR mediated endocytosis, complexes of FI-AsOR-PL–mitochondria should be stable such that FI-AsOR-PL remains bound to the mitochondria through whole process. Stability of the complexes was determined by centrifuging and re-suspending the mitochondria in fresh medium. If the complex is stable, FI-AsOR-PL would stay bound to mitochondria upon repeated centrifugation, otherwise loss of FI-AsOR-PL would be observed with repeated spins.

METHODS

CELLS AND CELL CULTURE

Huh 7, SK Hep1 and HTC cells were maintained in Dulbecco's Modified Eagle Medium (DMEM) (Gibco) supplemented with antibiotic/antimycotic solution (Invitrogen), 10% fetal bovine serum (FBS) (Invitrogen).

MITOCHONDRIA PREPARATION

Isolation of mitochondria is a delicate and time-consuming procedure. Composition of isolation buffers and storage buffers directly affect stability and function of isolated mitochondria [304]. It has been shown that the use of monosaccharides such as mannitol helps in isolation of better coupled isolated mitochondria [305]. Cells were lysed manually because detergents can cause denaturation of mitochondrial membrane proteins and result in swelling of mitochondria [306]. Since addition of tris chloride based buffers have shown to cause aggregation of isolated mitochondria [307], phosphate based buffers were used to isolate and store isolated mitochondria [308]. Recommended conditions and ionic concentrations were used to isolate mitochondria from hepatocytes and store isolated the mitochondria [309].

Mitochondria were isolated from HTC and Huh 7 cells using a mitochondria isolation kit for mammalian cells (Thermo Scientific, Rockford, IL, USA) according to manufacturer's instructions. In brief, cells were pelleted by centrifuging approximately 2×10^7 cells at $800 \times g$ for 5 min and re-suspended in 800 μ l of mitochondria isolation reagent A from mitochondria isolation kit. After 2 min incubation on ice, 10 μ l of isolation reagent B from

mitochondria isolation kit was added and cells were vortexed intermittently for 5 min on ice. Isolation reagent C from mitochondria isolation kit, 800 μ l, was added and mixed gently. Cell lysate was centrifuged at 1000 x g for 15 min at 4°C. Supernatant was collected and spun at 4000 x g for 20 min at 4°C. Mitochondria pellet was collected and washed with reagent C from mitochondria isolation kit. After purification, mitochondria were kept in isolation reagent C from the mitochondria isolation kit on ice until further use.

CARRIER PREPARATION

Orosomucoid (OR) was isolated from human serum (American Red Cross) by the procedure of Whitehead and Sammons [310]. OR was de-sialated by neuraminidase (Sigma) [311] to make asialo-orosomucoid (AsOR). AsOR was labeled with dylight 650 using an NHS ester reaction (Thermo Fisher Scientific Inc., Rockford, IL USA) according to manufacturer's instructions. AsOR and fluorescence labeled AsOR (FI-AsOR) were separately reacted with a carbodiimide cross-linker (Sigma) followed by addition of poly-L-lysine (PL) in 1 ml of 0.1 M MES (pH 6) for 24 h at 25°C. Excess PL was removed from AsOR-PL and FI-AsOR-PL separately using an exclusion column (10,000 MWCO, Millipore). FI-AsOR and FI-AsOR-PL, 1 μ g each in 100 μ l in phosphate buffered saline (PBS), were used to check fluorescence intensity using an XFLUOR4SAFIREII Version: V 4.62n spectrophotometer.

To evaluate the charge of proteins, samples were mixed with 60% glycerol and loaded in wells in the center of an 0.8% agarose gel, run at 100V for 1 h with Tris-acetate-EDTA (TAE) buffer (40 mM Tris (pH 7.6), 20 mM acetic acid, 1 mM EDTA) and stained

with 0.1% amido black (Bio-Rad) in 40% methanol and 10% acetic acid for 30 min, and de-stained with 40% methanol and 10% acetic acid for 10-13 h at 25°C on a rotary shaker.

MASS SPECTROMETRY

AsOR, FI-AsOR and FI-AsOR-PL were diluted to 1, 0.1, 0.025 and 0.001 mg/ml.

Lysozyme (MW 14.3 kDa) (Sigma) and bovine serum albumin (BSA) (MW 66.5 kDa) (Sigma) were used as controls. Matrix suitable for large analytes, 3, 5-dimethoxy-4-hydroxycinnamic acid (sinapinic acid), (Sequazym Peptide Mass Standards Kit, Applied Biosystems) was mixed with various concentrations of proteins with or without controls according to manufacturer's instructions, and submitted for mass spectrophotometry (Voyager-MALDI).

COMPLEX FORMATION AND STABILITY

Rat (HTC) cell mitochondria, 800 μ l (1.6 μ g/ μ l total mitochondria protein) in mitochondria isolation reagent C were incubated with 100 μ g of FI-AsOR-PL or FI-AsOR protein (in 52 μ l PBS) on ice for 45 min. Samples were repeatedly spun at 4000 rpm for 8-10 min at 4°C, and re-suspended in mitochondria isolation reagent C. After each spin, the mitochondria pellets and supernatants were collected, and fluorescence measured at 685 nm. Experiments were conducted in triplicate, and repeated 3 times. The results were expressed as mean \pm standard error in arbitrary fluorescence units.

PARTICLE SIZE ANALYSIS

FI-AsOR-PL, 100 µg, was added to isolated mitochondria, 400 µl (3 µg/µl total mitochondrial protein) and incubated on ice for 45 min. FI-AsOR-PL–mitochondria complexes were centrifuged at 4000 rpm for 10 min at 0°C, washed and re-suspended twice in mitochondria reagent C, 800 µl. Mitochondria or FI-AsOR-PL–mitochondria complexes, 8 µl, were analyzed on a 90Plus Particle Size Analyzer (Brookhaven Instruments Corporation, Holtsville, NY, USA). Each sample was run eight times, and assays repeated with 4 independent replicates. Results are expressed as mean effective diameter ± standard error (nm).

UPTAKE ASSAY BY FLUORESCENCE MICROSCOPY

Cells were plated at 50% confluence on sterile cover slips 2-3 days before assay. When 95% confluent, cells were washed with PBS (Mg^{2+} - and Ca^{2+} -free) and maintained in phosphate-free DMEM with high glucose (Life Technologies, #11971) for 16 h. Cells were incubated with FI-AsOR-PL at 37°C for 1 h. After uptake, cells were washed 3 times with 10 mM EDTA in ice cold PBS (Mg^{2+} - and Ca^{2+} -free) and fixed with 4% paraformaldehyde for 30 min and nuclei were stained with DAPI (Invitrogen) for 20 min. Cells were mounted and imaged under a fluorescence microscope, and presented as single wavelength at 672, and merged dual wavelength images at 461, and 672 nm.

RESULTS AND DISCUSSION

Fluorescence spectrophotometric data showed high intensity of fluorescence in both FI-AsOR and FI-AsOR-PL (Figure 2.2). The fluorescence value of 1 μ g FI-AsOR was 28,000 units, and of FI-AsOR-PL it was 27,600 units in 100 μ l of PBS. This suggested that protein was labeled with a fluorescent tag, which could help to measure fluorescence levels in cells after uptake.

To determine if charge of FI-AsOR-PL is changed from negative to positive upon addition of poly-lysine chains, an agarose gel was run. Gel electrophoresis showed that AsOR and FI-AsOR were negatively charged, and migrated towards the positive terminal. FI-AsOR-PL migrated towards negative terminal indicating that the addition of poly-lysine chains converted the negatively charged molecule into a positively charged one (Figure 2.3).

Average masses determined by mass spectrometric analysis were AsOR, 32.8 kDa; FI-AsOR, 33.4 kDa; and FI-AsOR-PL, 35.2 kDa. From these data and the known approximate mass of dylight tag (0.25 kDa) and PL (1 kDa), it was calculated that an average of two fluorescent tags and two PL chains were bound per FI-AsOR-PL molecule (Figure 2.4).

Chemical linkage of fluorescent tags and poly-lysine chains to AsOR might have altered AsOR recognition by AsGRs. To evaluate binding of FI-AsOR-PL to AsGRs, Huh7 [AsGR (+)] cells and SK Hep1 [AsGR (-)] cells were incubated with FI-AsOR-PL. Fluorescence microscopy showed that approximately 78% of cell population had numerous small punctate red structures (Figure 2.5A). Some structures surrounded

nuclei (Figure 2.5C) suggesting that those structures were intracellular, and the size was consistent with that of endosomal vesicles. In contrast, SK Hep1 cells [AsGR (-)] lacked any similar red structures (Figure 2.5B and D). This suggested that FI-AsOR-PL was internalized by Huh 7 cells by AsGR-mediated endocytosis. Internalization was not found uniform in all the cells, but was in groups of cells where cells were lying in close proximity. This could be because of the higher expression of AsGR in confluent cells compared to dividing cells (See Chapter 1). Plane of focus of microscopy is another factor that affects the observation of FI-AsOR-PL in all cells in a field. Difference in localization of early and late endosome (See Chapter 1) makes it difficult to observe internalization in all cells in one plane since cells might take different amount of times in endosomal maturation and hence different plane of localization of internalized protein.

If there is stable binding of FI-AsOR-PL with mitochondria, particle size of mitochondria is anticipated to increase after coating those with FI-AsOR-PL. Particle size analysis of mitochondria alone showed a mean diameter of 700 ± 57.8 nm, while purified FI-AsOR-PL–mitochondria complexes had a mean diameter 1000 ± 62 nm, Figure 2.6, suggesting that the complexation increased the mean diameter of mitochondria by approximately 43%.

Complexes of positively charged FI-AsOR-PL and isolated mitochondria were anticipated to be stable with charge-charge interactions. The stability of the FI-AsOR-PL–mitochondria complexes was determined by repeatedly centrifuging and re-suspending the complexes in fresh medium. As shown in Figure 2.7A, fluorescence of the FI-AsOR-PL associated with the pelleted mitochondria decreased by about 15% after the second spin, and then remained constant at approximately 27,000 units

through three spins. Conversely, fluorescence in the supernatants of FI-AsOR-PL mixed with mitochondria decreased to 24% from 32,000 to 7,900 units in supernatant after 1st spin and remained low in subsequent spins, Figure 2.7B. The mitochondrial pellet-associated fluorescence after mixing of mitochondria with FI-AsOR that lacked PL, was 4,000 units (< 10% of fluorescence of the FI-AsOR added) after the first spin, and no longer detected with the pelleted mitochondria after the 2nd and 3rd spins, Figure 2.7A. These data suggested that FI-AsOR-PL binding to mitochondria required the presence of PL, and the binding was stable under the conditions of re-suspension and centrifugation.

These data showed that we were able to make stable complexes of FI-AsOR-PL–mitochondria. These stable FI-AsOR-PL–mitochondria complexes were used further to evaluate binding and internalization of complexes by hepatocytes.

FIGURES

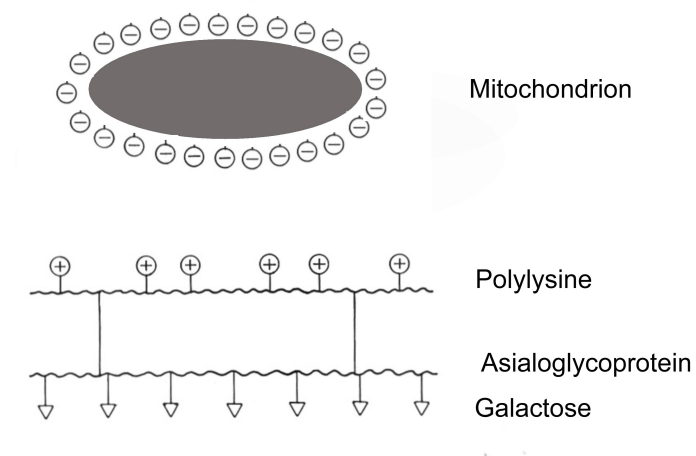


Figure 2.1. A representation of electrostatic binding of an FI-AsOR-PL conjugate to mitochondria.

Positively charged FI-AsOR-PL binds to negatively charged isolated mitochondria to form stable complexes of FI-AsOR-PL–mitochondria by electrostatic interactions.

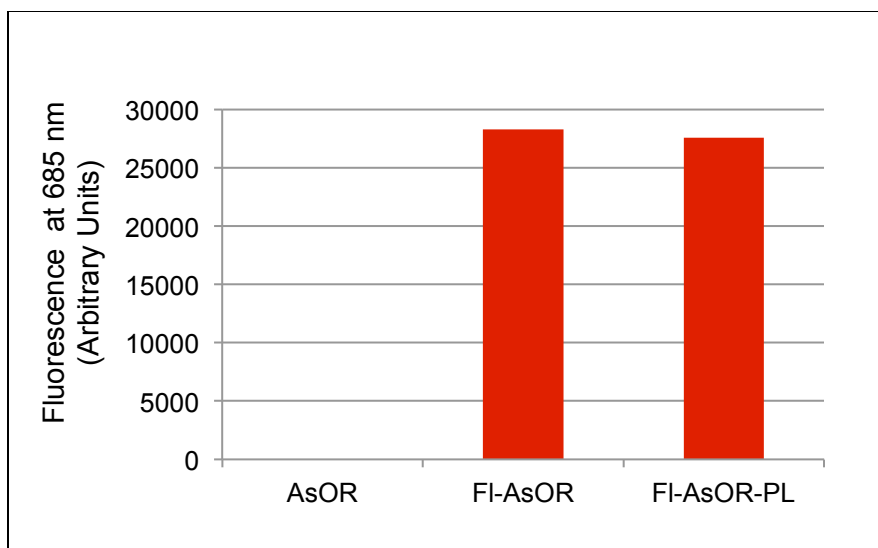


Figure 2.2. Fluorescence of proteins tagged with Dylight 650 dye.

One μg of each protein in 100 μl PBS was used to determine fluorescence intensity at 685 nm.

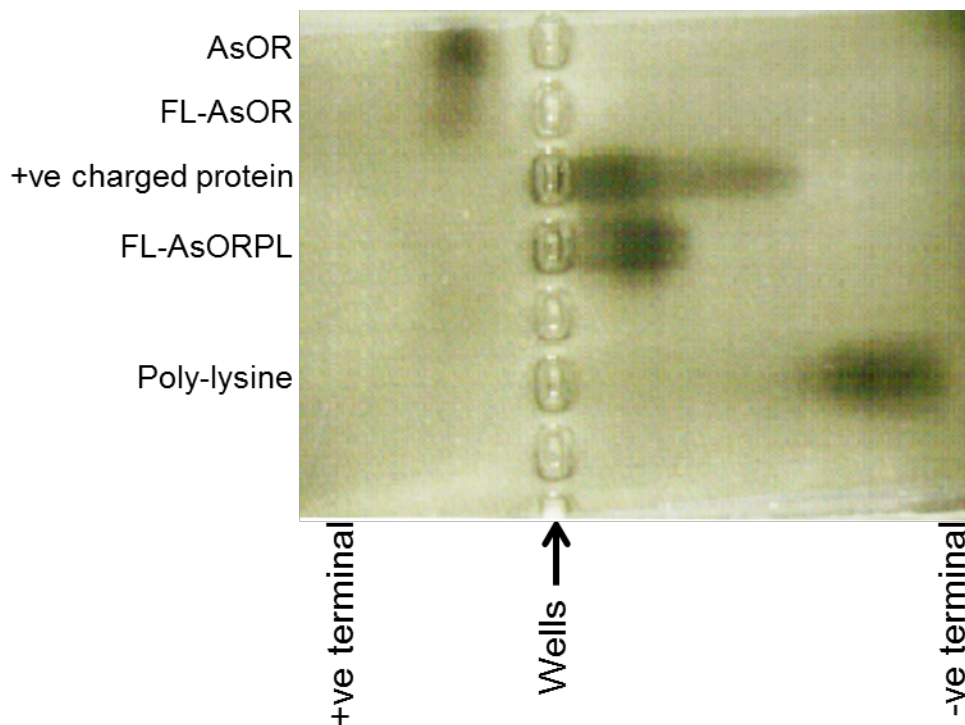
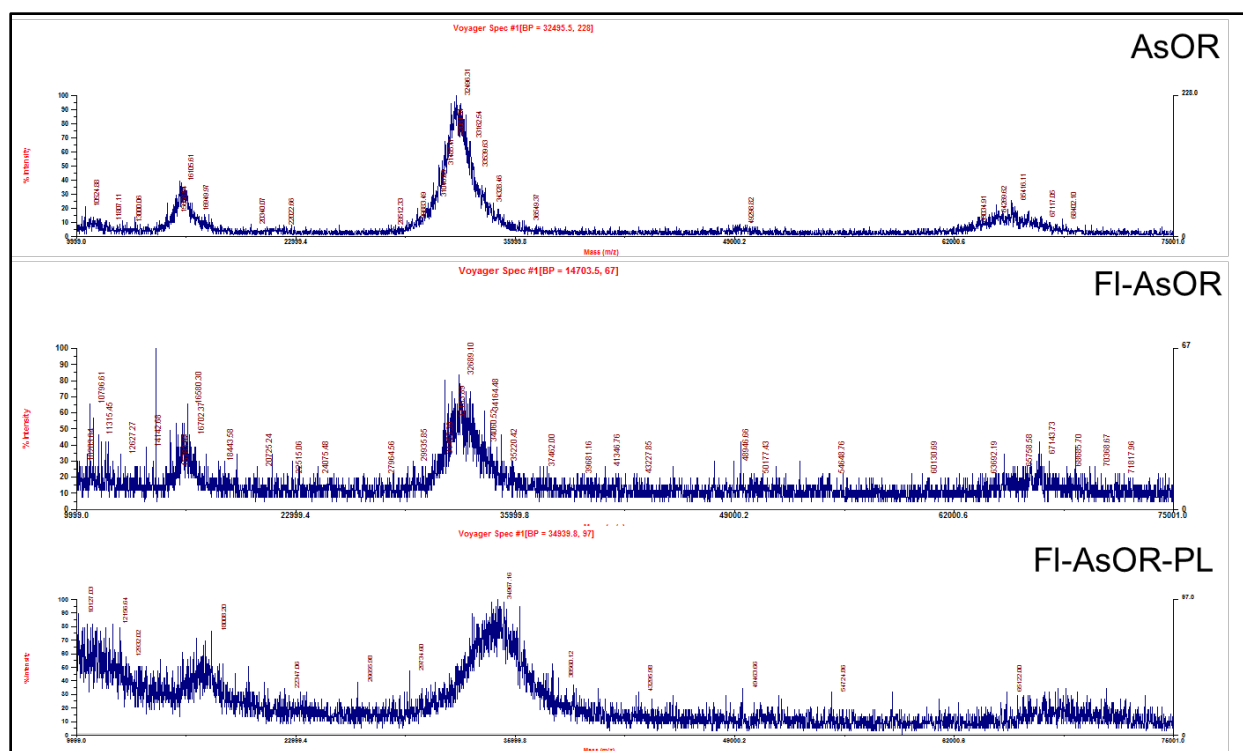


Figure 2.3. Gel electrophoresis showing the direction of migration of FI-AsOR and FI-AsOR-PL.

Proteins were loaded near the middle of a 0.8% agarose gel to determine the charge by direction of migration. Negatively charged proteins (AsOR and FI-AsOR) ran towards positive terminal and positively charged protein (FI-AsOR-PL), PL, and a positive charged control protein ran towards negative terminal.



Purified AsOR, FI-AsOR and FI-AsOR-PL with or without internal controls (lysozyme and bovine serum albumin (BSA)) were mixed with a sinapinic acid matrix, and loaded on a mass spectrometric plate to determine masses. Spectral peaks were calibrated as recommended by manufacturer using lysozyme and BSA as internal and external controls.

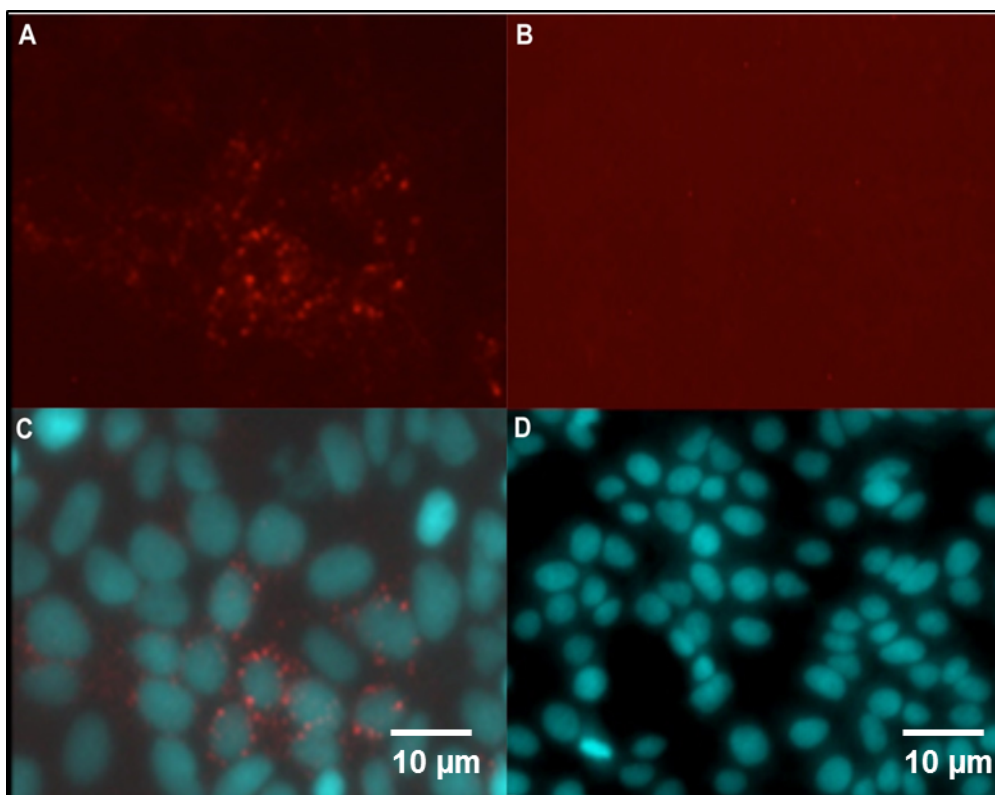


Figure 2.5. FI-AsOR-PL uptake analysis by fluorescence microscopy.

Uptake of FI-AsOR-PL by Huh 7 cells (A and C) and SK Hep1 cells (B and D) was determined with fluorescence microscopy after incubation for 1 h at 37°C. A-B, FI-AsOR-PL; C-D, FI-AsOR-PL + DAPI

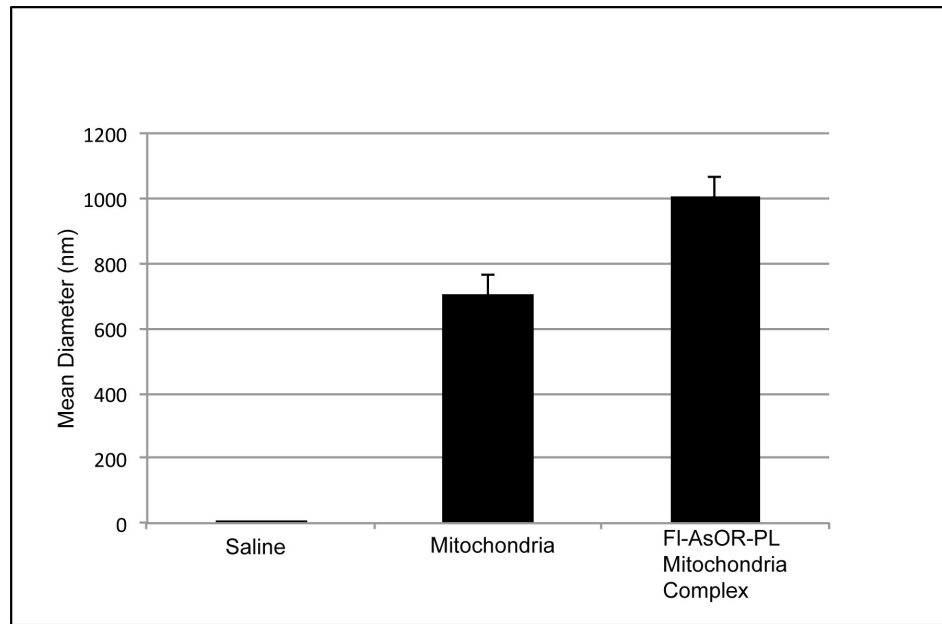
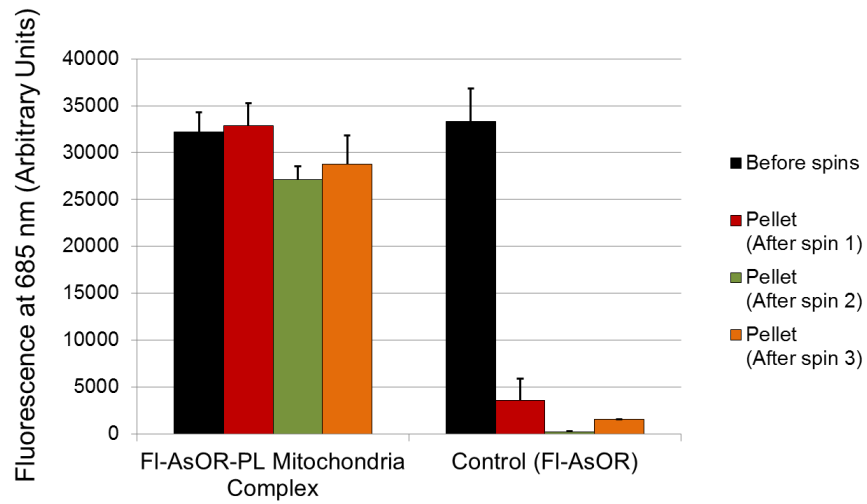


Figure 2.6. Particle size analysis by light scattering.

FI-AsOR-PL was added to isolated mitochondria to make complexes. The size of isolated mitochondria, and FI-AsOR-PL–mitochondria complexes in saline was determined using a 90Plus Particle Size Analyzer.

A



B

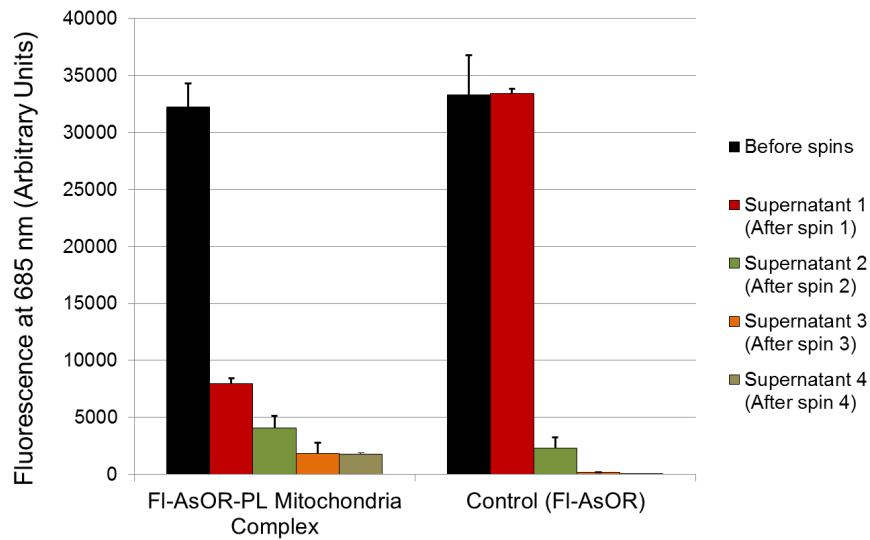


Figure 2.7. Stability of FI-AsOR-PL–mitochondria complexes.

Freshly isolated rat mitochondria were incubated with FI-AsOR-PL or FI-AsOR and repeatedly centrifuged and re-suspended in fresh medium. A. FI-AsOR-PL or FI-AsOR with pelleted mitochondria. B. FI-AsOR-PL or FI-AsOR in supernatant.

CHAPTER 3: ASSESSMENT OF BINDING AND UPTAKE OF FI-AsOR-PL-MITOCHONDRIAL COMPLEXES BY MODEL CELLS

To determine whether hepatocytes could recognize and internalize stable complexes of FI-AsOR-PL-mitochondria through AsGR-mediated endocytosis, Huh 7 cells and SK Hep1 cells were incubated separately with FI-AsOR-PL-mitochondria complex. We hypothesized that cells would be able to recognize the FI-AsOR-PL around the mitochondria, which would allow the cells to internalize the whole FI-AsOR-PL-mitochondria complexes.

Compared to dividing cells, AsGR expression is higher in confluent cells. So cells were grown to more than 95% confluence before uptake assays were performed. Human hepatocytes are maintained in cell culture media containing 10% serum. This serum competes with internalization of desired complexes. In order to avoid this competition, cells were washed and kept in serum free media for 12-18 h before uptake assays to allow recycling of receptors back to cell surface.

Cells were incubated with FI-AsOR protein alone as a positive control for AsGR-mediated endocytosis. In order to determine whether internalization was AsGR mediated and not random, cells were also incubated with mitochondria alone. Detection of internalized mitochondria in cells incubated with mitochondria alone would suggest that internalization was not specific. Cells were also pre-incubated with an excess AsOR prior exposure to FI-AsOR-PL-mitochondria complex at 37°C to compete with AsGR mediated endocytosis to determine specificity of uptake.

Endocytosis is a continuous process. Therefore, continuous internalization should show increasing levels of endocytosed substances in cells with time before degradation begins. Uptake assays were performed for different time periods to determine if increase in internalized complexes is a function of time.

After uptake assays, internalization of the protein carrier, FI-AsOR-PL was determined by measuring fluorescence intensity in cells. HTC cells were used as source of mitochondria as mitochondrial DNA sequences in HTC cells are distinguishable from human hepatocyte mitochondrial DNA sequences. This allows differentiating between endogenous mitochondria and internalized mitochondria in cells. Uptake of HTC mitochondria by human hepatocytes was measured by qPCR.

METHODS

UPTAKE ASSAY

Cells were plated at 50% confluence on tissue culture plates 2-3 days before assay.

When 95% confluent, cells were washed with PBS (Mg^{2+} - and Ca^{2+} -free) and maintained in phosphate-free DMEM with high glucose (Life Technologies, #11971) for 16 h. Mitochondria were isolated from HTC cells, and complexed with FI-AsOR-PL. Uptake assays were conducted at 37°C in DMEM, 2.8 mM Ca^{2+} [312] to which was added either 20 µg/ml mitochondria alone, 4 µg/ml FI-AsOR alone, 25 µl/ml FI-AsOR-PL–mitochondria complex, or 25 µl/ml FI-AsOR-PL–mitochondria complex + 200 µg/ml AsOR (100-fold molar excess added 4 min prior to uptake). Assays were repeated with 3 independent replicates.

After uptake, cells were washed 3 times with 10 mM EDTA in ice cold PBS (Mg^{2+} -and Ca^{2+} -free) followed by washes with ice cold PBS at each time point or at 2 h for extended experiments. Cells were either trypsinized with 0.05% trypsin-EDTA (Gibco, Life Technologies) and collected by centrifugation at 800 rpm for 4 min at 4°C or lysed with 200 µl lysis buffer (Buffer A, mitochondria isolation kit, Thermo Scientific).

Fluorescence intensity of FI-AsOR-PL in lysed cells was measured using XFLUOR4SAFIREII Version: V 4.62n spectrophotometer. HTC mitochondrial DNA levels in trypsinized cells or cell lysates were quantitated by qPCR. Experiments were conducted in triplicate, and repeated at least 3 times.

QUANTITATIVE PCR (qPCR)

To measure uptake of mitochondria, primers (Table 3.1) were designed using Primer3 [313] and Primer-BLAST [314] to specifically amplify Huh 7 mitochondrial DNA or rat liver (HTC) mitochondrial DNA. Primer specificity was determined by PCR using DNA extracted from Huh 7 and HTC cells with QIAamp DNA mini kit (Qiagen) according to the manufacturer's instructions.

For uptake studies, whole cell DNA was isolated using QIAamp DNA mini kit (Qiagen) and mitochondrial DNA levels were quantified by qPCR with Power SYBR Green PCR Master Mix (Applied Biosystems) according to manufacturer's instructions. Human lactate dehydrogenase A (LDHA) DNA levels were quantified in each sample using primers specific for the human LDHA isomer, and the results used to normalize mitochondrial DNA levels (Table 3.1). The qPCR conditions were: one cycle of 2 min at 50°C, and 10 min at 95°C; 40 cycles of 15 sec at 95°C, and 1 min at 60°C followed by one cycle of 10 min at 55°C. Melt curves were obtained following each qPCR to search for primer dimers, and analyze the specificity of the reaction with following conditions: 15 sec at 95°C, 15 sec at 60°C and 15 sec at 95°C. Assays were repeated with 3 independent replicates. Raw data from qPCR were analyzed using comparative real-time PCR kinetics formula [315] and the results expressed as means \pm standard error of fold changes in mitochondrial DNA levels (i.e. mitochondrial DNA number per cell) compared to untreated controls. Non-specific uptake was determined from amplification levels in untreated cells. The number of specific mitochondrial DNA copies in treated cells was determined by difference between total amplification in treated cells and non-specific amplification in untreated cells. The number of mitochondrial DNA copies per cell was calculated by dividing number of specific mitochondrial DNA copies in treated

cells by the number of nuclear LDHA DNA copies per cell [316]. The average number of mitochondria per cell was calculated by dividing number of mitochondrial DNA copies calculated per cell by the average number of mitochondrial DNA copies per mitochondria.

RESULTS AND DISCUSSION

After washing of the cells with EDTA-PBS to remove surface bound protein, the level of fluorescence in Huh 7 cells, AsGR (+) incubated with FI-AsOR alone was approximately 15,000 units at 15 min, and increased to more than 20,000 units at 60 min, Figure 3.2A. Similarly, fluorescence in Huh 7 cells incubated with FI-AsOR-PL-mitochondria complex was 20,000 units at 15 min, and increased to more than 35,000 units at 60 min. As expected, fluorescence levels after incubation of mitochondria alone (lacking labeled AsG) had no fluorescence. Furthermore, addition of a large molar excess of AsOR prior to FI-AsOR-PL-mitochondria complex resulted in fluorescence levels less than 2,500 units at both 15 min and 60 min in Huh 7 cells, Figure 3.2A. These results indicated that association of protein carrier with Huh 7 cells was time-dependent, and inhibited by competition with excess of free AsOR supporting the conclusion that association of protein carrier with Huh 7 cells was mediated by the AsGR. Fluorescence in SK Hep1, AsGR (-) cells was barely detectable under all conditions, Figure 3.2B which further suggest that time-dependent increase in fluorescence levels in Huh 7 cells was not random.

However, because the fluorescent tag was only on the FI-AsOR-PL carrier, it is possible that the carrier alone, without mitochondria, was internalized. To determine whether uptake of complexed mitochondria by Huh 7 cells had occurred, primers were designed, Table 3.1, and shown to amplify HTC (rat) mitochondrial DNA, and specifically distinguish that from Huh 7 (human) mitochondrial DNA, Figure 3.1.

Huh7 cells incubated with FI-AsOR-PL-mitochondria complex resulted in a 990-fold increase of HTC mitochondrial DNA levels (approximately 6-14 HTC mitochondria per cell) compared to untreated cells at 15 min, and an increase to more than double (approximately 14-36 HTC mitochondria per cell) ($p < 0.001$) at 60 min, Figure 3.3A. This showed that similar to fluorescence levels, mitochondrial DNA levels also increase with time in Huh 7 cells. Huh7 cells incubated with either mitochondria alone or FI-AsOR alone failed to show any significant HTC mitochondrial DNA levels suggesting that internalization of FI-AsOR-PL-mitochondria complex was not random. Pre-incubation of cells with an excess free AsOR prior to FI-AsOR-PL-mitochondria complex resulted in HTC mitochondrial DNA levels in Huh 7 cells that were 76% lower than in cells incubated with complexes without excess AsOR further suggesting that internalization of FI-AsOR-PL-mitochondria complex was AsGR mediated. In contrast, HTC mitochondrial DNA levels in SK Hep1 cells were barely detectable under any condition, Figure 3.3B. The data suggested that complexed mitochondria were taken up by Huh 7 cells specifically through the AsGR, and not due to some non-specific interaction.

Collectively, these data suggest that Huh 7 cells could bind and internalize FI-AsOR-PL-mitochondria complexes through AsGR mediated endocytosis. These complexes are destined to digestion unless their escape is facilitated before lysosomal fusion.

FIGURES AND TABLES

Table 3.1. Sequences of Primers Used For Quantification

Primers	Sequences
LDHA FW	5'-TAATGAAGGACTTGGCAGATGAACT-3'
LDHA RV	5'-ACGGCTTTCTCCCTCTTGCT-3'
HTC Mito FW	5'-AGGCTTAAAAGCAGCCATCA-3'
HTC Mito RV	5'-GACAATGGTTATCCGGGTTG-3'
Huh 7 Mito FW	5'-CCTGACTCCTACCCCTCA-3'
Huh 7 Mito RV	5'-ATCGGGTGATGATAGCCAAG-3'

FW, forward; RV, reverse; LDHA, human lactate dehydrogenase A; mito, mitochondria.

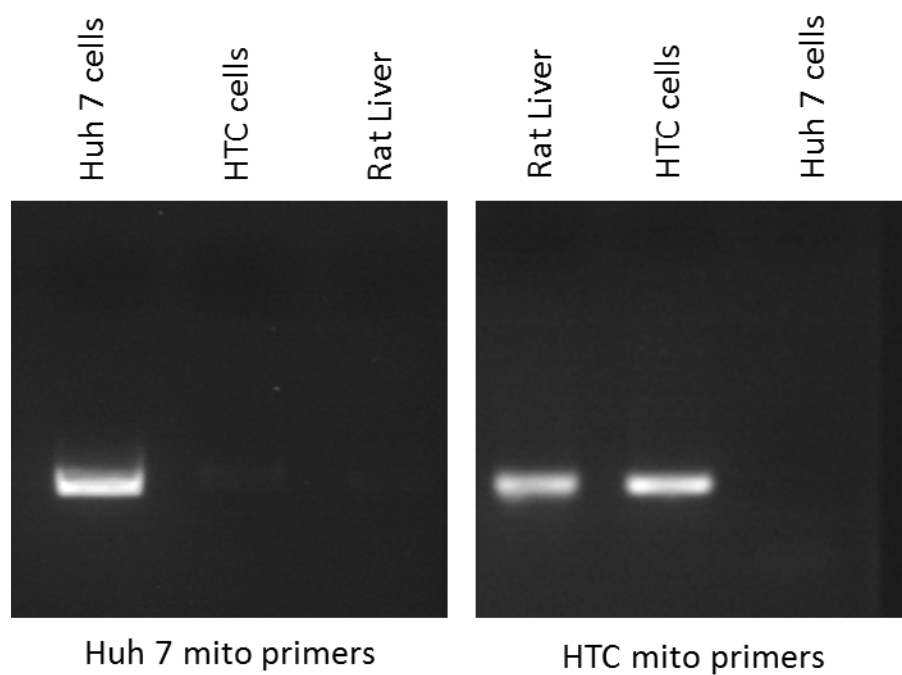


Figure 3.1. Primer specificity for mitochondrial DNA by amplification.

Primers were designed using Primer 3 and Primer-BLAST to amplify Huh7 mitochondrial DNA or HTC and rat liver mitochondrial DNA specifically. Cell mitochondrial DNA and rat liver cell DNA was used to determine specificity of primers.

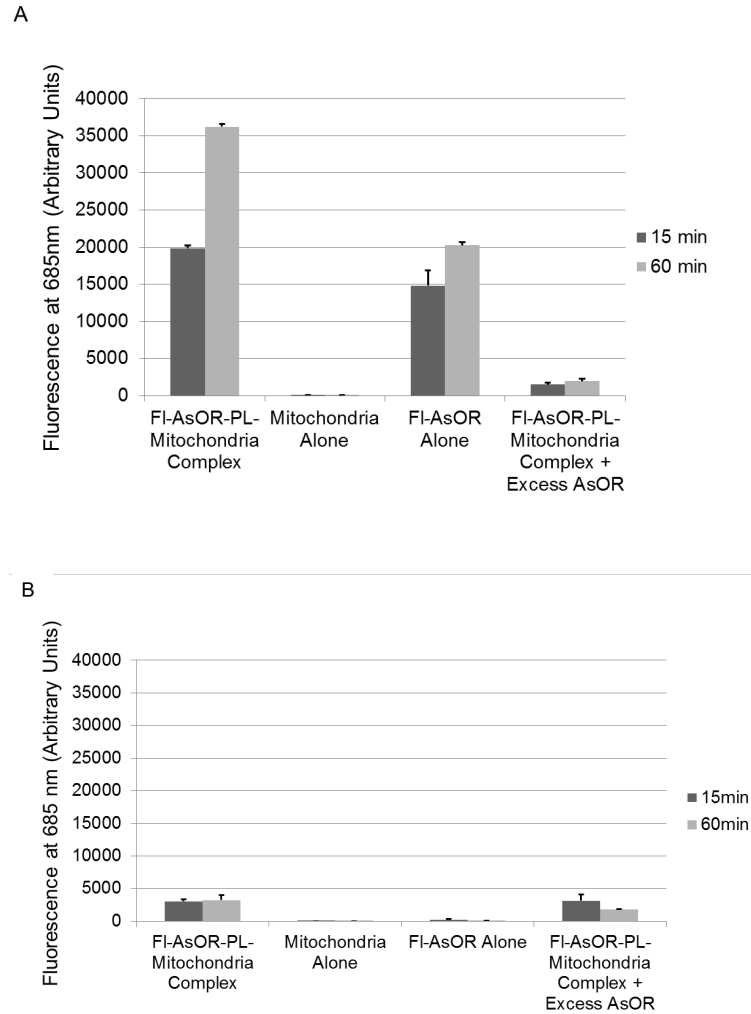


Figure 3.2. Uptake of FI-AsOR-PL–mitochondria complexes as measured by fluorescence.

Cells were incubated with FI-AsOR-PL–mitochondria complex, mitochondria alone, FI-AsOR alone or excess AsOR + complex at 37°C. At 15 min and 60 min, cells were collected and fluorescence levels measured by a fluorescence spectrophotometer. A, Huh 7 cells; B, SK Hep1 cells.

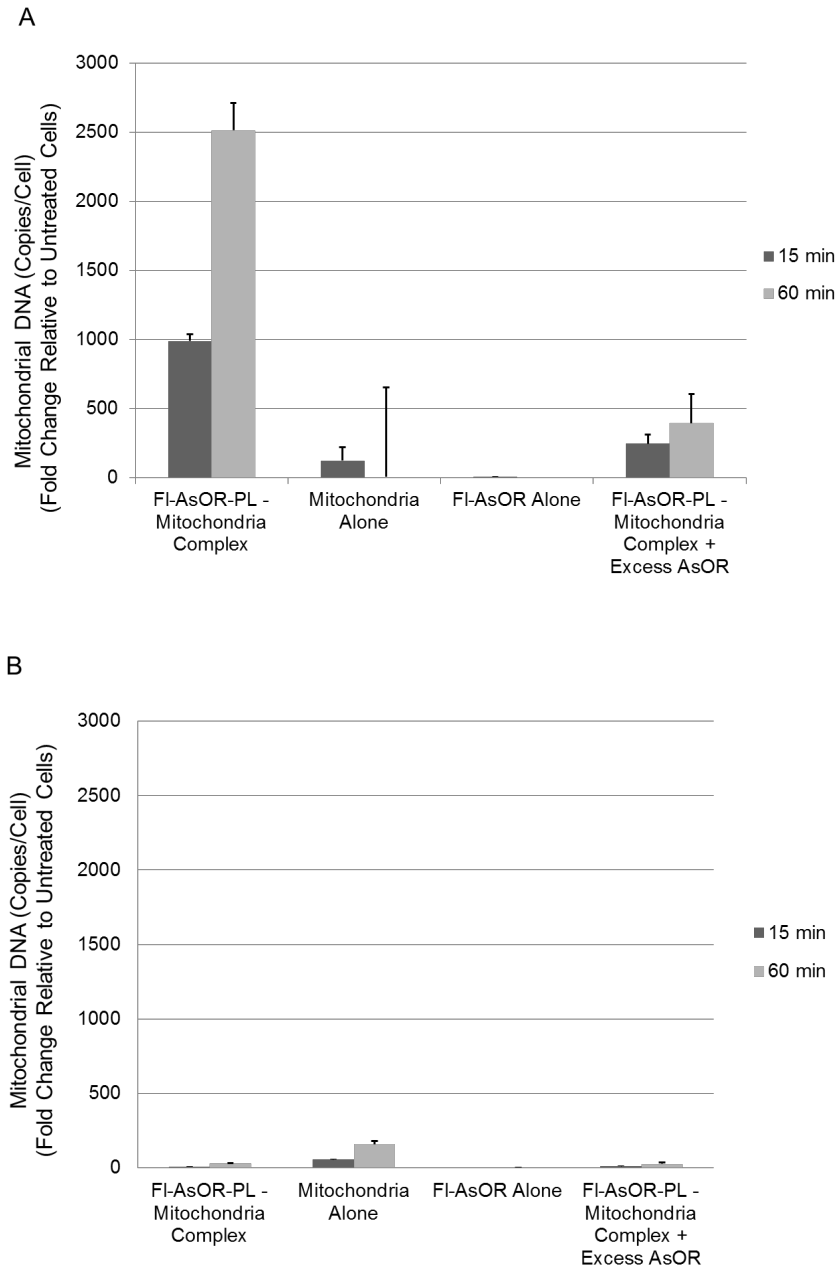


Figure 3.3. Uptake of FI-AsOR-PL–mitochondria complexes as measured by qPCR.

Cells were incubated with FI-AsOR-PL–mitochondria complex, mitochondria alone, FI-AsOR alone or excess AsOR + complex at 37°C. At 15 min and 60 min, cells were collected to measure HTC mitochondrial DNA in Huh 7 and SK Hep1 cells compared to untreated controls. A, Huh 7 cells; B, SK Hep1 cells.

CHAPTER 4: EFFECTS OF ENDOSOMAL DISRUPTION AGENTS ON INTRACELLULAR LOCALIZATION OF TARGETED MITOCHONDRIA

AsGR-mediated endocytosis is known to be a degradative pathway. Therefore, mitochondria internalized by Huh 7 cells were expected to be digested by lysosomal enzymes. Release of internalized mitochondria by hepatocytes into the cytoplasm should occur before exposure to lysosomal contents; otherwise internalization would not be helpful to develop a potential therapy for mitochondrial dysfunctional disorders. A number of microbes including viruses, and especially bacteria have evolved systems by which endosomes, into which they are endocytosed, are induced to rupture (See Chapter 1).

LISTERIOLYSIN O (LLO) FACILITATED ENDOSOMAL ESCAPE

Bacteria, *Listeria monocytogenes* produces a cholesterol-dependent toxin listeriolysin O (LLO) which gets activated at low pH and in reducing conditions that exist in endosomes, and induces pore formation in the cholesterol-containing membranes [317]. The pores result in influx of aqueous cytoplasmic content due to an osmotic gradient, and eventually rupture of endosomes resulting in escape of the bacteria, and endosomal contents into the cytoplasm [318, 319]. Because of its pH-dependent activity and rapid degradation in cytosol, cytotoxic effects of LLO are potentially reduced [271, 320]. LLO has been used as an endosomal escape agent alone [293] or in combination with lipid carriers [321, 322] and polymers [318]. Hence, we planned to use

LLO along with FI-AsOR-PL–mitochondria for targeted delivery to hepatocytes. Because it is known that the simultaneous binding of many AsGR is required to trigger endocytosis, it is possible that mitochondria and LLO could be targeted to the same endosome. Such a co-internalization event could result in endosomal escape and cytoplasmic delivery of targeted molecules to hepatocytes [293] (Figure 1.3).

AsOR-LLO CONJUGATES

To facilitate endosomal escape and intra-cytoplasmic delivery of mitochondria, advantage was taken of a bacterial protein, listeriolysin O (LLO), which is known to produce pores in endosomal membranes under the acidic and reducing conditions that exist in endosomes.

Conjugation of LLO to AsOR could result in targeting of the protein to hepatocytes. Co-internalization of the LLO-conjugate could result in rupture of endosomes, endosomal escape, and intracytoplasmic delivery of mitochondria (Figure 1.3). An irreversible linkage between AsOR and LLO might interfere with the ability of LLO to interact with the endosomal membranes after internalization to form pores. Therefore, an AsOR-LLO conjugate was prepared by chemically coupling AsOR to LLO using an SPDP cross-linker (N-succinimidyl 3-(2-pyridyldithio) propionate). The SPDP cross-linkers produce disulfide-containing linkages between protein molecules that can be cleaved later with reducing agents such as dithiothreitol (DTT) (Figure 4.1). These disulfide bonds would allow cleavage of AsOR and LLO under reducing conditions of endosomes after

internalization. Stability of the conjugate and release of LLO from AsOR under reducing conditions was demonstrated *in vitro*, Figure 4.2 and Table 4.1.

LLO is a membranolytic protein and could cause potential damage to outer membrane of isolated mitochondria leading to exposure of cytochrome c oxidase on inner membrane of mitochondria. Activity of cytochrome c oxidase was measured in mitochondria incubated with LLO and AsOR-LLO conjugate under different conditions to determine the damage to outer membrane of isolated mitochondria.

Activity of membranolytic proteins can also be measured with hemolytic assays where proteins are incubated with red blood cells (RBCs) to determine the membranolytic activity of proteins. Hemolytic assays were performed with LLO and AsOR-LLO conjugates under different conditions to determine their hemolytic activities.

Uptake assays were performed with and without AsOR-LLO conjugates for different time periods to determine change in internalization with time. To determine internalization was AsGR mediated; cells were pre-incubated with excess free AsOR to compete with internalization of FI-AsOR-PL–mitochondria complex. After uptake assays, internalization of the protein carrier, FI-AsOR-PL was determined by measuring fluorescence intensity in cells. Uptake of HTC mitochondria by human hepatocytes was measured by qPCR (See Chapter 3).

The specificity of AsGR-mediated internalization of mitochondrial complexes in presence of AsOR-LLO conjugates by hepatocytes was also determined by uptake assays in presence of colchicine and at lower temperature.

EFFECTS OF COLCHICINE TREATMENT

Colchicine is a toxic drug used to treat gout [323], pericarditis [324] and several other diseases. Colchicine treatment inhibits microtubule polymerization in cells by binding to tubulin [325]. Hence, colchicine induced impaired microtubule formation and restrained cytoskeletal movements in cells inhibits endocytosis [326]. Colchicine treatment of hepatocytes would allow recognition and binding of AsGs to AsGR on cell surface, but hindered endosomal formation would inhibit internalization of the ligand-receptor complexes. Therefore, cells were treated with colchicine prior to uptake of FI-AsOR-PL–mitochondria complexes with or without AsOR-LLO conjugates to determine non-specific association of FI-AsOR-PL–mitochondria complexes on cells surface.

EFFECTS OF LOW TEMPERATURES ON CELL MEMBRANES

A number of factors can affect cell membrane fluidity. Variations in temperature can cause changes in fluidity of cell membranes [327]. At low temperatures viscosity of plasma membranes increase and hence fluidity decreases which further hinders endosomal formation on cell surfaces. This allows recognition and binding of AsGs to AsGR on cell surface, but inhibits internalization of the ligand-receptor complexes. Henceforth, uptake assays of FI-AsOR-PL–mitochondria complexes with or without AsOR-LLO conjugates at low temperatures would help to determine non-specific association of FI-AsOR-PL–mitochondria complexes on hepatocytes surface.

To determine to localization of internalized AsOR-PL–mitochondria complexes by hepatocytes, GFP labeled mitochondria were used to make complexes with AsOR-PL.

After uptake of AsOR-PL–mitochondria complexes with or without AsOR-LLO conjugates, cells were labeled with early endosomal markers and localization of early endosomes and internalized mitochondria was observed under confocal microscope. Co-localization of early endosomes and GFP-labeled mitochondria in Z-axis of cell was also determined. Intensities of both early endosomal marker and GFP-labeled mitochondria in each stack of the image was measured and plotted against stack number of the image. Higher intensities from both labels in same stacks would determine co-localization of early endosomes and GFP-labeled mitochondria in Z-axis of cells.

METHODS

PREPARATION OF TARGETABLE LLO

Wild type (WT) listeriolysin O (LLO) was purified from a hypersecretor strain of *L. monocytogenes*, a generous gift from D. A. Portnoy, Stanford University, by a method described previously [328] with a modification that supernatants were concentrated using centrifugal devices (EMD Millipore Centricon® Plus-70 Centrifugal Filter Units, Membrane NMWL 30,000), washed with 3 L ice-cold distilled water, and concentrated to 400-600 ml. Supernatants were passed through a DEAE-Sephacel column, and purified LLO was washed, and then desalted with PD-10 columns (Sephadex G-25 M, Pharmacia Biotech). Purified LLO was aliquoted and stored at -20°C until further use. AsOR-LLO conjugates were synthesized using an SPDP cross-linker (Thermo Scientific) according to manufacturer's instructions. In brief, 1 mg of AsOR and LLO were dissolved in 12 µl of 20 mM SPDP and incubated separately at 25°C for 60 min. Preparations were desalted with PD-10 columns equilibrated with PBS. LLO-SPDP was reduced with DTT, and desalted on a PD-10 column equilibrated with PBS. Reduced LLO-SPDP (1 mg in 2.5 ml PBS) was mixed with AsOR-SPDP (1 mg in 2.5 ml PBS), and incubated for 18 h at 4°C to form AsOR-LLO conjugate. The conjugate was purified and concentrated using centrifugal devices (EMD Millipore Centricon® Plus-70 Centrifugal Filter Units, membrane NMWL (Nominal Molecular Weight Limit) 50,000). Final concentrations of proteins were measured using a Bio-Rad protein assay (BIO RAD) according to manufacturer's instructions. Purity and size of proteins was determined by electrophoresis on 10% SDS-PAGE. Gels were stained with 0.1%

Coomassie R250 (Sigma) in 10% acetic acid, 20% methanol and de-stained in 10% acetic acid, 20% methanol.

CYTOCHROME C OXIDASE ASSAY

LLO is known to cause pores in membranes, and because mitochondria are membrane-limited organelles, we sought to determine whether LLO would damage mitochondrial membranes. Effects on the integrity of the outer membrane of isolated mitochondria were assessed by measuring cytochrome C oxidase activity. LLO and AsOR-LLO conjugate were incubated separately with isolated HTC mitochondria with or without DTT at pH 7.5 and pH 5.6 for 45 min at 37°C. Cytochrome c oxidase activity was assayed by a kit (CYTOCOX1, Sigma-Aldrich) and the % cytochrome C oxidase activity relative to untreated controls was calculated according to manufacturer's instructions.

HEMOLYSIS

While, the gel showed cleavage under conditions known to exist in endosomes, a better measure of membranolytic activity is to measure hemolysis. To determine hemolytic activity, [293, 329], varying concentrations of LLO and AsOR-LLO conjugate were incubated, with or without DTT, with approximately 5 million human RBCs in 10 µl PBS separately at pH 7.4 and pH 5.6 for 30 min at 37°C. Effects of cholesterol on hemolytic activity were determined as described previously [330]. Samples were spun at 3000 rpm for 5 min, and absorbance of supernatants measured at 540 nm. The amounts of protein required for 50% hemolysis (50% complement hemolytic (CH50) activity) were calculated [331]. Assays were performed in 4 independent replicates, and the results are expressed as percent hemolysis relative to hemolysis of RBCs in distilled water.

CELL CULTURE

To create GFP-labeled mitochondria, HTC cells were transfected with pAcGFP1-Mito plasmid (Clontech Laboratories) using lipofectamine (Life Technologies) according to manufacturer's instructions. pAcGFP1-Mito plasmid encodes a mitochondrial targeting sequence (derived from the precursor of subunit VIII of human cytochrome C oxidase) fused to N-terminus of green fluorescent protein (GFP) from *Aequorea coerulescens* (AcGFP). Fluorescence-activated cell sorting (FACS) was used to separate GFP-labeled cells to make a stable cell line (Figure 4.8). HTC mito-GFP cells were maintained in DMEM supplemented with antibiotic/antimycotic solution, 10% FBS and 1.5 mg/ml G418 (Calbiochem). GFP-labeling was determined using MitoTracker RED FM (Molecular Probes - Life Technologies) according to the manufacturer's instructions. In brief, 200 nM MitoTracker red probe in Opti-MEM I medium (Invitrogen) was incubated with HTC mito-GFP cells for 30 min. Cells were washed twice PBS, fixed with 4% paraformaldehyde and washed 4 times with PBS. Labeled cells were mounted in ProLong® Gold reagent (Life Technologies), and used for fluorescent microscope imaging.

UPTAKE ASSAY

Uptake assays were performed as described in Chapter 3, Methods. Mitochondria were isolated from donor cells (HTC or HTC mito-GFP cells). Uptake assays were conducted at 37°C or 4°C in DMEM, 2.8 mM Ca^{2+} [312] to which was added 25 µl/ml FI-AsOR-PL–mitochondria complex, 25 µl/ml FI-AsOR-PL–mitochondria complex + 0.15 µg/ml AsOR-LLO conjugate, 25 µl/ml FI-AsOR-PL–mitochondria complex + 200 µg/ml AsOR (100-

fold molar excess added 4 min prior to uptake) or 25 μ l/ml FI-AsOR-PL–mitochondria complex + 0.15 μ g/ml AsOR-LLO conjugate + 200 μ g/ml AsOR (100-fold molar excess added 4 min prior to uptake). Assays were repeated with 3 independent replicates.

To determine the effects of colchicine on mitochondrial uptake, cells were incubated with 1 μ M colchicine for 2 h prior to uptake and during the uptake assay [326]. To determine the effects of low temperature on mitochondrial uptake, studies were also performed at 4°C using ice cold phosphate- and bicarbonate-free DMEM.

CONFOCAL MICROSCOPY

To determine the intracellular localization of targeted mitochondria in cells, Huh 7 cells were plated at 50% confluence, on sterile cover slips in 6-well tissue culture plate (Sigma). Cells were washed with PBS (Mg^{2+} - and Ca^{2+} -free) and maintained in supplement-free phosphate-free DMEM with high glucose (Life Technologies, #11971) for 16 h followed by exposure to AsOR-PL-mito-GFP complex, mito-GFP, and AsOR-PL-mito-GFP complex + AsOR-LLO conjugate separately for 2 h at 37°C. Cells were washed with EDTA-PBS and maintained in DMEM supplemented with antibiotic/antimycotic solution, and 10% FBS for 6 h. Cells were fixed with 4% paraformaldehyde for 30 min, and permeabilized with 0.25% Triton X-100 (Sigma) in PBS for 10 min followed by blocking solution (1% goat serum, 5% BSA, 0.3 M glycine) for 1 h at 25°C. Cells were incubated with anti-EEA1 antibody [1G11] (early endosome marker from Abcam Inc, #ab70521) overnight at 4°C. Alexa fluor 594 goat anti-mouse (Life Technologies) secondary antibody was added for 1 h. Nuclei were stained with DAPI (Invitrogen) for 20 min. Cells were mounted and imaged using a confocal

microscope, and images were analyzed with Image J for the presence of early endosomes (red), mitochondria (green), and nuclei (DAPI), and early endosomes and mitochondria merged (yellow).

To determine the localization of endosomes and mitochondria in the Z-plane, areas were randomly selected on the images taken by confocal microscopy. For each selected area, GFP and Alexa fluor 594 intensities were measured from each slice of Z-stacks of the image, and plotted together against the slice number of the image. High fluorescence intensity of both GFP and Alexa fluor 594 in close proximity were considered to indicate co-localization of HTC mitochondria and early endosomes in Z-plane.

RESULTS AND DISCUSSION

AsOR-LLO conjugates were made using SPDP cross-linkers (Figure 4.1). Proteins alone and conjugate were run on SDS-PAGE to determine approximate masses and purity. Figure 4.2 shows that AsOR runs around as 37 kDa and LLO around 50 kDa. The AsOR-LLO conjugate preparation did not contain free LLO or AsOR, but did have two bands, one at about 74 kDa, a position expected for AsOR-LLO. The higher mass band at about 90 kDa could be an LLO-dimer. Exposure of the conjugate preparation to reducing conditions, i.e. DTT, caused both bands to disappear, and the return of bands corresponding to AsOR and LLO, Figure 4.2. This showed that an AsOR-LLO conjugate was formed which was cleavable under reducing conditions.

Cytochrome C assays with LLO show some damage to outer membrane of mitochondria at pH 7.5 which increased at pH 5.6. Damage became significantly high in presence of DTT. Whereas AsOR-LLO conjugate did not affect the mitochondrial outer membrane and expose cytochrome c on the inner membrane of mitochondria, Figure 4.3 at pH 7.5 or 5.6 in absence of DTT. This suggested that AsOR-LLO conjugates would not cause damage to outer membrane of mitochondria while performing uptake assay. LLO should be released in an endosomal environment where it could facilitate the release of complexes in cytoplasm.

Using hemolysis as a measure of membrane-disruptive activity, LLO alone at pH 5.6 resulted in hemolysis of 32.8% of red blood cells. This increased to 88.6% in the presence of a reducing agent, DTT ($p < 0.0001$). In contrast, AsOR-LLO conjugate had no hemolytic activity in the absence of DTT at pH 7.4 or pH 5.6, but had 32.7% activity at pH 7.4, and 55.3% hemolysis at pH 5.6 in the presence of DTT. Cholesterol inhibited

the activity of both LLO and LLO-AsOR complex, Table 4.1, which was consistent with membranolytic properties of LLO. This further suggested that cleavage of LLO from AsOR-LLO conjugate was required for its membranolytic activity.

To determine whether the AsOR-LLO conjugate could affect intra-cytoplasmic delivery of mitochondria to hepatocytes, uptake assays were performed with Huh 7 cells and SK Hep1 cells at 37°C with or without AsOR-LLO conjugates. After incubation with FI-AsOR-PL-mitochondria complex alone, fluorescence levels in Huh 7 cells were 13,400 units at 15 min which increased to more than 30,000 units at 120 min, Figure 4.4A. However, co-administration of AsOR-LLO conjugate with complexed mitochondria led to an increase in fluorescence levels in Huh 7 cells from 13,000 units at 15 min to approximately 50,000 units at 120 min ($p < 0.0001$). This suggested that internalization of protein carrier was time-dependent, and increased in presence of AsOR-LLO. Pre-incubation of a large molar excess of AsOR for competition resulted in a >90% decrease in fluorescence in Huh 7 cells exposed to complexed mitochondria with or without AsOR-LLO. SK Hep1 cells did not show significant levels of fluorescence under any condition at any time point, Figure 4.4B which further suggested that internalization of protein carrier was AsGR mediated.

In addition to increased fluorescence levels, co-administration of AsOR-LLO conjugate with complexed mitochondria also resulted in increased HTC mitochondrial DNA levels in Huh 7 cells from 110-fold (approximately 1-2 HTC mitochondria per cell) at 15 min to approximately 23,800-fold (approximately 136-343 HTC mitochondria per cell) over untreated controls approximately at 120 min, Figure 4.5A. However, incubation of FI-AsOR-PL-mitochondria complex alone led to increased HTC mitochondrial DNA levels

from 690-fold (approximately 4-10 HTC mitochondria per cell) at 15 min to 7500-fold (approximately 43-107 HTC mitochondria per cell) over untreated controls at 120 min in Huh 7 cells ($p < 0.001$). This suggested that similar to the protein carrier, internalization of mitochondria was time-dependent and increased in presence of AsOR-LLO. Pre-incubation of excess free AsOR decreased HTC mitochondrial DNA levels by >75% in Huh 7 cells exposed to complexed mitochondria with or without AsOR-LLO. No significant levels of HTC mitochondrial DNA were found in SK Hep1 cells under any condition, Figure 4.5B. This further suggested that internalization of complexes was AsGR mediated.

For further confirmation that the observed levels of HTC mitochondrial DNA in Huh 7 cells had resulted from entry into the cells by receptor-mediated endocytosis, cells were pre-treated with colchicine for 120 min. Colchicine inhibits endocytosis and hinders internalization. The amount of HTC mitochondrial DNA associated with these cells was, 2,100-fold (approximately 13-29 HTC mitochondria per cell) over untreated controls at 120 min Figure 4.6, which was significantly lower than in Huh 7 cells not pre-treated with colchicine ($p < 0.00001$). This suggested that higher levels of mitochondrial DNA observed in Huh 7 cells exposed to FI-AsOR-PL-mitochondria complexes and AsOR-LLO conjugates in non-colchicine treated cells were not because of 'non-specific' association.

In addition, endocytosis is also inhibited at 4°C because of decreased fluidity of plasma membrane. Uptake in Huh 7 cells at 4°C showed no significant levels of HTC mitochondrial DNA at any time point, Figure 4.7. This further suggested that higher levels of mitochondrial DNA observed in Huh 7 cells after uptake at 37°C were internal.

To determine the localization of internalized mitochondria, a cell line stably expressing GFP-labeled mitochondria, HTC mito-GFP cells were used (Figure 4.8) (See Chapter 1). Cells were stained with MitoTracker RED, which intercalates between intermembrane space of mitochondria. Co-localization of mito-tracker red staining mitochondria and GFP in HTC mito-GFP cells showed that mitochondria were labeled with GFP (Figure 4.9). HTC mito-GFP cells were used as source for GFP labeled mitochondria. GFP-labeled mitochondria were isolated, and complexes were with AsOR-PL were made as described in Chapter 2, Methods. AsOR-PL–mitochondria complexes and controls were incubated for 120 min with Huh 7 cells. Six h later, cells were stained with an endosomal marker (EEA1- Alexa Fluor 594). Huh 7 cells incubated with GFP-labeled HTC mitochondria showed endosomal (red) staining, Figure 4.10A1, but no GFP staining was observed, Figure 4.10B1. Cells incubated with AsOR-PL–mitochondria complex showed endosomal staining; Figure 4.10A2, but little GFP, Figure 4.10B2. Most of the GFP-stained structures were overlapping Alexa Fluor 594 in the merged view (yellow), Figure 4.10D2, suggesting co-localization of mitochondria and endosomes. Co-localization of GFP and Alexa Fluor 594 was supported by fluorescence plot intensities in Z-axis of cell images from random fields, Figure 4.11. Higher intensities of both GFP and Alexa Fluor 594 in same stacks of image suggest that both GFP-labeled mitochondria and endosomes co-localize. Cells incubated with both AsOR-PL–mitochondria complex and AsOR-LLO conjugate also showed endosomal vesicles, Figure 4.10A3, and many GFP- and Alexa Fluor 594-stained punctate structures, Figure 4.10D3. However, most GFP structures remained green in the merged view, i.e. did not overlap with early endosomes suggesting the presence of

mitochondria not co-localized with endosomes. These data supported conclusion that co-administration of AsOR-LLO and complexed mitochondria resulted in escape of HTC mitochondria from endosomes. Internalization was not found uniform in all cells, which might be because of differential expression of AsGR in hepatocytes based on many factors (See Chapter 1 and 2).

FIGURES AND TABLES

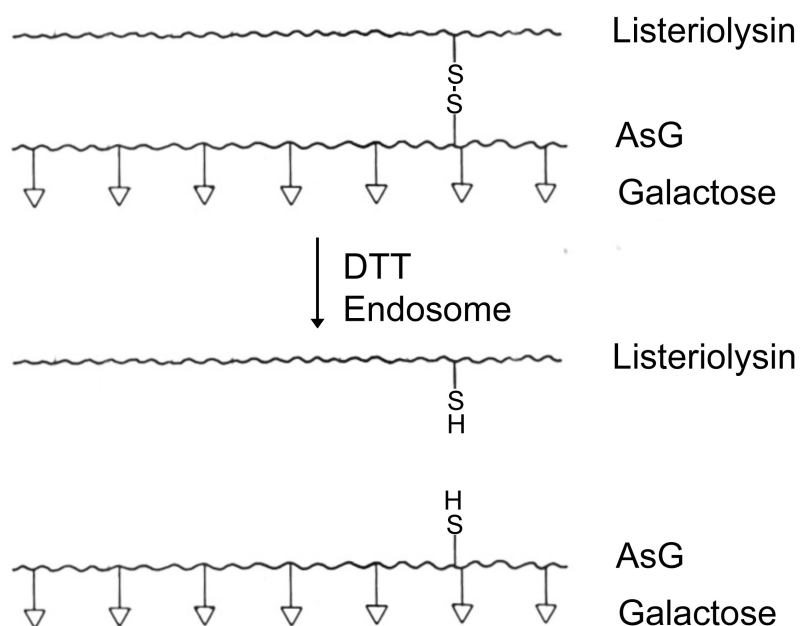


Figure 4.1. A diagram of a targetable AsG–LLO conjugate cleavable under reducing conditions.

AsOR and LLO were coupled with a disulfide linker to form an AsOR-LLO conjugate cleavable under low pH and reducing environment of endosomes.

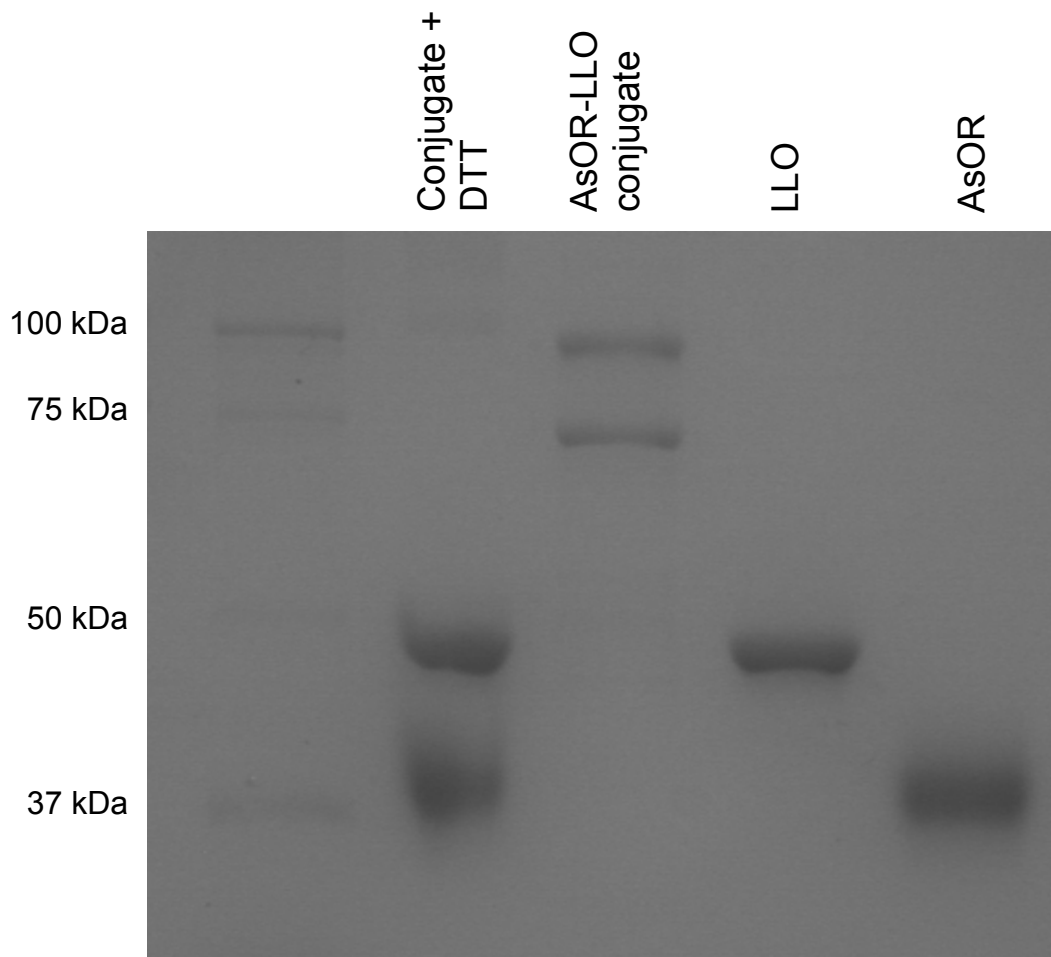


Figure 4.2. SDS-PAGE of AsOR-LLO conjugate and components stained with Coomassie Brilliant Blue.

Proteins were run on a 10% SDS-PAGE and stained with Coomassie blue. Lanes: 1, AsOR-LLO conjugate reduced with DTT; 2, AsOR-LLO conjugate; 3, LLO; 4, AsOR.

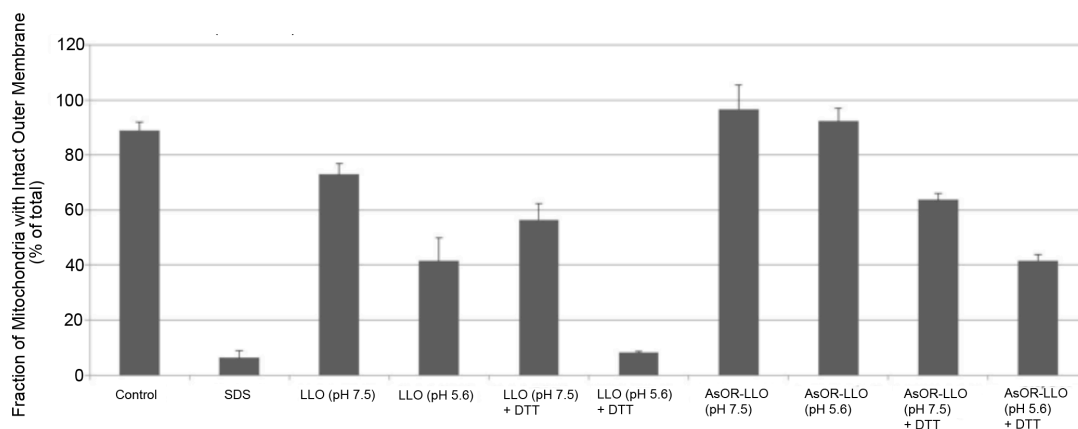


Figure 4.3. Cytochrome C oxidase assay.

Mitochondria were incubated with LLO and AsOR-LLO conjugate at pH 7.5 or 5.6, with or without DTT for 45 min, and damage to outer membrane of mitochondria was measured by quantitation of the amount of ferrocytochrome c oxidized to ferricytochrome c relative to untreated mitochondria.

Table 4.1. Hemolytic Activity of LLO and AsOR-LLO Conjugate.

		HEMOLYSIS (% of that in water)							
		pH 7.4				pH 5.6			
	Protein (μg)	PBS	DTT (5 mM)	Cholesterol (10 μg)	DTT (5 mM) + cholesterol (10 μg)	PBS	DTT (5 mM)	Cholesterol (10 μg)	DTT (5 mM) + cholesterol (10 μg)
LLO	0.001	0.00	0.09	0.34	6.69	1.30	1.03	0.10	0.01
	0.01	0.12	10.23	0.22	6.29	16.03	17.58	0.89	0.25
	0.1	0.87	68.69	0.00	0.72	32.81	88.61	0.00	0.00
AsOR-LLO	0.6	0.00	5.96	0.96	1.35	0.00	2.81	0.00	0.00
Conjugate	1	0.00	13.99	0.11	0.80	0.00	12.49	0.00	0.00
	1.5	0.00	32.67	0.00	0.98	0.00	55.34	0.00	0.00

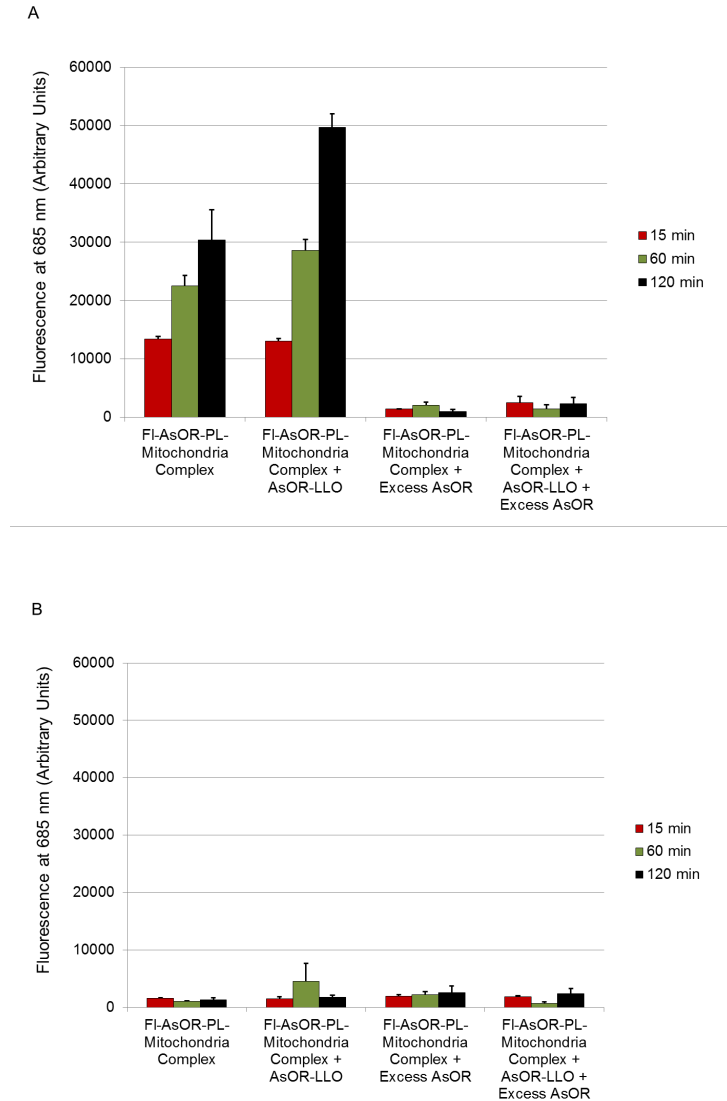


Figure 4.4. Changes in fluorescence after co-administration of complexed mitochondria and AsOR-LLO conjugates in cells.

Cells were incubated separately with FI-AsOR-PL–mitochondria complex, complexed mitochondria and AsOR-LLO conjugates, excess AsOR + complexed mitochondria or excess AsOR + complexed mitochondria + AsOR-LLO conjugates at 37°C. At 15 min, 60 min and 120 min, cells were collected to measure fluorescence. A, Huh 7 cells; B, SK Hep1 cells.

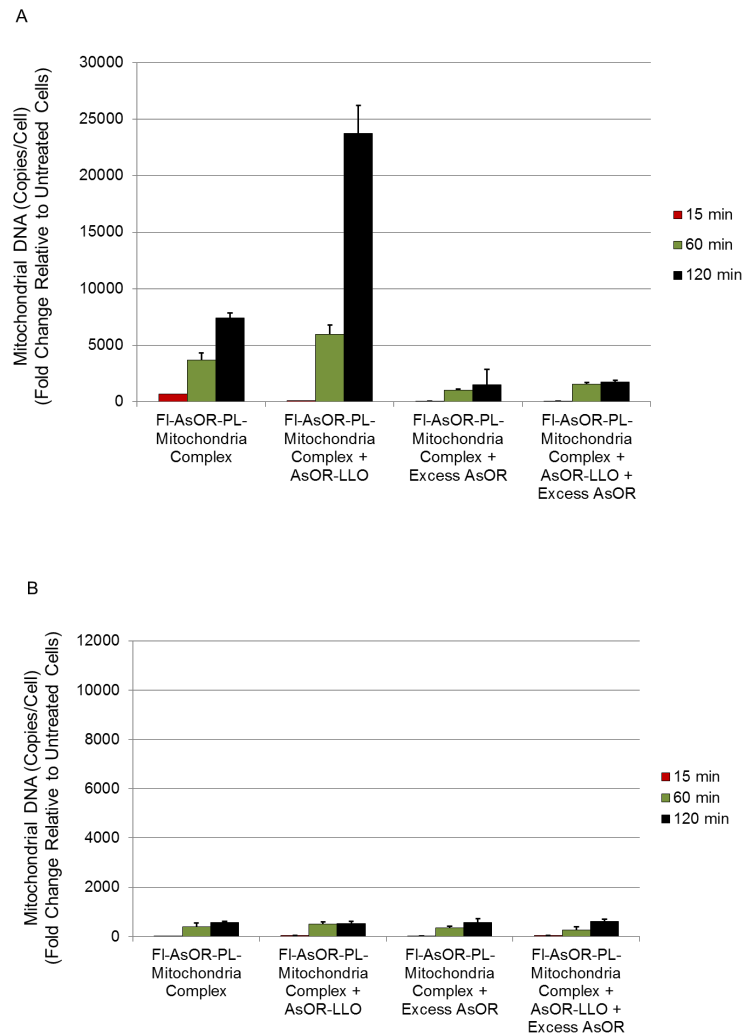


Figure 4.5. HTC mitochondrial DNA levels in cells after exposure to complexed mitochondria and AsOR-LLO conjugates.

Cells were incubated separately with FI-AsOR-PL–mitochondria complex, complexed mitochondria and AsOR-LLO conjugates, complexed mitochondria + excess AsOR, or complexed mitochondria + AsOR-LLO conjugates + excess AsOR at 37°C. At 15, 60 and 120 min, cells were collected and HTC mitochondrial DNA levels measured by qPCR compared to untreated controls. A, Huh 7 cells; B, SK Hep1 cells.

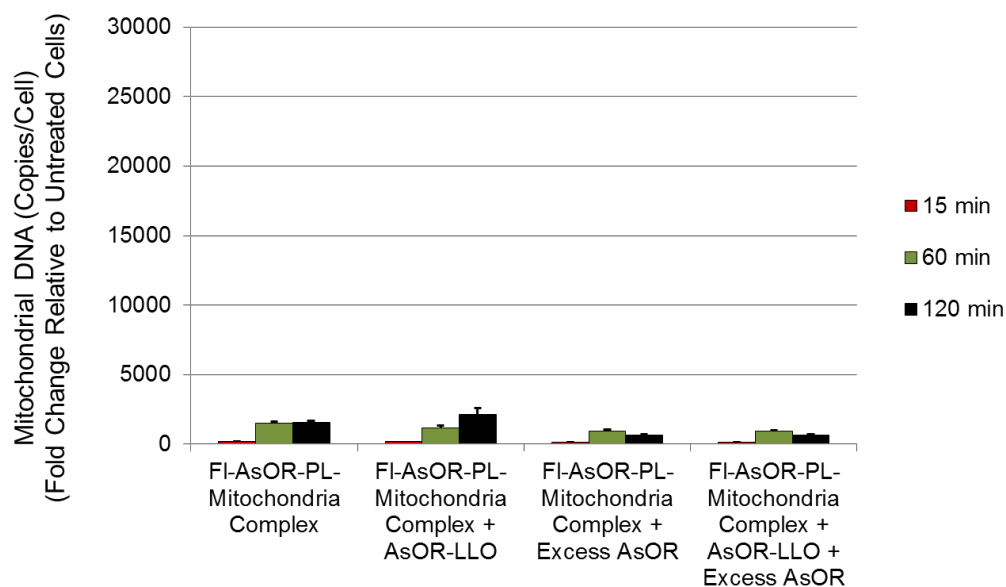


Figure 4.6. HTC mitochondrial DNA levels in colchicine-treated Huh 7 cells after exposure to complexed mitochondria and AsOR-LLO conjugates.

Huh 7 cells were treated with 1 μ M colchicine for 2 h prior and during exposure to FI-AsOR-PL-mitochondria complex, complexed mitochondria and AsOR-LLO conjugates, complexed mitochondria + excess AsOR or complexed mitochondria + AsOR-LLO conjugates + excess AsOR at 37°C. At 15, 60 and 120 min, cells were collected and HTC mitochondrial DNA levels measured by qPCR compared to untreated controls.

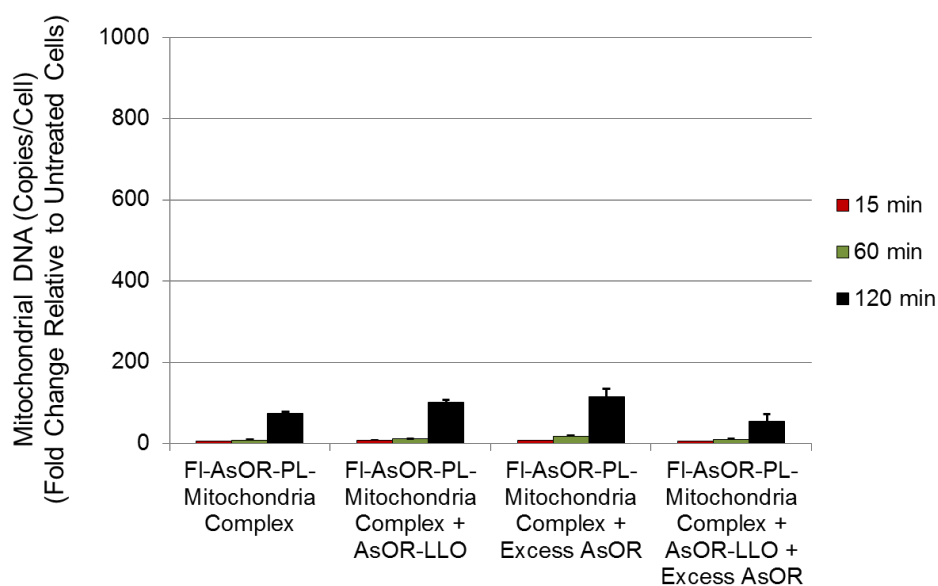


Figure 4.7. HTC mitochondrial DNA levels in Huh 7 cells at 4°C after exposure to complexed mitochondria and AsOR-LLO conjugates.

Huh 7 cells were incubated separately with FI-AsOR-PL–mitochondria complex, complexed mitochondria and AsOR-LLO conjugates, complexed mitochondria + excess AsOR or complexed mitochondria + AsOR-LLO conjugates + excess AsOR at 4°C. At 15, 60 and 120 min, cells were collected and HTC mitochondrial DNA measured by qPCR compared to untreated controls.

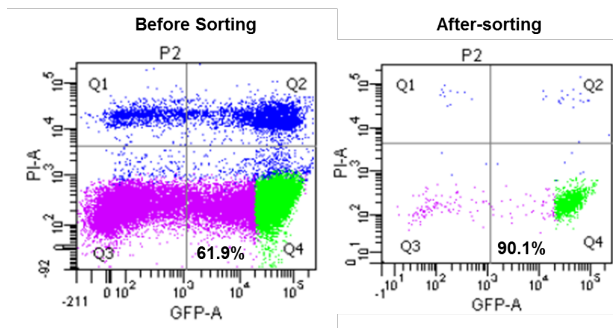


Figure 4.8. Isolation of an HTC mito-GFP cell line by fluorescence-activated cell sorting (FACS).

HTC cells stably expressing GFP-labeled mitochondria were sorted with FACS to establish an HTC mito-GFP cell line which was subsequently maintained in 1.5 mg/ml G418 media for selection.

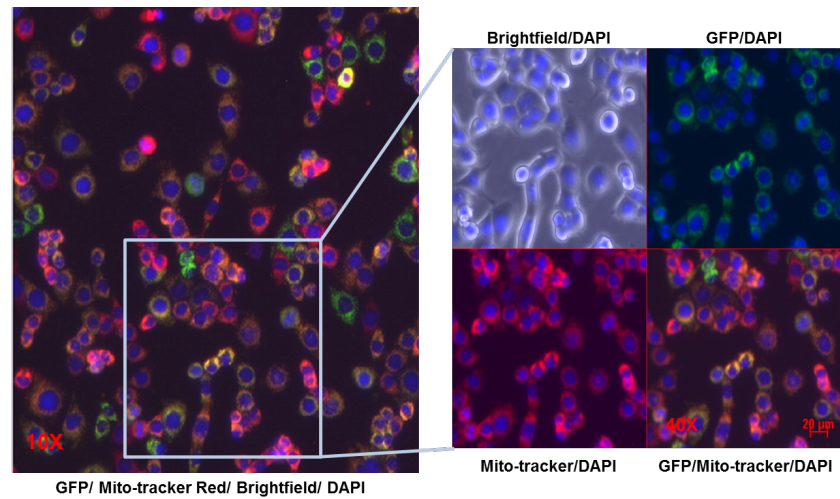


Figure 4.9. HTC Mito-GFP cells stained with Mito-Tracker Red.

HTC mito-GFP cells were incubated with MitoTracker red probe for 30 min, washed, fixed with paraformaldehyde and examined under a fluorescent microscope.

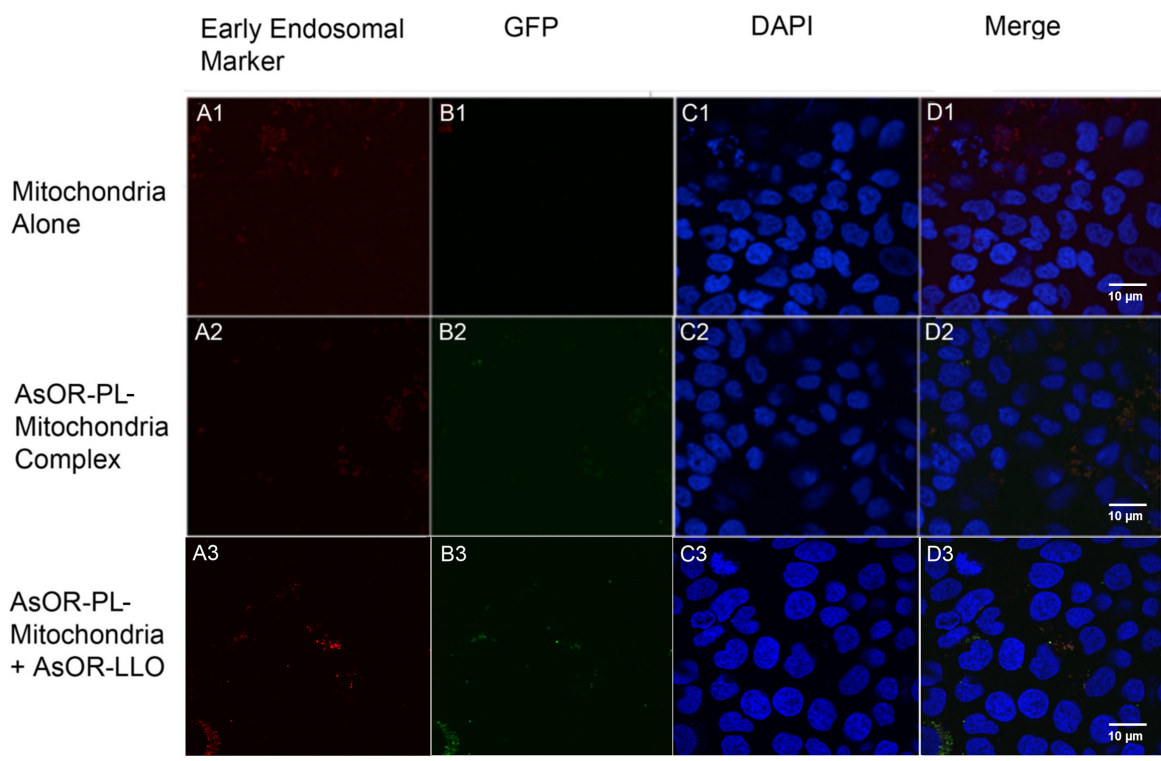


Figure 4.10. Localization of early endosomes and GFP-labeled HTC mitochondria by confocal fluorescence microscopy.

Huh 7 cells were incubated separately with GFP-mitochondria alone, AsOR-PL–GFP-mitochondria complex, or co-administered with complexed GFP-mitochondria and AsOR-LLO conjugates at 37°C for 2 h. Cells were washed with PBS and maintained in DMEM for 6 h before fixing with paraformaldehyde and staining for early-endosome marker EEA1. Cells were imaged under confocal fluorescence microscope. Panels A1–A3, endosomal marker (anti-EEA1-Alexa 594, red); B1–B3, GFP (green); C1–C3, DAPI nuclei (blue); and D1–D3, merged.

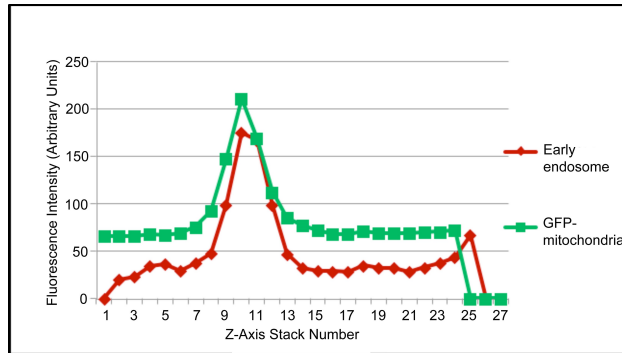


Figure 4.11. A plot of fluorescence intensities of confocal microscopic images versus stack number.

A plot of fluorescence intensities of early endosomal marker EEA1 and GFP-mitochondria, and stack number of confocal microscopic images of Huh 7 cells, 6 h post incubation with AsOR-PL-mitochondria-GFP complexes at 37°C.

CHAPTER 5: ASSESSMENT OF FUNCTION AND STABILITY OF MITOCHONDRIA TARGETED TO HEPATOCYTES LACKING MITOCHONDRIA

Being metabolically highly active, liver cells require high number of mitochondria to meet their energy needs. Damage to mitochondria in liver cells can result in severe liver dysfunction and eventually liver failure. The common effect of most mitochondrial disorders is insufficient energy production. Delivery of healthy and functional mitochondria to hepatocytes with damaged mitochondria may allow the cells to recover from such damage.

The objective of this study was to determine whether healthy and functional mitochondria could be delivered to hepatocytes with damaged mitochondria. Previous data, in this study, suggested that mitochondria can be internalized by hepatocytes through AsGR mediated endocytosis and escape from endosomes can be facilitated with hemolytic activity of LLO. Delivery of mitochondria to hepatocytes would be useful only if internalized mitochondria are stable and functional in hepatocytes, and could provide survival advantage to affected cells. A model (mitochondrial DNA free Huh 7-mito (-) and SK Hep1-mito (-) cells) for mitochondrial hepatopathies was developed by treating Huh 7 and SK Hep1 cells with ddC to deplete mitochondrial DNA levels in cells (See Chapter 1), Figure 5.1. Assays were performed to determine whether mitochondria could be targeted to Huh 7-mito (-) and SK Hep1-mito (-) cells.

Mitochondrial damage caused decreased energy levels in Huh 7-mito (-) and SK Hep1-mito (-) cells which would affect other processes and activities of cells. In order to

determine if cells can still recognize and internalize AsGs, uptake assays with FI-AsOR were performed.

Because of the lack of mitochondria, these cells required special supplemental media containing compensatory nutrients to permit survival, Figure 5.2. Withdrawal of the required special supplemental media containing compensatory nutrients results in death of the cells. Therefore, survival of cells in supplement-free media after exposure to complexed mitochondria could indicate appropriate mitochondrial function after internalization. Survival in mitochondria free cells was observed for long periods of time after exposure to FI-AsOR-PL–mitochondria complexes with or without AsOR-LLO conjugates and other controls (See Chapter 3), Stability of mitochondrial DNA levels in Huh 7-mito (-) and SK Hep1-mito (-) cells for long periods of time was also observed to determine long term stability of internalized mitochondria.

Functional stability of mitochondria in Huh 7-mito (-) and SK Hep1-mito (-) cells could be determined by determining the mitochondrial respiration in targeted cells. Since endogenous mitochondria of cells have depleted mitochondrial DNA and hence non-functional, stable mitochondrial respiration in mitochondrial DNA free cells exposed to FI-AsOR-PL–mitochondria complexes with or without AsOR-LLO conjugates and other controls could help in determining functional status of delivered mitochondria.

MITOCHONDRIAL RESPIRATION

Mitochondria undergo aerobic respiration which requires oxygen in order to generate ATP [332]. The outer membranes of mitochondria contain many complexes of integral membrane proteins that form channels through which a variety of molecules and ions move in and out of the mitochondria [333]. The inner membranes of mitochondria contain five complexes of integral membrane proteins as part of respiratory complex; NADH dehydrogenase (Complex I); succinate dehydrogenase (Complex II), cytochrome c reductase (Complex III; also known as the cytochrome b-c1 complex), cytochrome c oxidase (Complex IV); ATP synthase (Complex V) [334, 335]. Complexes I, III and IV constitutes the electron transport chain (ETC) of mitochondria [336, 337] and where stepwise shuttling of electrons from NADH (or FADH₂) to oxygen molecules with the help of two freely-diffusible molecules, ubiquinone and cytochrome c [338], form (with the aid of protons) water molecules [339]. ETC couples energy released by electron transfer to the pumping of protons (H⁺) from the matrix to the intermembrane space. The gradient of protons formed across the inner membrane by this process of active transport stores high amounts of intermediate energy [340]. The protons can flow back down this gradient only by re-entering the matrix through ATP synthase (complex V) in inner membrane [341]. The energy released as these protons flow down their gradient is coupled to the synthesis of ATP [342, 343] and the process is called oxidative phosphorylation (or OXPHOS) [344]. This allows the production of large amount of ATP supply of cells by mitochondria. Measurement of oxygen consumption rates (OCR) from cells or isolated mitochondria is useful to evaluate the mitochondrial stress, dysfunction and disease since ADP-dependent oxygen consumption directly reflects coupled

respiration or OXPHOS [345]. Several valuable methods are available in research to measure OCR in mitochondria like set of ETC complex inhibitors [346].

Several types of respiratory inhibitors for complexes of ETC in mitochondria have been identified. Inhibitors act by binding one or more electron carriers, preventing electron transport directly. An inhibitor may completely block electron transport by irreversibly binding to a binding site (example cyanide [347]) or bind competitively (example rotenone [348]). Injections of these inhibitors to cells result in inhibition of different complexes of ETC and hence OCR.

For mitochondrial stress assays, OCR is measured before and after the addition of a series of three different inhibitors to cells or isolated mitochondria. OCR measured before addition of inhibitors represents the basal respiration of cells.

Initially, addition of oligomycin, a complex V inhibitor, results in blocking of proton channels, and hence results in decreased electron flow [349]. This results in decreased OCR, which can be used to calculate ATP-linked respiration (by subtracting the oligomycin rate from baseline cellular OCR) and proton leak respiration (by subtracting non-mitochondrial respiration from the oligomycin rate).

Addition of a protonophore, carbonyl cyanide-p-trifluoromethoxyphenyl-hydrazon (FCCP), collapses the inner membrane gradient [350], and disrupts the mitochondrial inner membrane potential. This allows free flow of electrons across the membrane and ETC to function at its maximal rate increasing OCR to maximum in mitochondria. This allows calculating maximal respiratory capacity of mitochondria by subtracting non-mitochondrial respiration from the FCCP rate.

Lastly, addition of antimycin A and rotenone, inhibitors of complex III and I [351, 352] shuts ETC function down, and leads to complete inhibition of oxygen consumption by mitochondria. Resulting OCR is from non-mitochondrial respiration. Mitochondrial reserve capacity can be estimated by subtracting basal respiration from maximal respiratory capacity. These fluctuations in OCR on addition of these inhibitors determine the mitochondrial stress and disorders.

Mitochondrial stress assays can be used to measure mitochondrial functional status in cells.

METHODS

PREPARATION OF MITOCHONDRIA (-) CELLS

To create a model of cells lacking mitochondria, Huh 7 and SK Hep1 cells were seeded at 20% confluence, and then exposed to 10 μ M 2', 3'-dideoxycytidine (ddC) (Sigma-Aldrich #5782) for 3 weeks [120]. Cells were maintained in DMEM supplemented with antibiotic/antimycotic solution, 10% dialyzed FBS, 2 mM L-glutamine, 100 mg/ml sodium pyruvate (Invitrogen), and 50 mg/ml uridine (Sigma) [299]. Mitochondrial DNA levels were determined with qPCR periodically and cells lacking detectable mitochondrial DNA were considered to be mito (-). Huh 7-mito (-) and SK Hep1-mito (-) cells were frozen at -80°C until needed.

CELL PROLIFERATION ASSAY

Huh 7-mito (-) and SK Hep1-mito (-) cells were plated at 90% confluence, 2 days before uptake assay on 24-well tissue culture plate (Sigma). Equal numbers of Huh 7 and SK Hep1 cells were plated on 6-well tissue culture plates (Sigma). Cells were washed with PBS (Mg^{2+} - and Ca^{2+} -free) and maintained in supplement-free, phosphate-free DMEM with high glucose (Life Technologies, #11971) for 2 h followed by exposure to complexed mitochondria or controls for 2 h. Media containing complexed mitochondria were removed, and cells were washed with PBS (Mg^{2+} - and Ca^{2+} -free), and then maintained in supplement-free DMEM with antibiotic/antimycotic solution, and containing 1% dialyzed FBS. DNA levels were determined at various time points using a CyQUANT Cell proliferation assay kit (Molecular probes, Life technologies) according to manufacturer's instructions. Standard curves of DNA levels as a function of

fluorescence at 520 nm were generated, and used to calculate DNA concentrations. Experiments were conducted in triplicate, and repeated twice. Results are expressed as mean \pm standard error of total cellular DNA, (ng/well) per group. Cell cultures were not split at any time.

MITOCHONDRIA RESPIRATION ASSAYS

Huh 7-mito (-) cells were plated at 90% confluence in XF24 cell culture microplates (Seahorse Bioscience) 2 d before uptake assays. Cells were washed with PBS (Mg^{2+} - and Ca^{2+} -free) and maintained in supplement-free, phosphate-free high glucose DMEM (Life Technologies, #11971) for 2 h before uptake. Complexed mitochondria and controls were incubated with cells in the same media for 2 h. Cells were changed to supplement-free DMEM with antibiotic/antimycotic solution, 1% dialyzed FBS after uptake for 2 h, and respiration assays were performed using an XF Cell Mito Stress Kit (Seahorse) at various time points with Seahorse XFe Analyser according to manufacturer's instructions. Oxygen consumption rate (OCR) per well normalized to DNA levels were determined. Assays were performed in triplicate, and results are expressed as mean \pm standard error of OCR per group in units of pmol/min/DNA level at each time point. Huh 7 cells, positive controls, were plated 90% confluent 2 d before each OCR measurement.

MITOCHONDRIA (-) CELL UPTAKE ASSAY

Huh 7-mito (-) and SK Hep1 -mito (-) cells were plated 90% confluent 2 d before uptake assay. Cells were washed with PBS (Mg^{2+} - and Ca^{2+} -free) and maintained in supplement-free, phosphate-free DMEM with high glucose (Life Technologies, #11971)

for 2 h before uptake. Administration of complexed mitochondria and controls were performed as described in Chapter 4, Methods. Cells were maintained in supplement-free DMEM with antibiotic/antimycotic solution, 1% dialyzed FBS after uptake. Cells were collected at various time points for measurement of fluorescence and mitochondrial DNA levels as described in Chapter 3, Methods.

RESULTS AND DISCUSSION

Treatment of Huh 7 and SK Hep1 cells with ddC resulted in undetectable mitochondrial DNA after approximately 3 weeks, Figure 5.1. This indicated that in Huh 7-mito (-) and SK Hep1-mito (-) cells have dysfunctional mitochondria, and could be useful as study models of mitochondrial hepatopathies. Removal of supplements in cell culture media resulted in decreased cellular DNA in Huh 7 mito (-) and SK Hep1 mito (-) cells with time, whereas parental Huh 7 and SK Hep1 cells showed increased cellular DNA, Figure 5.2, indicating that mito (-) cells required supplements in the media for survival.

Mitochondrial damage in Huh 7-mito (-) and SK Hep1-mito (-) cells resulted in decreased energy levels, which affects the cellular activities including endocytosis [353]. Exposure of FI-AsOR, to Huh 7-mito (-) cells resulted in uptake of fluorescence, but levels were approximately 20% that of parental Huh 7 cells, Figure 5.3A. Pre-incubation of excess AsOR nearly abolished this uptake Figure 5.3A, and as expected SK Hep1-mito (-) cells did not show any significant levels of internalized FI-AsOR, Figure 5.3B. This suggested that, although significantly decreased, Huh 7-mito (-) cells were still able to recognize and internalize AsGs through AsGR mediated endocytosis.

Exposure of complexed Huh7-derived mitochondria alone to Huh 7-mito (-) cells showed that fluorescence levels increased from 6,400 units at 60 min to more than 11,000 units at 120 min ($p < 0.01$). Increased fluorescence levels in Huh 7-mito (-) cells with time showed that cells were able to internalize the protein carrier in complex. Further, after co-administration of complexed mitochondria with AsOR-LLO conjugate, fluorescence levels in Huh 7-mito (-) cells increased from 14,000 units at 60 min to more than 30,000 units at 120 min ($p < 0.00001$). This suggested that AsOR-LLO conjugate

facilitated the delivery of protein carrier in cytoplasm. Pre-incubation of excess AsOR resulted in decreased fluorescence levels >90%, Figure 5.4A indicating that internalization of the protein carrier was AsGR-mediated. Fluorescence levels in Huh 7-mito (-) cells decreased from 7,000 units at 12 h to 300 units by 7 d. Co-administration of complexed mitochondria and AsOR-LLO conjugate resulted in fluorescence levels that decreased from 27,000 units at 12 h to 11,000 units at 10 d, Figure 5.4B. Pre-incubation of excess free AsOR resulted in no significant levels of fluorescence in Huh 7-mito (-) cells after exposure to complexed mitochondria with or without AsOR-LLO conjugate. Decreasing levels of fluorescence at later time points in cells indicated decreasing levels of protein carrier over a longer period of time which could be accounted for by degradation of protein in cells, quenching of fluorescence of proteins in cytoplasm or diluted levels of protein with cell division.

There were no significant fluorescence levels in SK Hep1-mito (-) cells under any condition at any time point, Figure 5.5A and 5.5B further indicating that internalization of protein carrier in Huh 7-mito (-) cells was AsGR-mediated.

To determine whether levels of mitochondrial DNA in mitochondrial DNA free cells after uptake declined similar to fluorescence levels of protein carrier, Huh 7 mitochondrial DNA levels were assayed by qPCR. In contrast to the data on fluorescence, complexed mitochondria co-administered in presence of AsOR-LLO conjugate to Huh 7-mito (-) cells resulted in an increase in mitochondrial DNA levels from 5,300-fold (approximately 29-71 mitochondria per cell) over control at 12 h to more than 9,700-fold (approximately 57-143 mitochondria per cell) ($p < 0.0001$) over control at 7 d, and remained stable thereafter up to 10 d. Exposure to complexed mitochondria alone, in absence of AsOR-

LLO conjugate, resulted in mitochondrial DNA levels 900-fold (approximately 5-14 mitochondria per cell) over control at 12 h to barely detectable levels at 24 h, Figure 5.6A. These data suggest that complexed mitochondria were delivered to cytoplasm of Huh 7-mito (-) cells with the help of AsOR-LLO conjugate, and were stable for extended periods of time whereas internalized mitochondria in absence of AsOR-LLO conjugate were rapidly degraded. Mitochondrial DNA levels in SK Hep1-mito (-) cells were barely detectable under any condition at any time point, Figure 5.6B. Together, these results suggested that the fate of the fluorescence associated with FI-AsOR-PL-mitochondria complex was different from the fate of mitochondrial DNA. The protein marker gradually disappeared while the mitochondrial DNA levels increased with time eventually reaching a plateau. This also suggested a separation of the carrier from the mitochondria sometime within 8 h after internalization. Internalized mitochondrial DNA in Huh 7 cells (Appendix H) also declined over a period of time.

To determine whether uptake of mitochondria by mito (-) cells affected rates of cell proliferation in media lacking supplements, the numbers of cells were assayed by cellular DNA levels as a function of time after exposure to complexed mitochondria. Figure 5.7A shows that co-administration of complexed mitochondria and AsOR-LLO conjugate resulted in an increase in cell number to 3.5-fold over baseline ($p < 0.001$) by 10 d. In contrast, untreated cells decreased in cell numbers to 0.03-fold over baseline ($p < 0.004$). Cells exposed to complexed mitochondria or mitochondria alone also showed decreased cell numbers to 0.028-fold over baseline ($p < 0.004$). Pre-exposure to excess AsOR before co-administration of complexed mitochondria and AsOR-LLO conjugate also resulted in decreased cell numbers to 0.028-fold over baseline

($p < 0.004$). This indicated that AsOR-LLO conjugate facilitated cytoplasmic delivery of mitochondria and delivered mitochondria helped rescuing the cells from cell death in absence of required supplements.

SK Hep1-mito (-) cell numbers decreased under all conditions, Figure 5.7B. The data further suggested that internalization of mitochondria by Huh 7-mito (-) cells was AsGR-mediated.

Above assays strongly suggest that targeted mitochondria in presence of AsOR-LLO conjugates were delivered in cytoplasm of cells and were stable. To determine whether these internalized mitochondria were functional and were able to synthesize ATP in Huh 7-mito (-) cells, the OCR was measured before and after addition of inhibitors to quantitate mitochondrial respiration levels in cells. While Huh 7-mito (-) and SK Hep1-mito (-) cells showed no measurable mitochondrial respiration, Huh 7 and SK Hep1 cells showed higher basal OCR which varied on addition of oligomycin, carbonyl cyanide-p-trifluoromethoxyphenyl-hydrazone (FCCP) or rotenone in a manner consistent with mitochondrial respiration in cells, Figure 5.8. This further indicated that our cell culture models of mitochondrial hepatopathies had dysfunctional mitochondria.

Twelve h after co-administration of complexed mitochondria and AsOR-LLO conjugate to Huh 7-mito (-) cells resulted in a 70% increase in OCR compared to controls, Figure 5.9A ($p < 0.0001$). Exposure to mitochondria alone, complexed mitochondria with or without AsOR-LLO conjugate plus excess AsOR did not show any measurable mitochondrial respiration, Figure 5.9A. Ten d after co-administration of complexed mitochondria and AsOR-LLO conjugate, Huh 7-mito (-) cells had levels of mitochondrial

respiration comparable to parental Huh 7 cells, Figure 5.9B ($p < 0.00001$). The data indicate that internalized mitochondria were functional, and increased OCR in Huh 7-mito (-) cells, which became indistinguishable from that of parental cells by 10 d. Taken together, the data were consistent with proliferation of mitochondria after introduction into mito (-) cells, which can account for the observed rescue of Huh 7-mito (-) cells from cell death in supplement-free media.

FIGURES AND TABLES

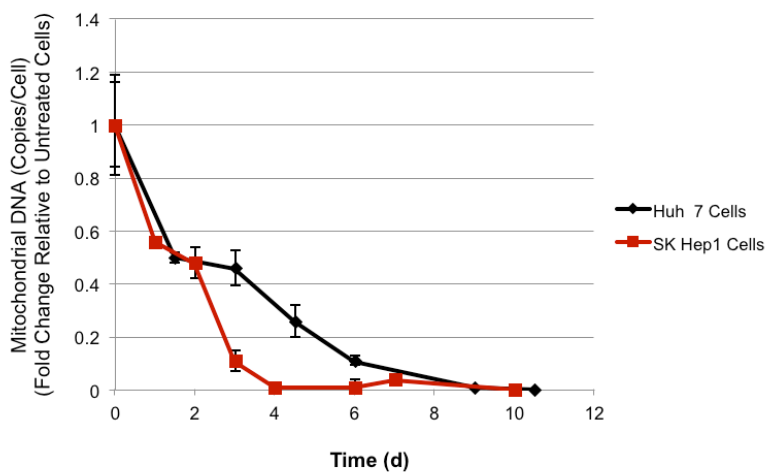


Figure 5.1. Mitochondrial DNA levels in Huh 7 and SK Hep1 cells treated with ddC.

Huh 7 and SK Hep1 cells were treated with ddC for 3 weeks and mitochondrial DNA levels were determined with qPCR with time.

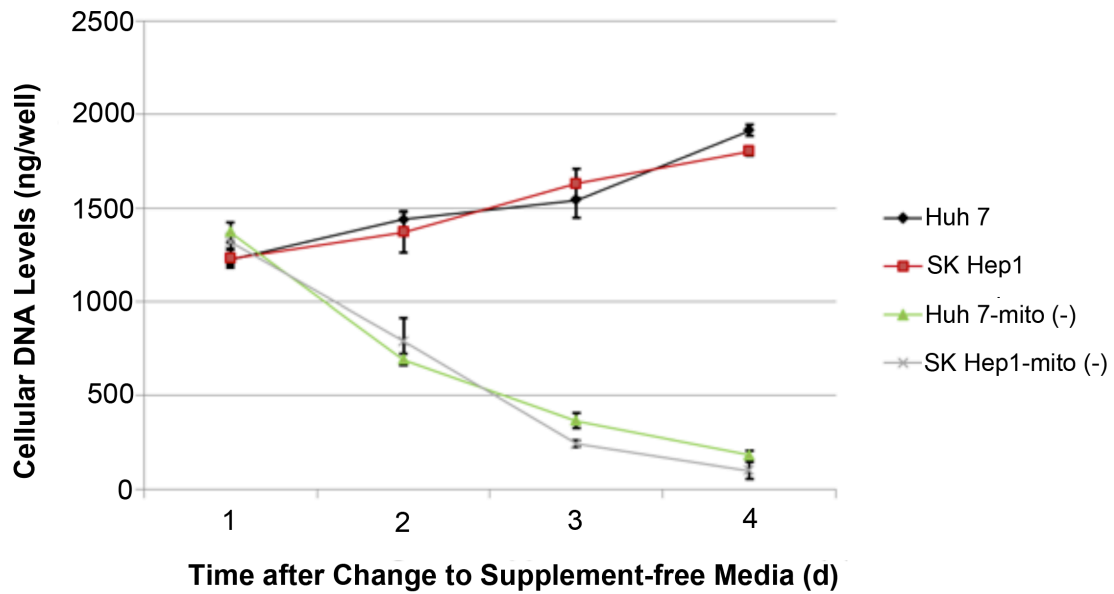


Figure 5.2. Cellular DNA levels (ng/well) of cells in wells after change to supplement-free media.

Cells were grown in supplement containing cell culture media, and then changed to supplement-free media. Cellular DNA levels as an estimate of the numbers of cells were measured as a function of time.

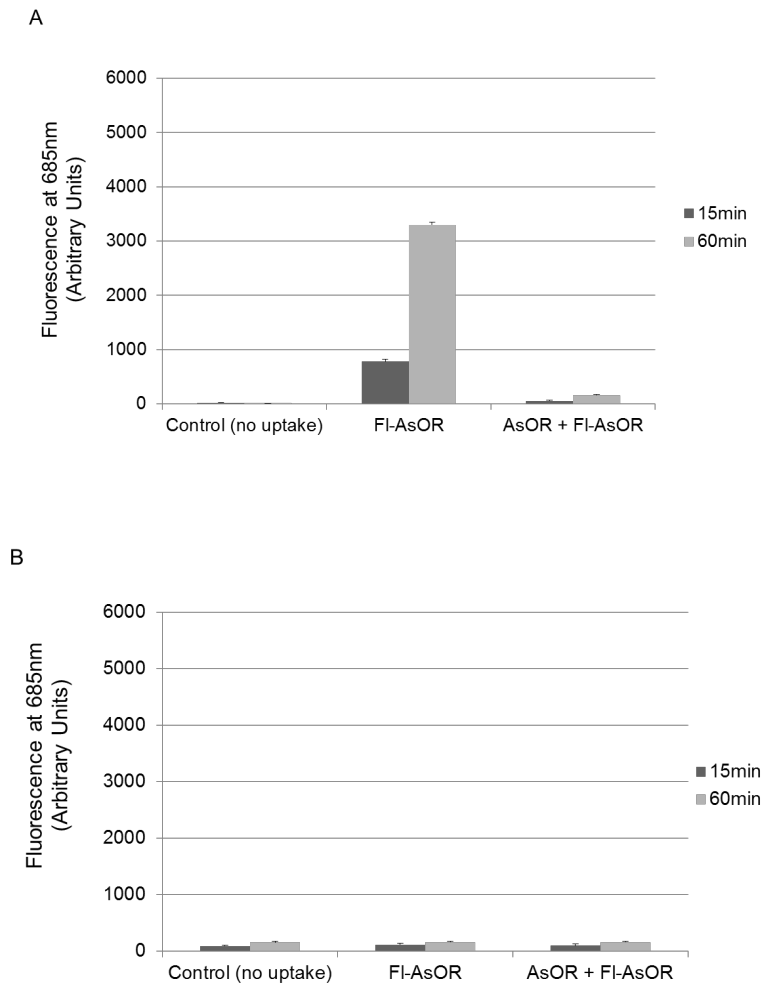


Figure 5.3. Determination of FI-AsOR uptake in mito (-) cells.

Uptake of FI-AsOR was determined by spectrophotometry after incubation for 1 h at 37°C. A, Huh 7-mito (-) cells; B, SK Hep1-mito (-) cells.

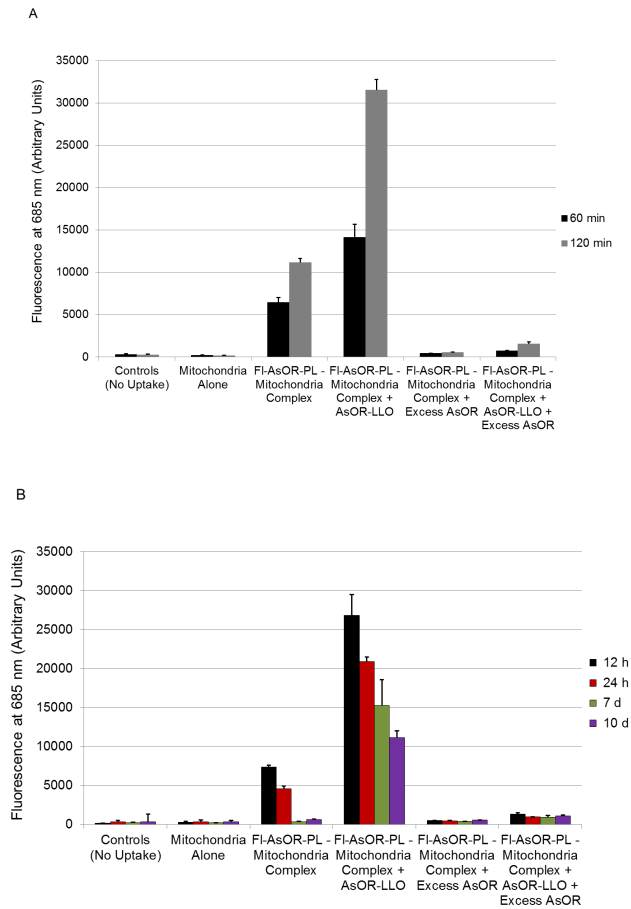


Figure 5.4. Fluorescence in Huh 7-mito (-) cells after co-administration of complexed mitochondria and controls.

Huh 7 -mito (-) cells were incubated separately with cell culture media, mitochondria alone, FI-AsOR-PL–mitochondria complex, complexed mitochondria and AsOR-LLO, complexed mitochondria + excess AsOR or complexed mitochondria + AsOR-LLO + excess AsOR at 37°C. After 2 h, cells were washed and maintained in supplement-free cell culture media. Cells were collected to measure FI-AsOR-PL levels taken up with spectrophotometer at different time points. A, Fluorescence levels in cells up to 120 min; B, Fluorescence levels in cells up to 10 d.

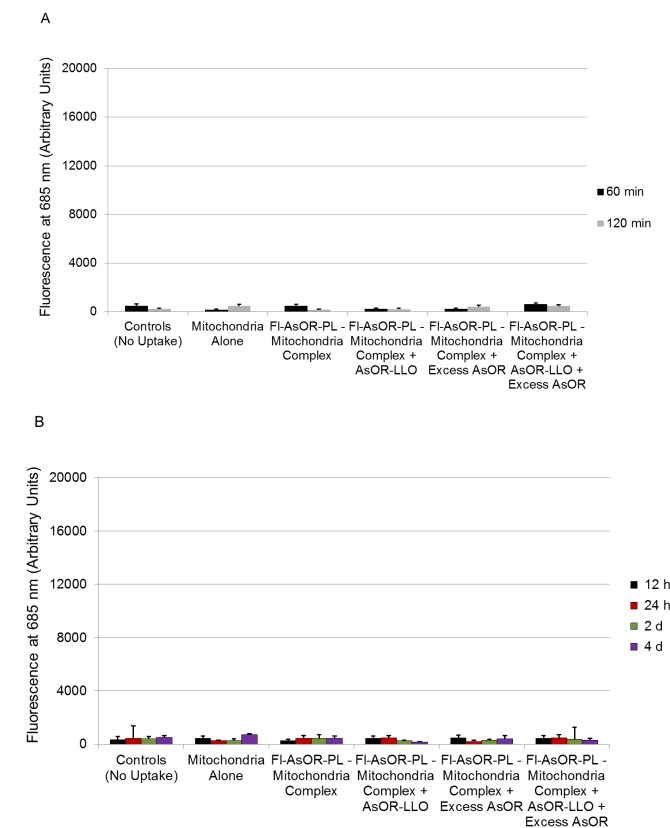


Figure 5.5. Fluorescence in SK Hep1-mito (-) cells after co-administration of complexed mitochondria and controls.

SK Hep1-mito (-) cells were incubated separately with cell culture media, mitochondria alone, FI-AsOR-PL–mitochondria complex, complexed mitochondria and AsOR-LLO, complexed mitochondria + excess AsOR and complexed mitochondria + AsOR-LLO + excess AsOR at 37°C. After 2 h, cells were washed and maintained in supplement-free cell culture media. Cells were collected to measure FI-AsOR-PL levels taken up with spectrophotometer at different time points. A, Fluorescence levels in cells up to 120 min; B, Fluorescence levels in cells up to 10 d.

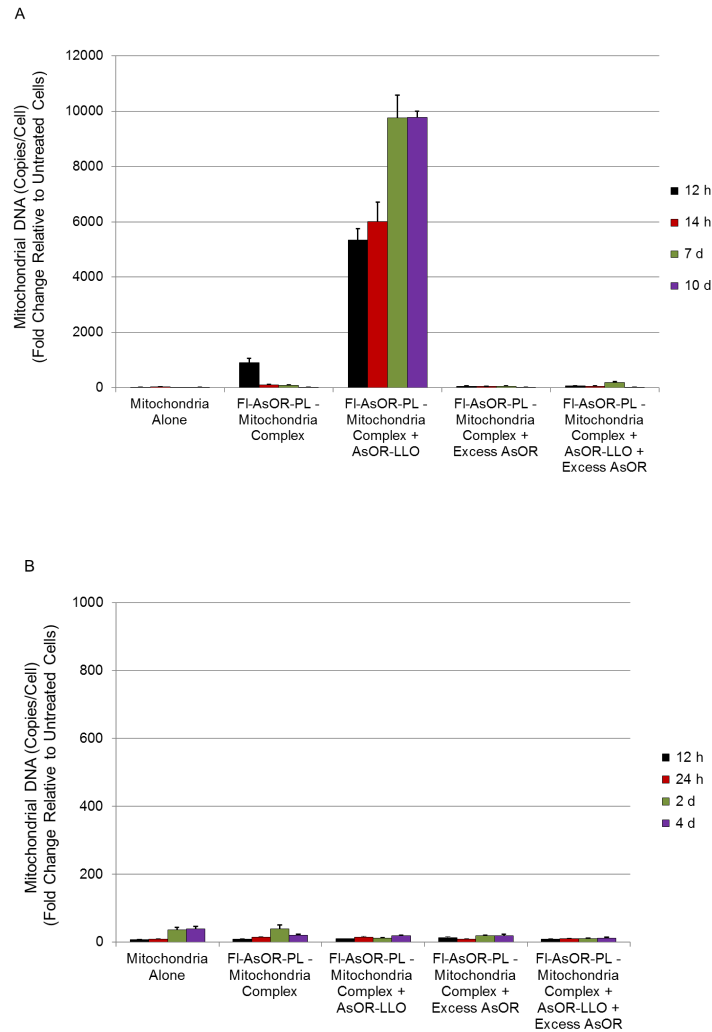


Figure 5.6. Mitochondrial DNA levels in mito (-) cells after co-administration of complexed mitochondria and AsOR-LLO, and controls.

Cells were incubated separately with cell culture media, mitochondria alone, FI-AsOR-PL–mitochondria complex, complexed mitochondria and AsOR-LLO conjugates, complexed mitochondria + excess AsOR or complexed mitochondria + AsOR-LLO + excess AsOR at 37°C. After 2 h, cells were washed and maintained in supplement-free cell culture media. Cells were collected to measure mitochondrial DNA levels by qPCR and compared to untreated controls. A, Huh 7-mito (-) cells; B, SK Hep1-mito (-) cells.

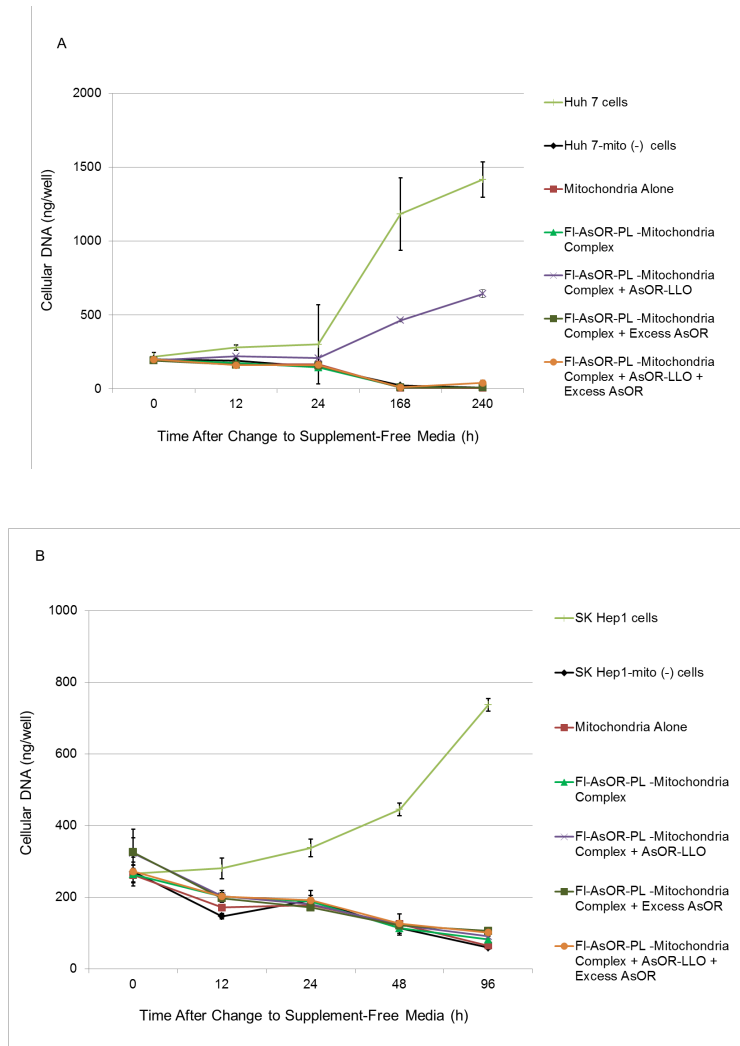


Figure 5.7. Cellular DNA levels in mito (-) cells after co-administration of complexed mitochondria and controls.

Cells were incubated separately with cell culture media, mitochondria alone, FI-AsOR-PL-mitochondria complex, complexed mitochondria and AsOR-LLO conjugates, complexed mitochondria + excess AsOR or complexed mitochondria + AsOR-LLO conjugates + excess AsOR at 37°C. After 2 h, cells were washed and maintained in supplement-free cell culture media. Total cellular DNA was measured in each well. A, Huh 7-mito (-) cells; B, SK Hep1-mito (-) cells.

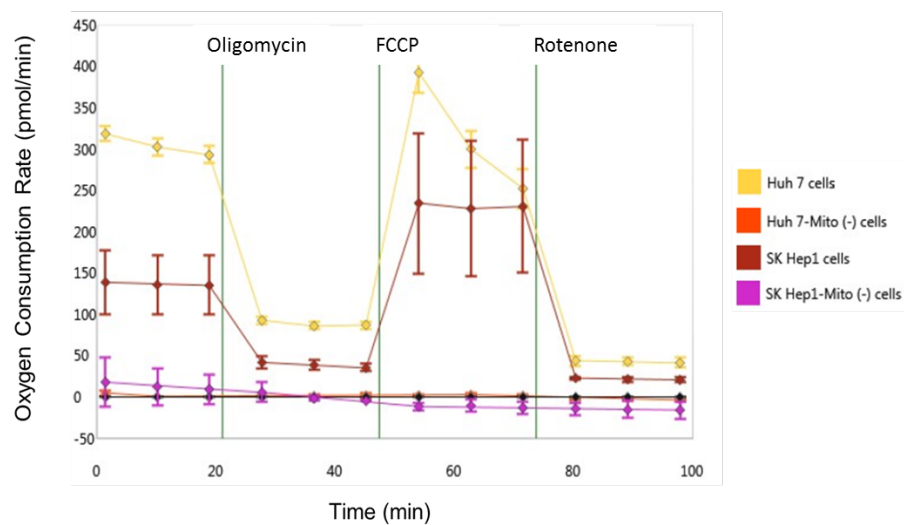


Figure 5.8. Characterization of mitochondrial respiration.

Cells were plated in XF24 cell culture microplates 1 day before mitochondria respiration assays. Oxygen consumption rates were measured with a Seahorse XFe Analyser to determine mitochondrial respiration in cells.

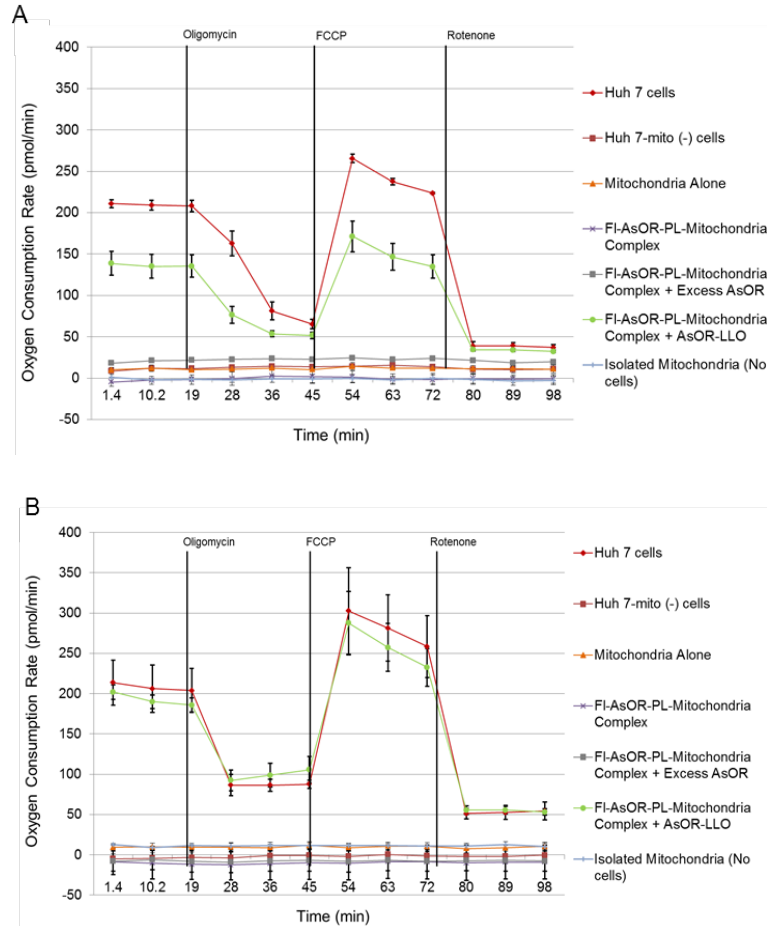


Figure 5.9. Oxygen consumption rates in Huh 7-mito (-) cells after co-administration of complexed mitochondria and controls.

Huh 7-mito (-) cells were incubated separately with cell culture media, mitochondria alone, FI-AsOR-PL-mitochondria complex, complexed mitochondria + excess AsOR, or complexed mitochondria + AsOR-LLO at 37°C. After 2 h, cells were washed and maintained in supplement-free cell culture media for various times. Oxygen consumption rates were measured after exposure to various inhibitors of regulators of mitochondrial respiration. A, 12 h; B, 10 d.

CHAPTER 6: CONCLUSIONS AND SIGNIFICANCE

The data indicate that covalent linkage of an AsG to PL forms a conjugate that can bind mitochondria in a stable electrostatic interaction. The AsG component can target mitochondria specifically to hepatocytes. Co-internalization of an endosomolytic agent co-targeted to hepatocytes through the AsG receptor enhances escape from endosomes, facilitating entry of mitochondria into the cytoplasm of cells. The targeted mitochondria replicate independent of cell division to restore the complement of mitochondria required by the host cells. Normal mitochondria targeted to cells lacking mitochondria resulted in restoration of the rates of cell proliferation, and rescue those cells from death. The transplanted mitochondria possessed the characteristics of normal mitochondrial respiration, and the oxygen consumption rates per cell approached normal after mitochondrial transplantation.

These data represent the first description of targeted introduction of foreign mitochondria into recipient cells other by cell fusion. It is also the first description of the use of receptors to target organelles to hepatocytes.

Currently, there is no treatment for mitochondrial dysfunction, and no means to repair or replace damaged mitochondria. The data demonstrate a method for mitochondrial transplantation, and is potentially curative for diseases caused by hepatic mitochondrial damage. Because the liver is the primary target of mitochondrial dysfunction induced by drugs/alcohol, in cases of liver failure, transplantation of healthy mitochondria to hepatocytes could be a potential treatment. This study forms the scientific basis for a potential therapy for mitochondrial disorders of hepatocytes where healthy and

functional mitochondria could be transplanted in cells with mitochondrial dysfunction. This could provide a generic and safe treatment for the mitochondrial hepatopathies where mitochondria renders dysfunctional because of genetic defect in mitochondrial DNA or mitochondrial damage is induced. Several nucleoside-based drugs and alcohol are known to induce such damage in liver. This therapy would be very helpful where use of mitochondrial damaging drugs is inevitable.

The endosymbiotic theory was first articulated by the Russian botanist Mereschkowski in 1905 [354]. Since then it has been modified and revised several times [355, 356]. According to this theory, mitochondria originated as free-living proteo-bacteria that were taken inside by primitive eukaryotic cell where they developed symbiotic relationship later. This study provides evidence in favor of endosymbiosis theory. Successful uptake of FI-AsOR-PL-mitochondrial complex by hepatocytes provides evidence that mitochondria might have become a part of eukaryotic cell during evolution.

CHAPTER 7: FUTURE DIRECTIONS

ENHANCED ESCAPE OF AsG-MITOCHONDRIA COMPLEXES FROM ENDOSOMES AFTER INTERNALIZATION

FI-AsOR-PL-mitochondria complexes exposed to hepatocytes in presence of AsOR-LLO conjugate leads to facilitate delivery of complex in cytoplasm of the hepatocytes. There have been reports that multiple ligands bind to the receptors and are internalized together in same endosomes [318]. In this case, both ligands recognize same receptor on cells surface, which might lead to competition in binding. Competition is unlikely due to the low ratio (1:30::AsOR-LLO conjugate: AsG-mitochondria complex) of AsOR-LLO conjugate is added to facilitate the escape of FI-AsOR-PL-mitochondria complex from endosomes. However, in order to eliminate the chances of competition for binding to the receptor on cell surface and, improve the escape after internalization from endosomes before lysosomal digestion, a ternary complex can be formed by complexing AsOR-LLO conjugates directly to mitochondria rather than by delivering them separately by separate receptor. It may improve the chances of escape of internalized FI-AsOR-PL-mitochondria complexes from endosomes as it would ensure co-uptake and co-internalization of both FI-AsOR-PL-mitochondria complexes and AsOR-LLO conjugate in same endosomes. Studies on various methods to form such ternary complexes are anticipated. Complexes of AsOR-PL to LLO or AsOR to LLO-PL can be formed to make a conjugate of AsOR-LLO-PL. Presence of PL in conjugate would provide positive charge to the conjugate which would help making stable complexes with mitochondria by binding to negatively charged isolated mitochondria through non-damaging charge-

charge interactions. Disulfide cross-linkers can be used to make complexes of LLO with AsOR-PL to avoid conformational changes in LLO and allow release of LLO from conjugates in reducing environment of endosomes for its membranolytic activity. Release of LLO from the AsOR-LLO-PL conjugates could be determined by reduction with DTT. Hemolytic assays can be performed with and without DTT at pH 7.4 and pH 5.6 to determine the membranolytic activity of LLO in AsOR-LLO-PL conjugate. LLO in form of AsOR-LLO-PL conjugate is expected to be non-damaging to the membranes till it is reduced in reducing environment of endosomes. To determine if AsOR-LLO-PL conjugates damage the outer membrane of mitochondria after making complexes with mitochondria before internalization, cytochrome c assays can be performed with and without DTT at pH 7.4 and pH 5.6. Optimum ratios of AsOR-LLO-PL and AsOR-PL can be calculated to make the ternary complex with isolated mitochondria for efficient binding to receptors on cell surface and internalization of the ternary complexes as well as efficient escape of complexes from the endosomes before lysosomal degradation. Increased efficiency of mitochondrial delivery with ternary complexes can be determined by comparing mitochondrial delivery to the hepatocytes in presence and absence of AsOR-LLO-PL conjugates. Function and stability of targeted mitochondria to hepatocytes as a form of ternary complex can be determined by rescuing the mitochondria free hepatocytes from cell death in supplement free media and measuring mitochondrial respiration levels in mitochondria free hepatocytes exposed to ternary complexes.

Mitochondria to be used for making complexes with AsG for targeted transplantation to hepatocytes should be healthy and functional for successful treatment and rescue of cells with damaged mitochondria. Isolation of intact mitochondria from cells is a very delicate and time consuming process in which any damage can induce structural alterations and functional impairments associated with oxidative phosphorylation. Isolation of fresh mitochondria each time before complex formation and internalization process causes increased chances of artificial damage induced by repeated technical handling. Also assessment of mitochondrial isolation efficiency and stability of isolated mitochondria after each isolation process adds to delay in further use of isolated mitochondria for targeting to hepatocytes. Delivery of damaged mitochondria to cells will not only result into in-effective treatment of mitochondrial disorders of hepatocytes, but it can also augment the chances apoptosis in targeted cells because of damaged mitochondria. Because mitochondria are fragile and easily deteriorate, to be of practical use, the development of a method of cryopreservation of mitochondria would be helpful. Isolated mitochondria have to be stored in appropriate media to provide stability to mitochondrial membranes and suitable ionic levels for mitochondrial function before use [309]. More appropriate storage buffers are required to provide proper environment for long-term storage and cryopreservation of mitochondria [357, 358]. If satisfactory cryopreservation could be achieved, mitochondria for transplantation could be stored and complex formation for targeting to hepatocytes conducted immediately prior to use. Studies in this area are planned. Proper conditions of long term storage of isolated mitochondria in suitable medium and temperature can be determined. Morphological

and biochemical parameters can be obtained in isolated mitochondrial suspensions [359] to determine long term stability and efficient function of isolated mitochondria in mitochondrial storage buffers. Damage to mitochondrial membrane due to long term storage can be determined with cytochrome c assays. Half-life and functional abilities of preserved isolated mitochondria in appropriate medium at different temperatures can be determined by measuring the damage to isolated mitochondria over time at different temperatures using membrane potential determining dyes such as JC-1 [360]. Identification of storage conditions and development of method of cryopreservation of mitochondria would eliminate the step of assessment of efficiency of mitochondrial isolation and stability each time before complex formation and will allow obtaining more consistent results.

ASGR-MEDIATED HEALTHY AND FUNCTIONAL MITOCHONDRIA DELIVERY TO HEPATOCYTES IN ANIMALS

Evidence shows that stable complexes of positively charged AsGs and mitochondria could be targeted specifically to hepatocytes and endosomolytic agents can facilitate escape of targeted mitochondria from endosomes to cytoplasm in cell culture. AsGR-mediated mitochondria delivery to hepatocytes *in vivo* would help developing a potential method of treatment for hepatic mitochondrial dysfunctional disorders. Rats can be used to develop the procedure of delivering mitochondria to hepatocytes *in vivo*. Studies in this area are on-going.

Huh 7 cells can be used as source of mitochondria since DNA sequence of Huh 7 mitochondria is distinguishable from rat cell mitochondrial DNA. Complexes of FI-AsOR-PL and mitochondria could be injected in a rat tail vein. Since extensive blood supply allows liver cells to filter blood off the toxins, we anticipate that blood would carry the complexes to liver cells where those could be recognized and internalized by hepatocytes.

Several potential problems are anticipated for the process:

1. Stability of the complexes in the blood can be affected by different types of serum proteins with different sizes and charges [361]. Some positively charged serum proteins [362-364] may also compete with the carrier protein for binding to mitochondria. Aggregation of complexes might also occur in presence of some serum proteins.

2. Blood macrophages have been shown to cause poor efficiency of delivery of biomolecules to desired tissues [365]. Interactions between macrophages and mitochondria complexes could be a potential problem.
3. Non-specific adherence of mitochondrial complexes to RBCs [366] may hinder the uptake of complexes by hepatocytes.
4. Optimum size of the mitochondrial complexes that could be internalized by hepatocytes *in vivo* will have to be studied [363, 367].
5. Because of larger size of the complexes, filtration of complexes in alveolar capillaries may also hinder the complexes enriched blood to reach hepatocytes [364, 368].
6. The rat liver sinusoidal (capillaries carrying blood in liver) diameter is approximately 5 μm and fenestrae (small pores in endothelial cells that allow for rapid exchange of molecules between sinusoid blood vessels and surrounding tissue) are approximately 100 nm diameter. Smaller size of fenestrae could hinder the delivery of large sized mitochondrial complexes to hepatocytes *in vivo*.
7. Kupffer cells (liver macrophages) could engulf the mitochondrial complexes that reach the liver and hinder the AsGR mediated uptake of complexes by hepatocytes.

The following are few alternative strategies for above mentioned anticipated problems:

Mitochondria complexes could be filtered before injecting to obtain a suspension of smaller sized complexes.

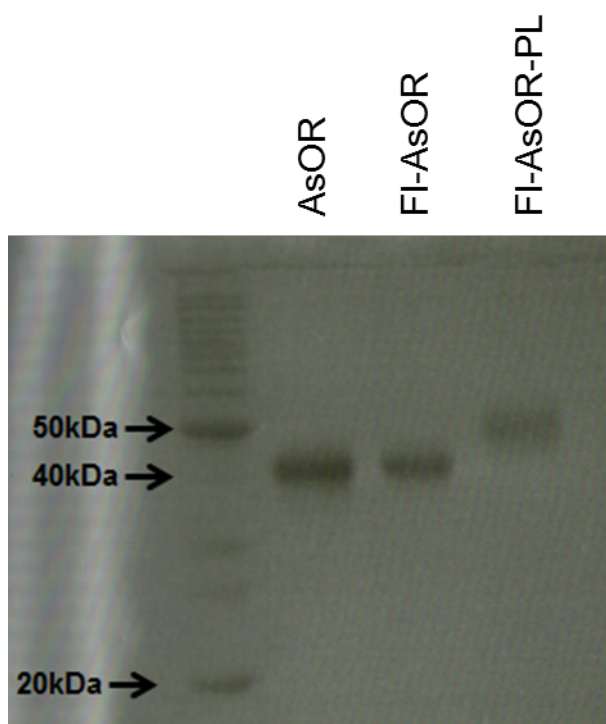
Some types of ultrafine aggregates and carbon particles could inhibit phagocytosis in macrophages [369, 370]. Use of these particles might reduce the interactions between macrophages and mitochondria complexes. These particles would also increase the availability of complexes to hepatocytes by inhibiting Kupffer cells.

Endothelin is a vasoconstrictor which causes release of calcium by the sarcoplasmic reticulum (SR) and results in increased smooth muscle contraction and vasoconstriction [371]. Endothelin receptor antagonist can help in inhibition of vasoconstriction and help in un-restricted movement of large cargos injected in blood for delivery to liver. Several FDA approved endothelin receptor antagonist (ERA) are available like ambrisentan (selective for the type A endothelin receptor (ETA) [372]) and bosentan (antagonist of endothelin-1 at the endothelin-A (ET-A) and endothelin-B (ET-B) receptors [373]). These antagonist are also used to treat pulmonary arterial hypertension [374]. These ERA could allow the free circulation of complexes in blood and through alveolar capillaries as well as liver sinusoid blood vessels and fenestrae.

Delivery of Huh 7 mitochondria to hepatocytes could be determined with qPCR, electron-microscopy or FISH (fluorescence-based in situ hybridization) assays. Localization of protein carriers could be determined by electron microscopy and immunohistochemistry. Specific delivery of mitochondria to hepatocytes can be determined by measuring the Huh 7 mitochondrial DNA levels in other organs such as lungs, heart, spleen and muscles.

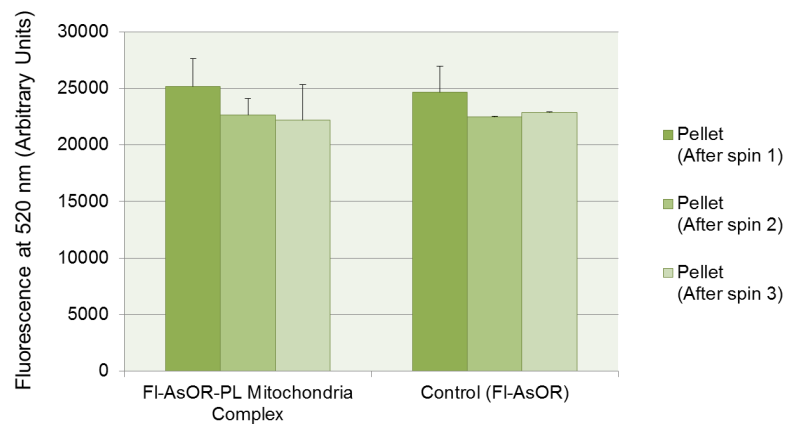
APPENDICES

APPENDIX A: DETERMINATION OF CHANGE IN SIZE OF ASOR AFTER ADDING FLUORESCENCE TAGS AND POLY-LYSINE CHAINS BY SDS-PAGE



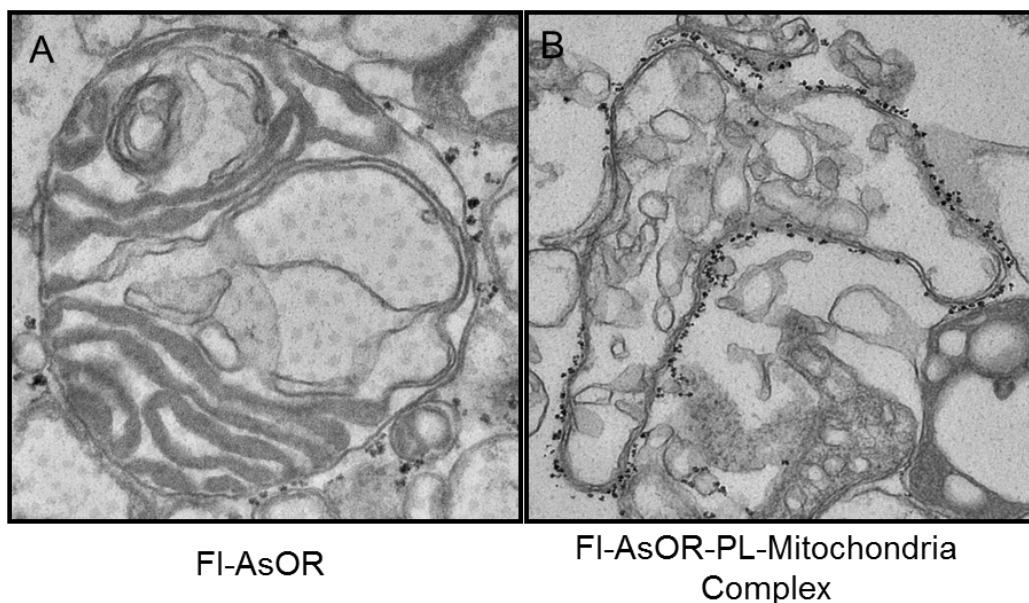
AsOR, FI-AsOR and FI-AsOR-PL were run on 15% SDS-PAGE and stained with Coomassie Brilliant Blue to determine size. SDS-PAGE illustrates that FI-AsOR is slightly larger than AsOR and FI-AsOR-PL is larger than both AsOR and FI-AsOR. Data show that addition of fluorescence tags and poly-lysine chains to AsOR results in increased size of protein.

APPENDIX B: FLUORESCENCE OF GFP-LABELED MITOCHONDRIA WHILE DETERMINING STABILITY OF FI-ASOR-PL- MITOCHONDRIA COMPLEXES.



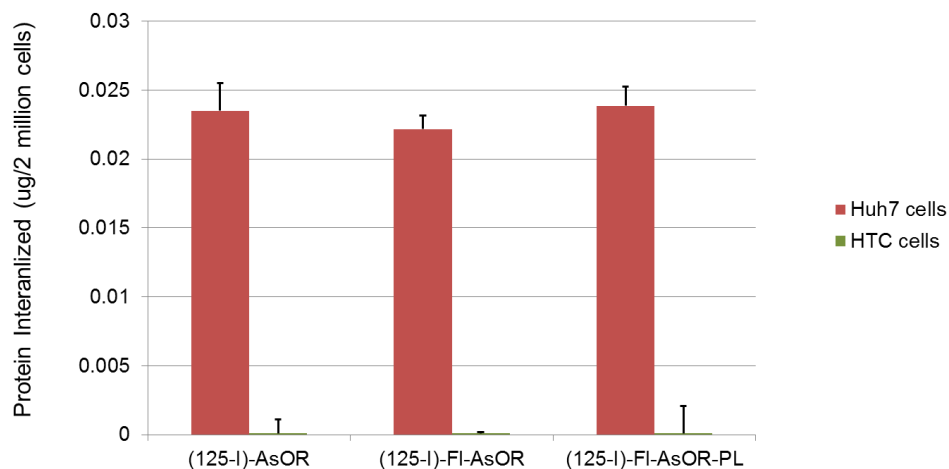
Freshly isolated GFP labeled rat mitochondria were incubated with FI-AsOR-PL or FI-AsOR and repeatedly centrifuged and re-suspended in fresh medium. Fluorescence levels of GFP labeled mitochondria at 520 nm were determined with fluorescence levels of proteins at 685 nm (Figure 2.7). The data show that GFP-labeled mitochondria fluorescence decreased from 25,000 units to 23,000 units after second spin, and remained stable thereafter ($p < 0.01$). Fluorescence levels of proteins (Figure 2.7) in corresponding spin cycle shows that in contrast to FI-AsOR, FI-AsOR-PL remained bound to mitochondria.

APPENDIX C: DETERMINATION OF STABILITY OF FI-ASOR-PL-MITOCHONDRIA COMPLEX BY ELECTRON MICROSCOPY



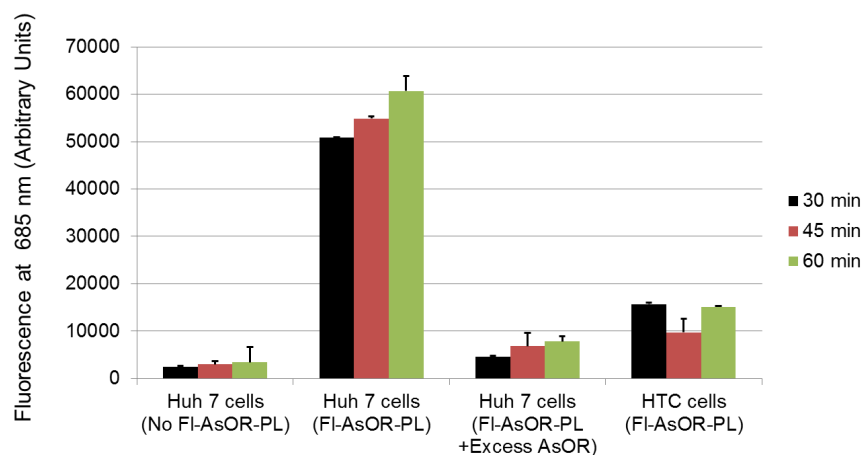
Freshly isolated rat mitochondria were incubated with FI-AsOR-PL or FI-AsOR to form stable complexes. Complexes were fixed with 4% paraformaldehyde for 10 min, and then washed with PBS. Cells were incubated with anti-orosomucoid antibody (Abcam, ab88869) for 2 h at 4°C. Goat Anti-Mouse IgG H&L (10nm Gold) (Abcam) secondary antibody was added for 1 h. Complexes were washed 3 times with PBS for 5 min each and fixed with 2.5% glutaraldehyde in 0.1 M sodium cacodylate buffer, and embedded in 3% agarose. Pellets were post fixed in OsO₄, dehydrated in ethanol and embedded in Poly/Bed 812 (Poly sciences, Inc.). Ultrathin 70 nm sections were mounted on 300 mesh Cu grids, stained with uranyl acetate and Sat's lead citrate, and examined with Hitachi H-7650 TEM. The data showed that unlike FI-AsOR (Figure A), FI-AsOR-PL stably bound to the mitochondria (Figure B) on the outer membrane.

APPENDIX D: DETERMINATION OF UPTAKE OF PROTEINS BY USING RADIOACTIVE TAG (^{125}I)



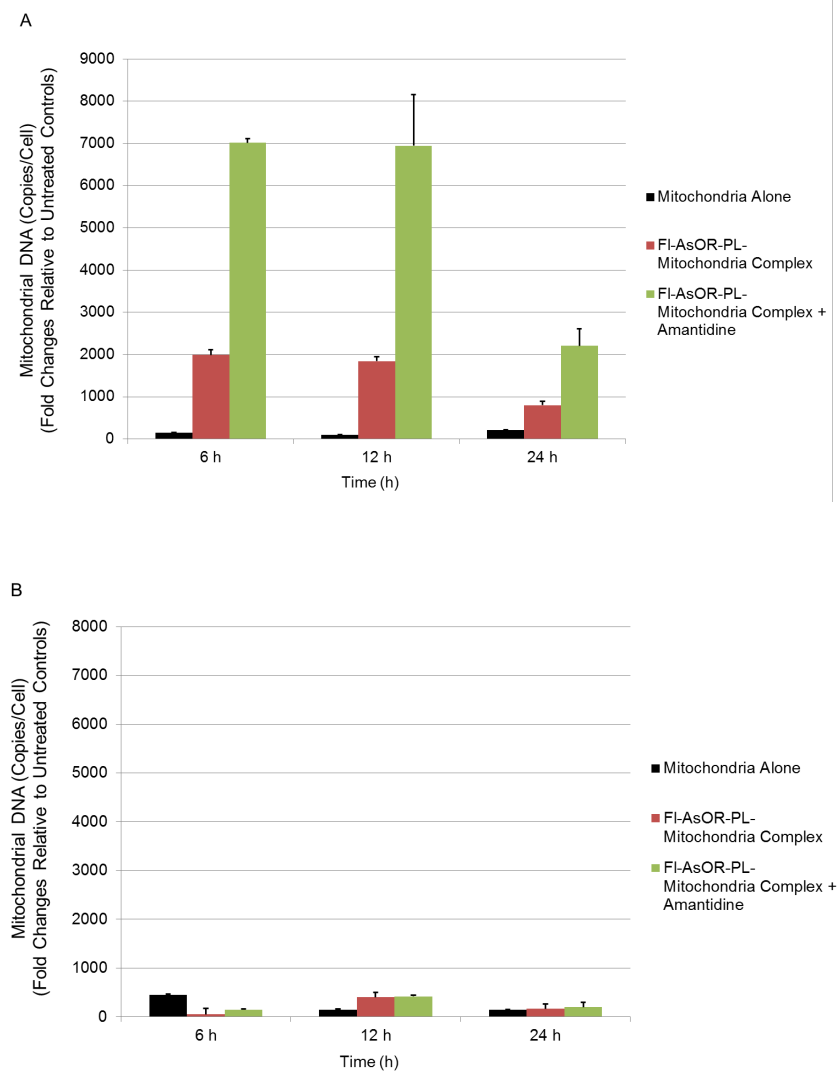
AsOR, FI-AsOR and FI-AsOR-PL were labeled with Na^{125}I using Pierce™ Iodination Beads according to manufacturer's specification [375] to form ^{125}I -AsOR, ^{125}I -FI-AsOR and ^{125}I -FI-AsOR-PL. Labeled protein was purified using PD-10 column according to manufacturer's instructions. Uptake assays were performed for 1 h as explained in Chapter 2, Methods. After washing extensively with 10 mM EDTA in ice cold PBS, cells were collected and radioactivity was measured using gamma counter (Packard gamma counter). Non-specific uptake was determined in presence of 100-fold excess of unlabeled AsOR, and specific uptake was determined by difference between total and non-specific accumulation of radioactivity in cell lysates. The amount of protein internalized by cells was calculated using specific activity of ^{125}I labeled protein used (cpm/ug). HTC cells (AsGR (-)) were used as negative controls. The data showed that 2 million Huh 7 cells internalized approximately 0.022 μg of ^{125}I -AsOR, ^{125}I -FI-AsOR and ^{125}I -FI-AsOR-PL whereas there was no significant uptake of proteins by HTC cells.

APPENDIX E: DETERMINATION OF UPTAKE OF PROTEINS BY FLUORESCENCE



Uptake of FI-AsOR-PL was performed with Huh 7 and HTC cells as explained in Chapter 2, Methods. Cells were collected at 30 min, 45 min and 60 min, and fluorescence levels were measured as explained in Chapter 3, Methods. The data showed that fluorescence levels increase in Huh 7 cells with time. Addition of excess AsOR led to decreased levels of fluorescence in Huh 7 cells at all-time points ($p < 0.001$). HTC cells (AsGR (-)) had fluorescence less than 25% of the fluorescence levels in Huh 7 cells, the levels did not increase with time. This suggests that association of FI-AsOR-PL with Huh 7 cells was time dependent, and AsGR-mediated.

APPENDIX F: EFFECTS OF AMANTADINE ON MITOCHONDRIAL DNA LEVELS AFTER UPTAKE OF FL-ASOR-PL-MITOCHONDRIA COMPLEX.

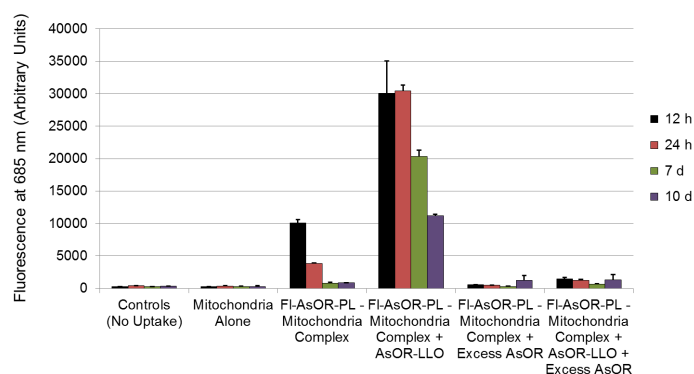


Cells were treated with 20 μ M amantadine (Sigma) for 1 h prior and during the uptake assay [376]. Uptake assays were performed as explained in Chapter 2, Methods for 2 h. Cells were collected to measure mitochondrial DNA levels with qPCR, and compared to untreated controls at various time points. A, HTC mitochondria DNA levels in Huh 7 cells; B, HTC mitochondria DNA levels in SK Hep1 cells. Amantadine increases the pH

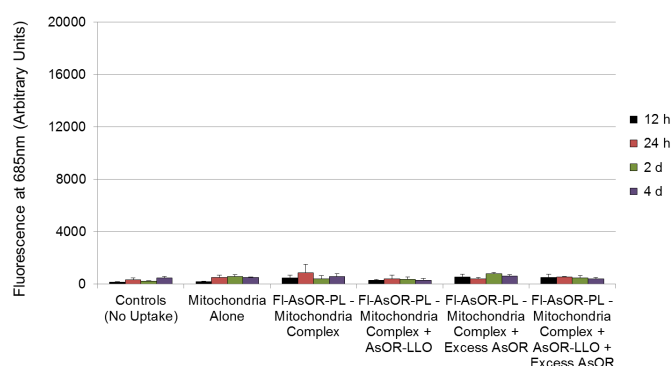
of endosomes, and inhibits lysosomal fusion and digestion [240]. Mitochondrial DNA levels in Huh 7 cells decreased from 2,000-fold over controls at 6 h to approximately 800-fold over controls at 24 h after exposure to complexed mitochondria. Amantadine-treated Huh 7 cells show 7,000-fold increase in mitochondrial DNA over controls at 6 h ($p < 0.04$). That level decreased to 2,000-fold over controls at 24 h. Huh 7 cells exposed to mitochondria alone did not show any significant levels of mitochondrial DNA. In addition, SK Hep1 cells also did not show any significant levels of mitochondrial DNA at any time point (Figure B). The data suggest that treatment of cells with amantadine inhibited the digestion of internalized mitochondria till amantadine treatment [240]. Afterwards, internalized complex was destroyed by lysosomal digestion.

APPENDIX G: FATE OF FLUORESCENCE IN CELLS AFTER UPTAKE

A



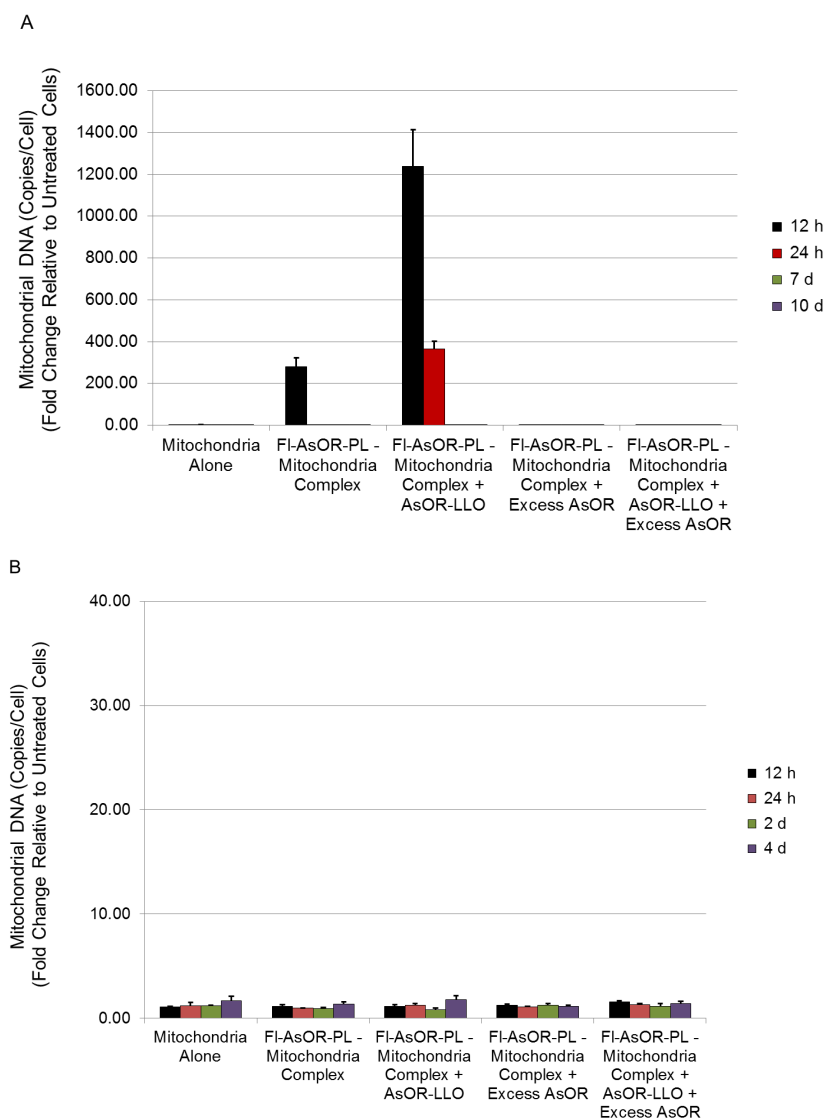
B



Cells were incubated separately with cell culture media, mitochondria alone, FI-AsOR-PL–mitochondria complex, complexed mitochondria and AsOR-LLO conjugate, excess AsOR + complexed mitochondria and excess AsOR + complexed mitochondria + AsOR-LLO conjugate at 37°C. After 2 h, cells were washed and maintained in supplement-free cell culture media. Cells were collected to measure FI-AsOR-PL levels taken up with spectrophotometer at different time points. A, Huh 7 cells; B, SK Hep1 cells.

The data showed that fluorescence levels in Huh 7 cells decreased from 10,000 units at 12 h to 4,000 units at 24 h when incubated with complexed mitochondria. Fluorescence levels become barely detectable on 7 d. Co-administration of AsOR-LLO conjugate with complexed mitochondria resulted in decrease in fluorescence levels from 30,000 units at 12 h to 11,000 units at 10 d, Figure A. Pre-incubation of excess free AsOR resulted in no significant levels of fluorescence in Huh 7 cells after exposure to complexed mitochondria with and without AsOR-LLO conjugate (Figure A). There were no significant fluorescence levels in SK Hep1 cells under any condition, at any time point, Figure B. Data suggest that fluorescence associated with Huh 7 cells after uptake of complexed mitochondria decreased rapidly with time.

APPENDIX H: FATE OF MITOCHONDRIAL DNA IN CELLS AFTER UPTAKE

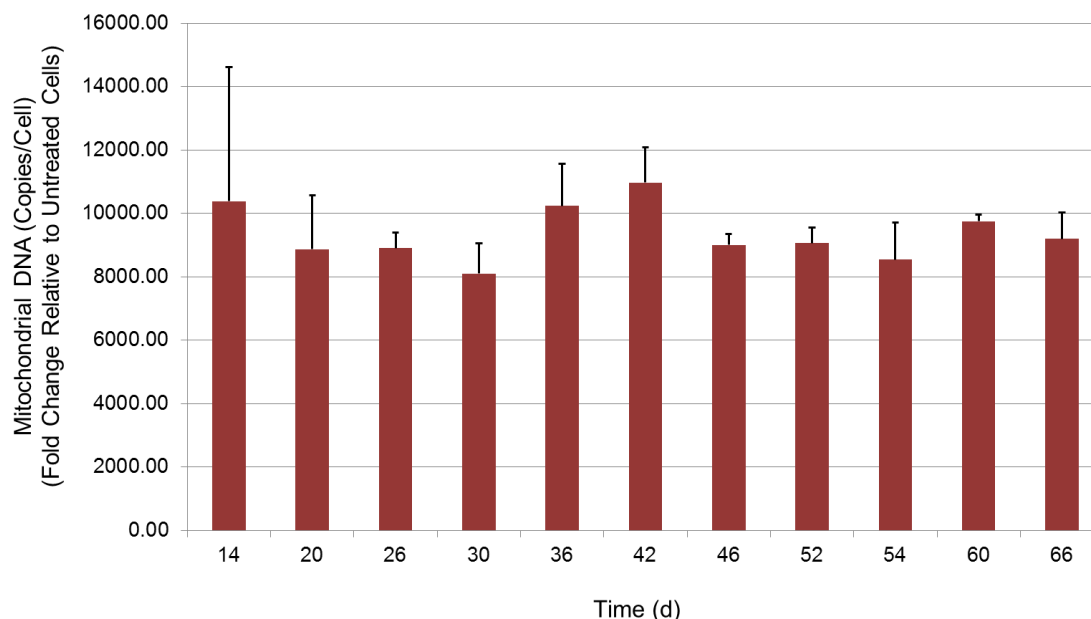


Cells were incubated separately with cell culture media, mitochondria alone, FI-AsOR-PL-mitochondria complex, complexed mitochondria and AsOR-LLO conjugate, excess AsOR + complexed mitochondria and excess AsOR + complexed mitochondria + AsOR-LLO conjugate at 37°C. After 2 h, cells were washed and maintained in supplement-free cell culture media. Cells were collected to measure mitochondrial DNA

levels with qPCR and compared to untreated controls at different time points. A, Huh 7 cells; B, SK Hep1 cells.

Mitochondrial DNA levels in Huh 7 cells incubated with complexed mitochondria declined from 300-fold over controls at 12 h to undetectable at 24 h. Co-administration of AsOR-LLO with complexed mitochondria in Huh 7 cells resulted in 1,250-fold mitochondrial DNA over controls at 12 h to less than 400-fold at 24 h and barely detectable at 7 d. Pre-incubation of excess free AsOR resulted in no significant levels of mitochondrial DNA in Huh 7 cells after exposure to complexed mitochondria with and without AsOR-LLO conjugate (Figure A). SK Hep1 cells did not show any significant levels of mitochondrial DNA under any condition, at any time point, Figure B.

APPENDIX I: FATE OF MITOCHONDRIAL DNA IN MITOCHONDRIA FREE CELLS AFTER UPTAKE FOR EXTENDED PERIODS OF TIME



Huh 7 mito (-) cells were incubated with complexed HTC mitochondria and AsOR-LLO conjugate at 37°C. After 2 h, cells were washed and maintained in supplement-free cell culture media. Cells were collected to measure HTC mitochondrial DNA levels by qPCR and compared to untreated controls. Data showed that mitochondrial DNA levels were stable after uptake over a longer period of time.

REFERENCES

1. Hayashi, J., et al., *Human mitochondria and mitochondrial genome function as a single dynamic cellular unit*. J Cell Biol, 1994. **125**(1): p. 43-50.
2. Tait, S.W. and D.R. Green, *Mitochondria and cell signalling*. J Cell Sci, 2012. **125**(Pt 4): p. 807-15.
3. Zhdanov, A.V., et al., *A novel effect of DMOG on cell metabolism: Direct inhibition of mitochondrial function precedes HIF target gene expression*. Biochim Biophys Acta, 2015.
4. Vega-Naredo, I., et al., *Mitochondrial metabolism directs stemness and differentiation in P19 embryonal carcinoma stem cells*. Cell Death Differ, 2014. **21**(10): p. 1560-74.
5. Kasahara, A. and L. Scorrano, *Mitochondria: from cell death executioners to regulators of cell differentiation*. Trends Cell Biol, 2014. **24**(12): p. 761-70.
6. Mandal, S., et al., *Mitochondrial function controls proliferation and early differentiation potential of embryonic stem cells*. Stem Cells, 2011. **29**(3): p. 486-95.
7. Tait, S.W. and D.R. Green, *Mitochondria and cell death: outer membrane permeabilization and beyond*. Nat Rev Mol Cell Biol, 2010. **11**(9): p. 621-32.
8. Ong, S.B. and A.B. Gustafsson, *New roles for mitochondria in cell death in the reperfused myocardium*. Cardiovasc Res, 2012. **94**(2): p. 190-6.
9. Lartigue, L., et al., *Caspase-independent mitochondrial cell death results from loss of respiration, not cytotoxic protein release*. Mol Biol Cell, 2009. **20**(23): p. 4871-84.
10. Tezel, G. and X. Yang, *Caspase-independent component of retinal ganglion cell death, in vitro*. Invest Ophthalmol Vis Sci, 2004. **45**(11): p. 4049-59.
11. Liu, Y.J., et al., *Germinal center cells express bcl-2 protein after activation by signals which prevent their entry into apoptosis*. Eur J Immunol, 1991. **21**(8): p. 1905-10.

12. Karbowski, M. and R.J. Youle, *Regulating mitochondrial outer membrane proteins by ubiquitination and proteasomal degradation*. Curr Opin Cell Biol, 2011. **23**(4): p. 476-82.
13. Raffy, S. and J. Teissie, *Control of lipid membrane stability by cholesterol content*. Biophys J, 1999. **76**(4): p. 2072-80.
14. Colbeau, A., J. Nachbaur, and P.M. Vignais, *Enzymic characterization and lipid composition of rat liver subcellular membranes*. Biochim Biophys Acta, 1971. **249**(2): p. 462-92.
15. Weeber, E.J., et al., *The role of mitochondrial porins and the permeability transition pore in learning and synaptic plasticity*. J Biol Chem, 2002. **277**(21): p. 18891-7.
16. Yano, M., et al., *Identification and functional analysis of human Tom22 for protein import into mitochondria*. Mol Cell Biol, 2000. **20**(19): p. 7205-13.
17. Nargang, F.E., et al., *Role of the negative charges in the cytosolic domain of TOM22 in the import of precursor proteins into mitochondria*. Mol Cell Biol, 1998. **18**(6): p. 3173-81.
18. Haucke, V., et al., *The yeast mitochondrial protein import receptor Mas20p binds precursor proteins through electrostatic interaction with the positively charged presequence*. J Biol Chem, 1995. **270**(10): p. 5565-70.
19. Volman, H., *A morphologic and morphometric study of the mitochondria in several hepatoma cell lines and in isolated hepatocytes*. Virchows Arch B Cell Pathol, 1978. **26**(3): p. 249-59.
20. Comte, J., B. Maisterrena, and D.C. Gautheron, *Lipid composition and protein profiles of outer and inner membranes from pig heart mitochondria. Comparison with microsomes*. Biochim Biophys Acta, 1976. **419**(2): p. 271-84.
21. King, M.E., G.C. Godman, and D.W. King, *Respiratory enzymes and mitochondrial morphology of HeLa and L cells treated with chloramphenicol and ethidium bromide*. J Cell Biol, 1972. **53**(1): p. 127-42.
22. Birch-Machin, M.A. and D.M. Turnbull, *Assaying mitochondrial respiratory complex activity in mitochondria isolated from human cells and tissues*. Methods Cell Biol, 2001. **65**: p. 97-117.

23. van der Bliek, A.M., Q. Shen, and S. Kawajiri, *Mechanisms of mitochondrial fission and fusion*. Cold Spring Harb Perspect Biol, 2013. **5**(6).
24. Collins, T.J., et al., *Mitochondria are morphologically and functionally heterogeneous within cells*. EMBO J, 2002. **21**(7): p. 1616-27.
25. Park, M.K., et al., *Perinuclear, perigranular and sub-plasmalemmal mitochondria have distinct functions in the regulation of cellular calcium transport*. EMBO J, 2001. **20**(8): p. 1863-74.
26. Karbowski, M. and R.J. Youle, *Dynamics of mitochondrial morphology in healthy cells and during apoptosis*. Cell Death Differ, 2003. **10**(8): p. 870-80.
27. Imoto, M., I. Tachibana, and R. Urrutia, *Identification and functional characterization of a novel human protein highly related to the yeast dynamin-like GTPase Vps1p*. J Cell Sci, 1998. **111 (Pt 10)**: p. 1341-9.
28. Labrousse, A.M., et al., *C. elegans dynamin-related protein DRP-1 controls severing of the mitochondrial outer membrane*. Mol Cell, 1999. **4**(5): p. 815-26.
29. Tieu, Q. and J. Nunnari, *Mdv1p is a WD repeat protein that interacts with the dynamin-related GTPase, Dnm1p, to trigger mitochondrial division*. J Cell Biol, 2000. **151**(2): p. 353-66.
30. Shin-ya Miyagishima¹, R.I., Kyoko Toda¹, Haruko Kuroiwa², Tsuneyoshi Kuroiwa¹, *Real-time analyses of chloroplast and mitochondrial division and differences in the behavior of their dividing rings during contraction*. Planta Springer-Verlag, 1999.
31. Shepard, K.A. and M.P. Yaffe, *The yeast dynamin-like protein, Mgm1p, functions on the mitochondrial outer membrane to mediate mitochondrial inheritance*. J Cell Biol, 1999. **144**(4): p. 711-20.
32. Alexander, C., et al., *OPA1, encoding a dynamin-related GTPase, is mutated in autosomal dominant optic atrophy linked to chromosome 3q28*. Nat Genet, 2000. **26**(2): p. 211-5.
33. Rapaport, D., et al., *Fzo1p is a mitochondrial outer membrane protein essential for the biogenesis of functional mitochondria in Saccharomyces cerevisiae*. J Biol Chem, 1998. **273**(32): p. 20150-5.

34. Walberg, M.W. and D.A. Clayton, *In vitro* transcription of human mitochondrial DNA. Identification of specific light strand transcripts from the displacement loop region. J Biol Chem, 1983. **258**(2): p. 1268-75.
35. Kunisada, T. and H. Yamagishi, *Sequence repetition and genomic distribution of small polydisperse circular DNA purified from HeLa cells*. Gene, 1984. **31**(1-3): p. 213-23.
36. Bonawitz, N.D., D.A. Clayton, and G.S. Shadel, *Initiation and beyond: multiple functions of the human mitochondrial transcription machinery*. Mol Cell, 2006. **24**(6): p. 813-25.
37. Alberts B, J.A., Lewis J, et al., *Molecular Biology of the Cell. The Mitochondrion*. New York: Garland Science . , 2002(4th edition).
38. Tessman, I. and M.A. Kennedy, *DNA polymerase II of Escherichia coli in the bypass of abasic sites in vivo*. Genetics, 1994. **136**(2): p. 439-48.
39. Clayton, D.A., J.N. Doda, and E.C. Friedberg, *Absence of a pyrimidine dimer repair mechanism for mitochondrial DNA in mouse and human cells*. Basic Life Sci, 1975. **5B**: p. 589-91.
40. Longley, M.J., et al., *The fidelity of human DNA polymerase gamma with and without exonucleolytic proofreading and the p55 accessory subunit*. J Biol Chem, 2001. **276**(42): p. 38555-62.
41. Thorslund, T., et al., *Repair of 8-oxoG is slower in endogenous nuclear genes than in mitochondrial DNA and is without strand bias*. DNA Repair (Amst), 2002. **1**(4): p. 261-73.
42. He, Y., et al., *Heteroplasmic mitochondrial DNA mutations in normal and tumour cells*. Nature, 2010. **464**(7288): p. 610-4.
43. Limongelli, A., et al., *Variable penetrance of a familial progressive necrotising encephalopathy due to a novel tRNA(Ile) homoplasmic mutation in the mitochondrial genome*. J Med Genet, 2004. **41**(5): p. 342-9.
44. Westermann, B., *Bioenergetic role of mitochondrial fusion and fission*. Biochim Biophys Acta, 2012. **1817**(10): p. 1833-8.

45. Nakada, K., et al., *Inter-mitochondrial complementation: Mitochondria-specific system preventing mice from expression of disease phenotypes by mutant mtDNA*. Nat Med, 2001. **7**(8): p. 934-40.
46. Ivanov, P.L., et al., *Mitochondrial DNA sequence heteroplasmy in the Grand Duke of Russia Georgij Romanov establishes the authenticity of the remains of Tsar Nicholas II*. Nat Genet, 1996. **12**(4): p. 417-20.
47. Kocher, T.D., et al., *Dynamics of mitochondrial DNA evolution in animals: amplification and sequencing with conserved primers*. Proc Natl Acad Sci U S A, 1989. **86**(16): p. 6196-200.
48. Hall, P.A., et al., *Regulation of cell number in the mammalian gastrointestinal tract: the importance of apoptosis*. J Cell Sci, 1994. **107 (Pt 12)**: p. 3569-77.
49. Lawson, J.A., et al., *Inhibition of Fas receptor (CD95)-induced hepatic caspase activation and apoptosis by acetaminophen in mice*. Toxicol Appl Pharmacol, 1999. **156**(3): p. 179-86.
50. Liu, X., et al., *Induction of apoptotic program in cell-free extracts: requirement for dATP and cytochrome c*. Cell, 1996. **86**(1): p. 147-57.
51. Susin, S.A., et al., *Molecular characterization of mitochondrial apoptosis-inducing factor*. Nature, 1999. **397**(6718): p. 441-6.
52. Hao, Z., et al., *Specific ablation of the apoptotic functions of cytochrome C reveals a differential requirement for cytochrome C and Apaf-1 in apoptosis*. Cell, 2005. **121**(4): p. 579-91.
53. Aouacheria, A., et al., *Modulating mitochondria-mediated apoptotic cell death through targeting of Bcl-2 family proteins*. Recent Pat DNA Gene Seq, 2007. **1**(1): p. 43-61.
54. Lee, W.S. and R.J. Sokol, *Liver disease in mitochondrial disorders*. Semin Liver Dis, 2007. **27**(3): p. 259-73.
55. Treem, W.R. and R.J. Sokol, *Disorders of the mitochondria*. Semin Liver Dis, 1998. **18**(3): p. 237-53.
56. Meyers, D.E., H.I. Basha, and M.K. Koenig, *Mitochondrial cardiomyopathy: pathophysiology, diagnosis, and management*. Tex Heart Inst J, 2013. **40**(4): p. 385-94.

57. Haas, R.H., *Autism and mitochondrial disease*. Dev Disabil Res Rev, 2010. **16**(2): p. 144-53.
58. Taylor, R.W. and D.M. Turnbull, *Mitochondrial DNA mutations in human disease*. Nat Rev Genet, 2005. **6**(5): p. 389-402.
59. Moraes, C.T., et al., *Mitochondrial DNA deletions in progressive external ophthalmoplegia and Kearns-Sayre syndrome*. N Engl J Med, 1989. **320**(20): p. 1293-9.
60. Rahman, S., et al., *Decrease of 3243 A-->G mtDNA mutation from blood in MELAS syndrome: a longitudinal study*. Am J Hum Genet, 2001. **68**(1): p. 238-40.
61. Larsson, N.G., et al., *Progressive increase of the mutated mitochondrial DNA fraction in Kearns-Sayre syndrome*. Pediatr Res, 1990. **28**(2): p. 131-6.
62. Weber, K., et al., *A new mtDNA mutation showing accumulation with time and restriction to skeletal muscle*. Am J Hum Genet, 1997. **60**(2): p. 373-80.
63. Larsson, N.G., et al., *Segregation and manifestations of the mtDNA tRNA(Lys) A->G(8344) mutation of myoclonus epilepsy and ragged-red fibers (MERRF) syndrome*. Am J Hum Genet, 1992. **51**(6): p. 1201-12.
64. Taylor, R.W., et al., *A homoplasmic mitochondrial transfer ribonucleic acid mutation as a cause of maternally inherited hypertrophic cardiomyopathy*. J Am Coll Cardiol, 2003. **41**(10): p. 1786-96.
65. Sacconi, S., et al., *A functionally dominant mitochondrial DNA mutation*. Hum Mol Genet, 2008. **17**(12): p. 1814-20.
66. Schon EA1, R.R., Moraes CT, Nakase H, Zeviani M, DiMauro S., *A direct repeat is a hotspot for large-scale deletion of human mitochondrial DNA*. Science, 1989. **Apr 21;244(4902):346-9**.
67. Cortopassi, G.A., et al., *A pattern of accumulation of a somatic deletion of mitochondrial DNA in aging human tissues*. Proc Natl Acad Sci U S A, 1992. **89**(16): p. 7370-4.
68. Bender, A., et al., *High levels of mitochondrial DNA deletions in substantia nigra neurons in aging and Parkinson disease*. Nat Genet, 2006. **38**(5): p. 515-7.

69. Sciacco, M., et al., *Distribution of wild-type and common deletion forms of mtDNA in normal and respiration-deficient muscle fibers from patients with mitochondrial myopathy*. Hum Mol Genet, 1994. **3**(1): p. 13-9.
70. Macmillan, C., et al., *Pedigree analysis of French Canadian families with T14484C Leber's hereditary optic neuropathy*. Neurology, 1998. **50**(2): p. 417-22.
71. Thorburn, D.R., et al., *Biochemical and molecular diagnosis of mitochondrial respiratory chain disorders*. Biochim Biophys Acta, 2004. **1659**(2-3): p. 121-8.
72. Gorman, G.S., et al., *Prevalence of nuclear and mitochondrial DNA mutations related to adult mitochondrial disease*. Ann Neurol, 2015. **77**(5): p. 753-9.
73. Ozawa, T., *Mechanism of somatic mitochondrial DNA mutations associated with age and diseases*. Biochim Biophys Acta, 1995. **1271**(1): p. 177-89.
74. Chiu, A.Y., et al., *Age-dependent penetrance of disease in a transgenic mouse model of familial amyotrophic lateral sclerosis*. Mol Cell Neurosci, 1995. **6**(4): p. 349-62.
75. Schneider, S. and L. Excoffier, *Estimation of past demographic parameters from the distribution of pairwise differences when the mutation rates vary among sites: application to human mitochondrial DNA*. Genetics, 1999. **152**(3): p. 1079-89.
76. Reeve, A.K., K.J. Krishnan, and D. Turnbull, *Mitochondrial DNA mutations in disease, aging, and neurodegeneration*. Ann N Y Acad Sci, 2008. **1147**: p. 21-9.
77. Chol, M., et al., *The mitochondrial DNA G13513A MELAS mutation in the NADH dehydrogenase 5 gene is a frequent cause of Leigh-like syndrome with isolated complex I deficiency*. J Med Genet, 2003. **40**(3): p. 188-91.
78. Maceluch, J.A. and M. Niedziela, *The clinical diagnosis and molecular genetics of kearns-sayre syndrome: a complex mitochondrial encephalomyopathy*. Pediatr Endocrinol Rev, 2006. **4**(2): p. 117-37.
79. Rahman, S. and J. Poulton, *Diagnosis of mitochondrial DNA depletion syndromes*. Arch Dis Child, 2009. **94**(1): p. 3-5.
80. Corona, P., et al., *A novel mtDNA mutation in the ND5 subunit of complex I in two MELAS patients*. Ann Neurol, 2001. **49**(1): p. 106-10.

81. Goto, Y., I. Nonaka, and S. Horai, *A mutation in the tRNA(Leu)(UUR) gene associated with the MELAS subgroup of mitochondrial encephalomyopathies*. Nature, 1990. **348**(6302): p. 651-3.
82. Tatuch, Y., et al., *Heteroplasmic mtDNA mutation (T----G) at 8993 can cause Leigh disease when the percentage of abnormal mtDNA is high*. Am J Hum Genet, 1992. **50**(4): p. 852-8.
83. Man, P.Y., D.M. Turnbull, and P.F. Chinnery, *Leber hereditary optic neuropathy*. J Med Genet, 2002. **39**(3): p. 162-9.
84. Riordan-Eva, P., et al., *The clinical features of Leber's hereditary optic neuropathy defined by the presence of a pathogenic mitochondrial DNA mutation*. Brain, 1995. **118 (Pt 2)**: p. 319-37.
85. Shoffner, J.M., et al., *Myoclonic epilepsy and ragged-red fiber disease (MERRF) is associated with a mitochondrial DNA tRNA(Lys) mutation*. Cell, 1990. **61**(6): p. 931-7.
86. Fowler, B.A., J.S. Woods, and C.M. Schiller, *Ultrastructural and biochemical effects of prolonged oral arsenic exposure on liver mitochondria of rats*. Environ Health Perspect, 1977. **19**: p. 197-204.
87. Moraes, C.T., et al., *Phenotype-genotype correlations in skeletal muscle of patients with mtDNA deletions*. Muscle Nerve Suppl, 1995. **3**: p. S150-3.
88. Taylor, R.W., et al., *The diagnosis of mitochondrial muscle disease*. Neuromuscul Disord, 2004. **14**(4): p. 237-45.
89. Jancura, D., et al., *How hydrogen peroxide is metabolized by oxidized cytochrome c oxidase*. Biochemistry, 2014. **53**(22): p. 3564-75.
90. Szuhai, K., et al., *Simultaneous A8344G heteroplasmy and mitochondrial DNA copy number quantification in myoclonus epilepsy and ragged-red fibers (MERRF) syndrome by a multiplex molecular beacon based real-time fluorescence PCR*. Nucleic Acids Res, 2001. **29**(3): p. E13.
91. Kirby, D.M., et al., *Biochemical assays of respiratory chain complex activity*. Methods Cell Biol, 2007. **80**: p. 93-119.
92. Janssen, A.J., et al., *Muscle 3243A-->G mutation load and capacity of the mitochondrial energy-generating system*. Ann Neurol, 2008. **63**(4): p. 473-81.

93. Holt, I.J., A.E. Harding, and J.A. Morgan-Hughes, *Deletions of muscle mitochondrial DNA in patients with mitochondrial myopathies*. *Nature*, 1988. **331**(6158): p. 717-9.
94. Holt, I.J., A.E. Harding, and J.A. Morgan-Hughes, *Deletions of muscle mitochondrial DNA in mitochondrial myopathies: sequence analysis and possible mechanisms*. *Nucleic Acids Res*, 1989. **17**(12): p. 4465-9.
95. Haas, R.H., et al., *The in-depth evaluation of suspected mitochondrial disease*. *Mol Genet Metab*, 2008. **94**(1): p. 16-37.
96. Taylor, R.W., et al., *The determination of complete human mitochondrial DNA sequences in single cells: implications for the study of somatic mitochondrial DNA point mutations*. *Nucleic Acids Res*, 2001. **29**(15): p. E74-4.
97. Fischer, S.G. and L.S. Lerman, *Length-independent separation of DNA restriction fragments in two-dimensional gel electrophoresis*. *Cell*, 1979. **16**(1): p. 191-200.
98. van Den Bosch, B.J., et al., *Mutation analysis of the entire mitochondrial genome using denaturing high performance liquid chromatography*. *Nucleic Acids Res*, 2000. **28**(20): p. E89.
99. Zhou, S., et al., *An oligonucleotide microarray for high-throughput sequencing of the mitochondrial genome*. *J Mol Diagn*, 2006. **8**(4): p. 476-82.
100. McFarland, R., et al., *Assigning pathogenicity to mitochondrial tRNA mutations: when "definitely maybe" is not good enough*. *Trends Genet*, 2004. **20**(12): p. 591-6.
101. Taivassalo, T., et al., *Endurance training and detraining in mitochondrial myopathies due to single large-scale mtDNA deletions*. *Brain*, 2006. **129**(Pt 12): p. 3391-401.
102. Wenz, T., et al., *Endurance exercise is protective for mice with mitochondrial myopathy*. *J Appl Physiol* (1985), 2009. **106**(5): p. 1712-9.
103. Taivassalo, T., et al., *Gene shifting: a novel therapy for mitochondrial myopathy*. *Hum Mol Genet*, 1999. **8**(6): p. 1047-52.
104. Murphy, J.L., et al., *Resistance training in patients with single, large-scale deletions of mitochondrial DNA*. *Brain*, 2008. **131**(Pt 11): p. 2832-40.

105. Taylor, R.W., et al., *Selective inhibition of mutant human mitochondrial DNA replication in vitro by peptide nucleic acids*. Nat Genet, 1997. **15**(2): p. 212-5.
106. Bacman, S.R., et al., *Modulating mtDNA heteroplasmy by mitochondria-targeted restriction endonucleases in a 'differential multiple cleavage-site' model*. Gene Ther, 2007. **14**(18): p. 1309-18.
107. Minczuk, M., et al., *Sequence-specific modification of mitochondrial DNA using a chimeric zinc finger methylase*. Proc Natl Acad Sci U S A, 2006. **103**(52): p. 19689-94.
108. Manfredi, G., et al., *Rescue of a deficiency in ATP synthesis by transfer of MTATP6, a mitochondrial DNA-encoded gene, to the nucleus*. Nat Genet, 2002. **30**(4): p. 394-9.
109. Bonnet, C., et al., *Allotopic mRNA localization to the mitochondrial surface rescues respiratory chain defects in fibroblasts harboring mitochondrial DNA mutations affecting complex I or v subunits*. Rejuvenation Res, 2007. **10**(2): p. 127-44.
110. Rubio, M.A., et al., *Mammalian mitochondria have the innate ability to import tRNAs by a mechanism distinct from protein import*. Proc Natl Acad Sci U S A, 2008. **105**(27): p. 9186-91.
111. Ma, H., et al., *Metabolic rescue in pluripotent cells from patients with mtDNA disease*. Nature, 2015.
112. Brown, D.T., et al., *Random genetic drift determines the level of mutant mtDNA in human primary oocytes*. Am J Hum Genet, 2001. **68**(2): p. 533-6.
113. White, S.L., et al., *Two cases of prenatal analysis for the pathogenic T to G substitution at nucleotide 8993 in mitochondrial DNA*. Prenat Diagn, 1999. **19**(12): p. 1165-8.
114. Sato, A., et al., *Gene therapy for progeny of mito-mice carrying pathogenic mtDNA by nuclear transplantation*. Proc Natl Acad Sci U S A, 2005. **102**(46): p. 16765-70.
115. Craven, L., et al., *Pronuclear transfer in human embryos to prevent transmission of mitochondrial DNA disease*. Nature, 2010. **465**(7294): p. 82-5.

116. Amato, P., et al., *Three-parent in vitro fertilization: gene replacement for the prevention of inherited mitochondrial diseases*. Fertil Steril, 2014. **101**(1): p. 31-5.
117. Callaway, E., *World hails embryo vote*. Nature, 2015. **518**(7538): p. 145-6.
118. Degli Esposti, D., et al., *Mitochondrial roles and cytoprotection in chronic liver injury*. Biochem Res Int, 2012. **2012**: p. 387626.
119. Labbe, G., D. Pessayre, and B. Fromenty, *Drug-induced liver injury through mitochondrial dysfunction: mechanisms and detection during preclinical safety studies*. Fundam Clin Pharmacol, 2008. **22**(4): p. 335-53.
120. Chariot, P., et al., *Zidovudine-induced mitochondrial disorder with massive liver steatosis, myopathy, lactic acidosis, and mitochondrial DNA depletion*. J Hepatol, 1999. **30**(1): p. 156-60.
121. Cormier-Daire, V., et al., *Neonatal and delayed-onset liver involvement in disorders of oxidative phosphorylation*. J Pediatr, 1997. **130**(5): p. 817-22.
122. Moraes, C.T., et al., *mtDNA depletion with variable tissue expression: a novel genetic abnormality in mitochondrial diseases*. Am J Hum Genet, 1991. **48**(3): p. 492-501.
123. Narkewicz, M.R., et al., *Liver involvement in Alpers disease*. J Pediatr, 1991. **119**(2): p. 260-7.
124. Morikawa, Y., et al., *Pearson's marrow/pancreas syndrome: a histological and genetic study*. Virchows Arch A Pathol Anat Histopathol, 1993. **423**(3): p. 227-31.
125. Cormier-Daire, V., et al., *Mitochondrial DNA rearrangements with onset as chronic diarrhea with villous atrophy*. J Pediatr, 1994. **124**(1): p. 63-70.
126. Holve, S., et al., *Liver disease in Navajo neuropathy*. J Pediatr, 1999. **135**(4): p. 482-93.
127. Sokol, R.J. and W.R. Treem, *Mitochondria and childhood liver diseases*. J Pediatr Gastroenterol Nutr, 1999. **28**(1): p. 4-16.
128. Mahoney, D.J., G. Parise, and M.A. Tarnopolsky, *Nutritional and exercise-based therapies in the treatment of mitochondrial disease*. Curr Opin Clin Nutr Metab Care, 2002. **5**(6): p. 619-29.

129. Eleff, S., et al., *³¹P NMR study of improvement in oxidative phosphorylation by vitamins K3 and C in a patient with a defect in electron transport at complex III in skeletal muscle*. Proc Natl Acad Sci U S A, 1984. **81**(11): p. 3529-33.
130. Chen, R.S., C.C. Huang, and N.S. Chu, *Coenzyme Q10 treatment in mitochondrial encephalomyopathies. Short-term double-blind, crossover study*. Eur Neurol, 1997. **37**(4): p. 212-8.
131. Dubern, B., et al., *Orthotopic liver transplantation for mitochondrial respiratory chain disorders: a study of 5 children*. Transplantation, 2001. **71**(5): p. 633-7.
132. Thomson, M., et al., *Generalised mitochondrial cytopathy is an absolute contraindication to orthotopic liver transplant in childhood*. J Pediatr Gastroenterol Nutr, 1998. **26**(4): p. 478-81.
133. Huang, Y.S., et al., *Cytochrome P450 2E1 genotype and the susceptibility to antituberculosis drug-induced hepatitis*. Hepatology, 2003. **37**(4): p. 924-30.
134. Fromenty, B. and D. Pessayre, *Inhibition of mitochondrial beta-oxidation as a mechanism of hepatotoxicity*. Pharmacol Ther, 1995. **67**(1): p. 101-54.
135. Gougeon, M.L., et al., *Adipocytes targets and actors in the pathogenesis of HIV-associated lipodystrophy and metabolic alterations*. Antivir Ther, 2004. **9**(2): p. 161-77.
136. Note, R., et al., *Mitochondrial and metabolic effects of nucleoside reverse transcriptase inhibitors (NRTIs) in mice receiving one of five single- and three dual-NRTI treatments*. Antimicrob Agents Chemother, 2003. **47**(11): p. 3384-92.
137. Masubuchi, Y., S. Kano, and T. Horie, *Mitochondrial permeability transition as a potential determinant of hepatotoxicity of antidiabetic thiazolidinediones*. Toxicology, 2006. **222**(3): p. 233-9.
138. Trost, L.C. and J.J. Lemasters, *The mitochondrial permeability transition: a new pathophysiological mechanism for Reye's syndrome and toxic liver injury*. J Pharmacol Exp Ther, 1996. **278**(3): p. 1000-5.
139. Bae, M.A. and B.J. Song, *Critical role of c-Jun N-terminal protein kinase activation in troglitazone-induced apoptosis of human HepG2 hepatoma cells*. Mol Pharmacol, 2003. **63**(2): p. 401-8.

140. Berson, A., et al., *Steatohepatitis-inducing drugs cause mitochondrial dysfunction and lipid peroxidation in rat hepatocytes*. Gastroenterology, 1998. **114**(4): p. 764-74.
141. Larosche, I., et al., *Tamoxifen inhibits topoisomerases, depletes mitochondrial DNA, and triggers steatosis in mouse liver*. J Pharmacol Exp Ther, 2007. **321**(2): p. 526-35.
142. Begriche, K., et al., *Drug-induced toxicity on mitochondria and lipid metabolism: mechanistic diversity and deleterious consequences for the liver*. J Hepatol, 2011. **54**(4): p. 773-94.
143. Deschamps, D., et al., *Inhibition by salicylic acid of the activation and thus oxidation of long chain fatty acids. Possible role in the development of Reye's syndrome*. J Pharmacol Exp Ther, 1991. **259**(2): p. 894-904.
144. Lewis, W., et al., *Fialuridine and its metabolites inhibit DNA polymerase gamma at sites of multiple adjacent analog incorporation, decrease mtDNA abundance, and cause mitochondrial structural defects in cultured hepatoblasts*. Proc Natl Acad Sci U S A, 1996. **93**(8): p. 3592-7.
145. Benbrik, E., et al., *Cellular and mitochondrial toxicity of zidovudine (AZT), didanosine (ddI) and zalcitabine (ddC) on cultured human muscle cells*. J Neurol Sci, 1997. **149**(1): p. 19-25.
146. Perlmutter, D.H., *Liver injury in alpha1-antitrypsin deficiency: an aggregated protein induces mitochondrial injury*. J Clin Invest, 2002. **110**(11): p. 1579-83.
147. McCormack, A.L., et al., *Environmental risk factors and Parkinson's disease: selective degeneration of nigral dopaminergic neurons caused by the herbicide paraquat*. Neurobiol Dis, 2002. **10**(2): p. 119-27.
148. Fromenty, B., et al., *Hepatic mitochondrial DNA deletion in alcoholics: association with microvesicular steatosis*. Gastroenterology, 1995. **108**(1): p. 193-200.
149. Levy, M., *Role of viral infections in the induction of adverse drug reactions*. Drug Saf, 1997. **16**(1): p. 1-8.
150. Prandota, J., *Important role of prodromal viral infections responsible for inhibition of xenobiotic metabolizing enzymes in the pathomechanism of idiopathic Reye's*

- syndrome, Stevens-Johnson syndrome, autoimmune hepatitis, and hepatotoxicity of the therapeutic doses of acetaminophen used in genetically predisposed persons.* Am J Ther, 2002. **9**(2): p. 149-56.
151. McClusky, D.A., 3rd, et al., *Hepatic surgery and hepatic surgical anatomy: historical partners in progress.* World J Surg, 1997. **21**(3): p. 330-42.
 152. Sakka, S.G., *Assessing liver function.* Curr Opin Crit Care, 2007. **13**(2): p. 207-14.
 153. Greengard, O., M. Federman, and W.E. Knox, *Cytomorphometry of developing rat liver and its application to enzymic differentiation.* J Cell Biol, 1972. **52**(2): p. 261-72.
 154. Bradley, S.E., et al., *The Estimation of Hepatic Blood Flow in Man.* J Clin Invest, 1945. **24**(6): p. 890-7.
 155. Srivastava, D., et al., *Hepatic venous blood and the development of pulmonary arteriovenous malformations in congenital heart disease.* Circulation, 1995. **92**(5): p. 1217-22.
 156. Man, K., et al., *Graft injury in relation to graft size in right lobe live donor liver transplantation: a study of hepatic sinusoidal injury in correlation with portal hemodynamics and intragraft gene expression.* Ann Surg, 2003. **237**(2): p. 256-64.
 157. Souba, W.W., R.J. Smith, and D.W. Wilmore, *Glutamine metabolism by the intestinal tract.* JPEN J Parenter Enteral Nutr, 1985. **9**(5): p. 608-17.
 158. Wisse, E., *An ultrastructural characterization of the endothelial cell in the rat liver sinusoid under normal and various experimental conditions, as a contribution to the distinction between endothelial and Kupffer cells.* J Ultrastruct Res, 1972. **38**(5): p. 528-62.
 159. Motta, P. and K.R. Porter, *Structure of rat liver sinusoids and associated tissue spaces as revealed by scanning electron microscopy.* Cell Tissue Res, 1974. **148**(1): p. 111-25.
 160. Wisse, E., *An electron microscopic study of the fenestrated endothelial lining of rat liver sinusoids.* J Ultrastruct Res, 1970. **31**(1): p. 125-50.

161. Popescu, D., et al., *Hydrodynamic effects on the solute transport across endothelial pores and hepatocyte membranes*. Phys Med Biol, 2000. **45**(11): p. N157-65.
162. Godoy, P., et al., *Recent advances in 2D and 3D in vitro systems using primary hepatocytes, alternative hepatocyte sources and non-parenchymal liver cells and their use in investigating mechanisms of hepatotoxicity, cell signaling and ADME*. Arch Toxicol, 2013. **87**(8): p. 1315-530.
163. Widmann, J.J., R.S. Cotran, and H.D. Fahimi, *Mononuclear phagocytes (Kupffer cells) and endothelial cells. Identification of two functional cell types in rat liver sinusoids by endogenous peroxidase activity*. J Cell Biol, 1972. **52**(1): p. 159-70.
164. Willekens, F.L., et al., *Liver Kupffer cells rapidly remove red blood cell-derived vesicles from the circulation by scavenger receptors*. Blood, 2005. **105**(5): p. 2141-5.
165. Arii, S. and M. Imamura, *Physiological role of sinusoidal endothelial cells and Kupffer cells and their implication in the pathogenesis of liver injury*. J Hepatobiliary Pancreat Surg, 2000. **7**(1): p. 40-8.
166. Hildebrand, F., et al., *Kupffer cells and their mediators: the culprits in producing distant organ damage after trauma-hemorrhage*. Am J Pathol, 2006. **169**(3): p. 784-94.
167. Matsuoka, M. and H. Tsukamoto, *Stimulation of hepatic lipocyte collagen production by Kupffer cell-derived transforming growth factor beta: implication for a pathogenetic role in alcoholic liver fibrogenesis*. Hepatology, 1990. **11**(4): p. 599-605.
168. Thurman, R.G., II. *Alcoholic liver injury involves activation of Kupffer cells by endotoxin*. Am J Physiol, 1998. **275**(4 Pt 1): p. G605-11.
169. Minato, Y., Y. Hasumura, and J. Takeuchi, *The role of fat-storing cells in Disse space fibrogenesis in alcoholic liver disease*. Hepatology, 1983. **3**(4): p. 559-66.
170. Han, Y.P., et al., *A matrix metalloproteinase-9 activation cascade by hepatic stellate cells in trans-differentiation in the three-dimensional extracellular matrix*. J Biol Chem, 2007. **282**(17): p. 12928-39.

171. Di Campli, C., et al., *Advances in extracorporeal detoxification by MARS dialysis in patients with liver failure*. Curr Med Chem, 2003. **10**(4): p. 341-8.
172. Ruepp, S.U., et al., *Genomics and proteomics analysis of acetaminophen toxicity in mouse liver*. Toxicol Sci, 2002. **65**(1): p. 135-50.
173. Igoudjil, A., et al., *High concentrations of stavudine impair fatty acid oxidation without depleting mitochondrial DNA in cultured rat hepatocytes*. Toxicol In Vitro, 2008. **22**(4): p. 887-98.
174. Maisonneuve, C., et al., *Effects of zidovudine, stavudine and beta-aminoisobutyric acid on lipid homeostasis in mice: possible role in human fat wasting*. Antivir Ther, 2004. **9**(5): p. 801-10.
175. Stacchino, C., et al., *Detoxification process for glutaraldehyde-treated bovine pericardium: biological, chemical and mechanical characterization*. J Heart Valve Dis, 1998. **7**(2): p. 190-4.
176. Moulson, C.L., et al., *Homozygous and compound heterozygous mutations in ZMPSTE24 cause the laminopathy restrictive dermopathy*. J Invest Dermatol, 2005. **125**(5): p. 913-9.
177. Karlsson, H.L., et al., *Copper oxide nanoparticles are highly toxic: a comparison between metal oxide nanoparticles and carbon nanotubes*. Chem Res Toxicol, 2008. **21**(9): p. 1726-32.
178. Dai, D., et al., *Identification of variants of CYP3A4 and characterization of their abilities to metabolize testosterone and chlorpyrifos*. J Pharmacol Exp Ther, 2001. **299**(3): p. 825-31.
179. Nakamura, Y., et al., *A phase II detoxification enzyme inducer from lemongrass: identification of citral and involvement of electrophilic reaction in the enzyme induction*. Biochem Biophys Res Commun, 2003. **302**(3): p. 593-600.
180. Van der Logt, E.M., et al., *Effects of dietary anticarcinogens and nonsteroidal anti-inflammatory drugs on rat gastrointestinal UDP-glucuronosyltransferases*. Anticancer Res, 2004. **24**(2B): p. 843-9.
181. Mizuno, N., et al., *Impact of drug transporter studies on drug discovery and development*. Pharmacol Rev, 2003. **55**(3): p. 425-61.

182. Keppler, D., *Multidrug resistance proteins (MRPs, ABCs): importance for pathophysiology and drug therapy*. Handb Exp Pharmacol, 2011(201): p. 299-323.
183. Liska, D.J., *The detoxification enzyme systems*. Altern Med Rev, 1998. **3**(3): p. 187-98.
184. Moyer, A.M., et al., *Acetaminophen-NAPQI hepatotoxicity: a cell line model system genome-wide association study*. Toxicol Sci, 2011. **120**(1): p. 33-41.
185. Farrell, G.C. and C.Z. Larter, *Nonalcoholic fatty liver disease: from steatosis to cirrhosis*. Hepatology, 2006. **43**(2 Suppl 1): p. S99-S112.
186. Fannin, R.D., et al., *Acetaminophen dosing of humans results in blood transcriptome and metabolome changes consistent with impaired oxidative phosphorylation*. Hepatology, 2010. **51**(1): p. 227-36.
187. Perno, C.F., et al., *Inhibition of human immunodeficiency virus (HIV-1/HTLV-III_{Ba-L}) replication in fresh and cultured human peripheral blood monocytes/macrophages by azidothymidine and related 2',3'-dideoxynucleosides*. J Exp Med, 1988. **168**(3): p. 1111-25.
188. Cuatrecasas, P., *Interaction of Vibrio cholerae enterotoxin with cell membranes*. Biochemistry, 1973. **12**(18): p. 3547-58.
189. Orrenius, S., M.J. McCabe, Jr., and P. Nicotera, *Ca²⁺-dependent mechanisms of cytotoxicity and programmed cell death*. Toxicol Lett, 1992. **64-65 Spec No**: p. 357-64.
190. Orrenius, S., D.J. McConkey, and P. Nicotera, *Role of calcium in toxic and programmed cell death*. Adv Exp Med Biol, 1991. **283**: p. 419-25.
191. Guengerich, F.P. and D.C. Liebler, *Enzymatic activation of chemicals to toxic metabolites*. Crit Rev Toxicol, 1985. **14**(3): p. 259-307.
192. Gosemann, J.H., et al., *TLR4 influences the humoral and cellular immune response during polymicrobial sepsis*. Injury, 2010. **41**(10): p. 1060-7.
193. Benali-Furet, N.L., et al., *Hepatitis C virus core triggers apoptosis in liver cells by inducing ER stress and ER calcium depletion*. Oncogene, 2005. **24**(31): p. 4921-33.

194. Leist, M., et al., *Tumor necrosis factor-induced hepatocyte apoptosis precedes liver failure in experimental murine shock models*. Am J Pathol, 1995. **146**(5): p. 1220-34.
195. Giannini, E., et al., *Progressive liver functional impairment is associated with an increase in AST/ALT ratio*. Dig Dis Sci, 1999. **44**(6): p. 1249-53.
196. Giannini, E., et al., *Validity and clinical utility of the aspartate aminotransferase-alanine aminotransferase ratio in assessing disease severity and prognosis in patients with hepatitis C virus-related chronic liver disease*. Arch Intern Med, 2003. **163**(2): p. 218-24.
197. Haukeland, J.W., et al., *Systemic inflammation in nonalcoholic fatty liver disease is characterized by elevated levels of CCL2*. J Hepatol, 2006. **44**(6): p. 1167-74.
198. Ramachandran, R. and S. Kakar, *Histological patterns in drug-induced liver disease*. J Clin Pathol, 2009. **62**(6): p. 481-92.
199. Bach, N., S.N. Thung, and F. Schaffner, *The histological features of chronic hepatitis C and autoimmune chronic hepatitis: a comparative analysis*. Hepatology, 1992. **15**(4): p. 572-7.
200. Grattagliano, I., et al., *Mitochondria in chronic liver disease*. Curr Drug Targets, 2011. **12**(6): p. 879-93.
201. Dimauro, S. and P. Rustin, *A critical approach to the therapy of mitochondrial respiratory chain and oxidative phosphorylation diseases*. Biochim Biophys Acta, 2009. **1792**(12): p. 1159-67.
202. Brodsky, F.M., et al., *Biological basket weaving: formation and function of clathrin-coated vesicles*. Annu Rev Cell Dev Biol, 2001. **17**: p. 517-68.
203. Valladeau, J., et al., *Langerin, a novel C-type lectin specific to Langerhans cells, is an endocytic receptor that induces the formation of Birbeck granules*. Immunity, 2000. **12**(1): p. 71-81.
204. Wang, L.H., K.G. Rothberg, and R.G. Anderson, *Mis-assembly of clathrin lattices on endosomes reveals a regulatory switch for coated pit formation*. J Cell Biol, 1993. **123**(5): p. 1107-17.
205. Parton, R.G., et al., *Plasticity of early endosomes*. J Cell Sci, 1992. **103 (Pt 2)**: p. 335-48.

206. Ramanathan, H.N. and Y. Ye, *The p97 ATPase associates with EEA1 to regulate the size of early endosomes*. Cell Res, 2012. **22**(2): p. 346-59.
207. Poteryaev, D., et al., *Identification of the switch in early-to-late endosome transition*. Cell, 2010. **141**(3): p. 497-508.
208. Falk, J., et al., *Rab5 and Rab4 regulate axon elongation in the Xenopus visual system*. J Neurosci, 2014. **34**(2): p. 373-91.
209. Killisch, I., et al., *Characterization of early and late endocytic compartments of the transferrin cycle. Transferrin receptor antibody blocks erythroid differentiation by trapping the receptor in the early endosome*. J Cell Sci, 1992. **103 (Pt 1)**: p. 211-32.
210. Wilson, J.M., et al., *EEA1, a tethering protein of the early sorting endosome, shows a polarized distribution in hippocampal neurons, epithelial cells, and fibroblasts*. Mol Biol Cell, 2000. **11**(8): p. 2657-71.
211. Viotti, C., et al., *Endocytic and secretory traffic in Arabidopsis merge in the trans-Golgi network/early endosome, an independent and highly dynamic organelle*. Plant Cell, 2010. **22**(4): p. 1344-57.
212. Barysch, S.V., et al., *Sorting in early endosomes reveals connections to docking- and fusion-associated factors*. Proc Natl Acad Sci U S A, 2009. **106**(24): p. 9697-702.
213. Grant, B.D. and J.G. Donaldson, *Pathways and mechanisms of endocytic recycling*. Nat Rev Mol Cell Biol, 2009. **10**(9): p. 597-608.
214. Tjelle, T.E., et al., *Isolation and characterization of early endosomes, late endosomes and terminal lysosomes: their role in protein degradation*. J Cell Sci, 1996. **109 (Pt 12)**: p. 2905-14.
215. Chia, P.Z., P. Gunn, and P.A. Gleeson, *Cargo trafficking between endosomes and the trans-Golgi network*. Histochem Cell Biol, 2013. **140**(3): p. 307-15.
216. Raiborg, C. and H. Stenmark, *The ESCRT machinery in endosomal sorting of ubiquitylated membrane proteins*. Nature, 2009. **458**(7237): p. 445-52.
217. Jovic, M., et al., *The early endosome: a busy sorting station for proteins at the crossroads*. Histol Histopathol, 2010. **25**(1): p. 99-112.

218. Ghosh, P. and S. Kornfeld, *The GGA proteins: key players in protein sorting at the trans-Golgi network*. Eur J Cell Biol, 2004. **83**(6): p. 257-62.
219. Seaman, M.N., *The retromer complex - endosomal protein recycling and beyond*. J Cell Sci, 2012. **125**(Pt 20): p. 4693-702.
220. Brown, W.J., J. Goodhouse, and M.G. Farquhar, *Mannose-6-phosphate receptors for lysosomal enzymes cycle between the Golgi complex and endosomes*. J Cell Biol, 1986. **103**(4): p. 1235-47.
221. Carroll, K.S., et al., *Role of Rab9 GTPase in facilitating receptor recruitment by TIP47*. Science, 2001. **292**(5520): p. 1373-6.
222. Wood, S.A., J.E. Park, and W.J. Brown, *Brefeldin A causes a microtubule-mediated fusion of the trans-Golgi network and early endosomes*. Cell, 1991. **67**(3): p. 591-600.
223. Levkowitz, G., et al., *c-Cbl/Sli-1 regulates endocytic sorting and ubiquitination of the epidermal growth factor receptor*. Genes Dev, 1998. **12**(23): p. 3663-74.
224. Ghosh, R.N., D.L. Gelman, and F.R. Maxfield, *Quantification of low density lipoprotein and transferrin endocytic sorting HEp2 cells using confocal microscopy*. J Cell Sci, 1994. **107** (Pt 8): p. 2177-89.
225. Piper, R.C. and J.P. Luzio, *Late endosomes: sorting and partitioning in multivesicular bodies*. Traffic, 2001. **2**(9): p. 612-21.
226. Vanlandingham, P.A. and B.P. Ceresa, *Rab7 regulates late endocytic trafficking downstream of multivesicular body biogenesis and cargo sequestration*. J Biol Chem, 2009. **284**(18): p. 12110-24.
227. Soldati, T., et al., *Rab7 and Rab9 are recruited onto late endosomes by biochemically distinguishable processes*. J Biol Chem, 1995. **270**(43): p. 25541-8.
228. Juuti-Uusitalo, K., et al., *Selective targeting of avidin/mannose 6-phosphate receptor chimeras to early or late endosomes*. Eur J Cell Biol, 2000. **79**(7): p. 458-68.
229. Luzio, J.P., et al., *Lysosome-endosome fusion and lysosome biogenesis*. J Cell Sci, 2000. **113** (Pt 9): p. 1515-24.

230. Antonin, W., et al., *A SNARE complex mediating fusion of late endosomes defines conserved properties of SNARE structure and function*. EMBO J, 2000. **19**(23): p. 6453-64.
231. Hirst, J., C.E. Futter, and C.R. Hopkins, *The kinetics of mannose 6-phosphate receptor trafficking in the endocytic pathway in HEp-2 cells: the receptor enters and rapidly leaves multivesicular endosomes without accumulating in a prelysosomal compartment*. Mol Biol Cell, 1998. **9**(4): p. 809-16.
232. Terman, A., et al., *Mitochondrial turnover and aging of long-lived postmitotic cells: the mitochondrial-lysosomal axis theory of aging*. Antioxid Redox Signal, 2010. **12**(4): p. 503-35.
233. Nishino, I., et al., *Primary LAMP-2 deficiency causes X-linked vacuolar cardiomyopathy and myopathy (Danon disease)*. Nature, 2000. **406**(6798): p. 906-10.
234. Fok, A.K., et al., *Modulation of the digestive lysosomal system in Paramecium caudatum. II. Physiological effects of cytochalasin B, colchicine and trifluoperazine*. Eur J Cell Biol, 1985. **37**: p. 27-34.
235. Ogata, M., et al., *Autophagy is activated for cell survival after endoplasmic reticulum stress*. Mol Cell Biol, 2006. **26**(24): p. 9220-31.
236. Ryter, S.W., S.M. Cloonan, and A.M. Choi, *Autophagy: a critical regulator of cellular metabolism and homeostasis*. Mol Cells, 2013. **36**(1): p. 7-16.
237. Bright, N.A., et al., *Dense core lysosomes can fuse with late endosomes and are re-formed from the resultant hybrid organelles*. J Cell Sci, 1997. **110** (Pt 17): p. 2027-40.
238. Bright, N.A., M.J. Gratian, and J.P. Luzio, *Endocytic delivery to lysosomes mediated by concurrent fusion and kissing events in living cells*. Curr Biol, 2005. **15**(4): p. 360-5.
239. Seguin, S.J., et al., *Inhibition of autophagy, lysosome and VCP function impairs stress granule assembly*. Cell Death Differ, 2014. **21**(12): p. 1838-51.
240. Fredericksen, B.L., et al., *Inhibition of endosomal/lysosomal degradation increases the infectivity of human immunodeficiency virus*. J Virol, 2002. **76**(22): p. 11440-6.

241. Hudgin, R.L., et al., *The isolation and properties of a rabbit liver binding protein specific for asialoglycoproteins*. J Biol Chem, 1974. **249**(17): p. 5536-43.
242. Halberg, D.F., et al., *Major and minor forms of the rat liver asialoglycoprotein receptor are independent galactose-binding proteins. Primary structure and glycosylation heterogeneity of minor receptor forms*. J Biol Chem, 1987. **262**(20): p. 9828-38.
243. McPhaul, M. and P. Berg, *Formation of functional asialoglycoprotein receptor after transfection with cDNAs encoding the receptor proteins*. Proc Natl Acad Sci U S A, 1986. **83**(23): p. 8863-7.
244. Fuhrer, C., et al., *The two subunits of the asialoglycoprotein receptor contain different sorting information*. J Biol Chem, 1994. **269**(5): p. 3277-82.
245. Ashwell, G. and J. Harford, *Carbohydrate-specific receptors of the liver*. Annu Rev Biochem, 1982. **51**: p. 531-54.
246. Morell, A.G., et al., *The role of sialic acid in determining the survival of glycoproteins in the circulation*. J Biol Chem, 1971. **246**(5): p. 1461-7.
247. Ashwell, G. and A.G. Morell, *The role of surface carbohydrates in the hepatic recognition and transport of circulating glycoproteins*. Adv Enzymol Relat Areas Mol Biol, 1974. **41**(0): p. 99-128.
248. Geuze, H.J., et al., *Intracellular site of asialoglycoprotein receptor-ligand uncoupling: double-label immunoelectron microscopy during receptor-mediated endocytosis*. Cell, 1983. **32**(1): p. 277-87.
249. Tycko, B., C.H. Keith, and F.R. Maxfield, *Rapid acidification of endocytic vesicles containing asialoglycoprotein in cells of a human hepatoma line*. J Cell Biol, 1983. **97**(6): p. 1762-76.
250. Stockert, R.J., et al., *Functional segregation of hepatic receptors for asialoglycoproteins during endocytosis*. J Biol Chem, 1980. **255**(19): p. 9028-9.
251. Wu, C.H. and G.Y. Wu, *Receptor-mediated delivery of foreign genes to hepatocytes*. Adv Drug Deliv Rev, 1998. **29**(3): p. 243-248.
252. Li, Y., et al., *Targeted delivery of macromolecular drugs: asialoglycoprotein receptor (ASGPR) expression by selected hepatoma cell lines used in antiviral drug development*. Curr Drug Deliv, 2008. **5**(4): p. 299-302.

253. Wu, G.Y. and C.H. Wu, *Receptor-mediated gene delivery and expression in vivo*. J Biol Chem, 1988. **263**(29): p. 14621-4.
254. Tokatlian, T. and T. Segura, *siRNA applications in nanomedicine*. Wiley Interdiscip Rev Nanomed Nanobiotechnol, 2010. **2**(3): p. 305-15.
255. Kay, M.A., J.C. Glorioso, and L. Naldini, *Viral vectors for gene therapy: the art of turning infectious agents into vehicles of therapeutics*. Nat Med, 2001. **7**(1): p. 33-40.
256. Leopold, P.L., et al., *Fluorescent virions: dynamic tracking of the pathway of adenoviral gene transfer vectors in living cells*. Hum Gene Ther, 1998. **9**(3): p. 367-78.
257. Fominaya, J. and W. Wels, *Target cell-specific DNA transfer mediated by a chimeric multidomain protein. Novel non-viral gene delivery system*. J Biol Chem, 1996. **271**(18): p. 10560-8.
258. Huang, H.W., F.Y. Chen, and M.T. Lee, *Molecular mechanism of Peptide-induced pores in membranes*. Phys Rev Lett, 2004. **92**(19): p. 198304.
259. Jenssen, H., P. Hamill, and R.E. Hancock, *Peptide antimicrobial agents*. Clin Microbiol Rev, 2006. **19**(3): p. 491-511.
260. Moreira, C., et al., *Improving chitosan-mediated gene transfer by the introduction of intracellular buffering moieties into the chitosan backbone*. Acta Biomater, 2009. **5**(8): p. 2995-3006.
261. Wiley, D.C. and J.J. Skehel, *The structure and function of the hemagglutinin membrane glycoprotein of influenza virus*. Annu Rev Biochem, 1987. **56**: p. 365-94.
262. Nishiyama, N., et al., *Photochemical enhancement of transgene expression by polymeric micelles incorporating plasmid DNA and dendrimer-based photosensitizer*. J Drug Target, 2006. **14**(6): p. 413-24.
263. Cabral, H., et al., *A photo-activated targeting chemotherapy using glutathione sensitive camptothecin-loaded polymeric micelles*. Pharm Res, 2009. **26**(1): p. 82-92.
264. Subramanian, A., et al., *Adenovirus or HA-2 fusogenic peptide-assisted lipofection increases cytoplasmic levels of plasmid in nondividing endothelium*

- with little enhancement of transgene expression. J Gene Med, 2002. 4(1): p. 75-83.*
265. Oliveira, S., et al., *Fusogenic peptides enhance endosomal escape improving siRNA-induced silencing of oncogenes. Int J Pharm, 2007. 331(2): p. 211-4.*
 266. Prchla, E., et al., *Virus-mediated release of endosomal content in vitro: different behavior of adenovirus and rhinovirus serotype 2. J Cell Biol, 1995. 131(1): p. 111-23.*
 267. Kwon, E.J., J.M. Bergen, and S.H. Pun, *Application of an HIV gp41-derived peptide for enhanced intracellular trafficking of synthetic gene and siRNA delivery vehicles. Bioconjug Chem, 2008. 19(4): p. 920-7.*
 268. Rudolph, C., et al., *Oligomers of the arginine-rich motif of the HIV-1 TAT protein are capable of transferring plasmid DNA into cells. J Biol Chem, 2003. 278(13): p. 11411-8.*
 269. Kamper, N., et al., *A membrane-destabilizing peptide in capsid protein L2 is required for egress of papillomavirus genomes from endosomes. J Virol, 2006. 80(2): p. 759-68.*
 270. Kimura, T. and A. Ohya, *Association between the pH-dependent conformational change of West Nile flavivirus E protein and virus-mediated membrane fusion. J Gen Virol, 1988. 69 (Pt 6): p. 1247-54.*
 271. Glomski, I.J., et al., *The Listeria monocytogenes hemolysin has an acidic pH optimum to compartmentalize activity and prevent damage to infected host cells. J Cell Biol, 2002. 156(6): p. 1029-38.*
 272. Browne, K.A., et al., *Cytosolic delivery of granzyme B by bacterial toxins: evidence that endosomal disruption, in addition to transmembrane pore formation, is an important function of perforin. Mol Cell Biol, 1999. 19(12): p. 8604-15.*
 273. Kakimoto, S., et al., *The conjugation of diphtheria toxin T domain to poly(ethylenimine) based vectors for enhanced endosomal escape during gene transfection. Biomaterials, 2009. 30(3): p. 402-8.*

274. Jia, L.T., et al., *Specific tumoricidal activity of a secreted proapoptotic protein consisting of HER2 antibody and constitutively active caspase-3*. Cancer Res, 2003. **63**(12): p. 3257-62.
275. Day, P.J., et al., *Binding of ricin A-chain to negatively charged phospholipid vesicles leads to protein structural changes and destabilizes the lipid bilayer*. Biochemistry, 2002. **41**(8): p. 2836-43.
276. Vago, R., et al., *Saporin and ricin A chain follow different intracellular routes to enter the cytosol of intoxicated cells*. FEBS J, 2005. **272**(19): p. 4983-95.
277. Foerg, C., et al., *Decoding the entry of two novel cell-penetrating peptides in HeLa cells: lipid raft-mediated endocytosis and endosomal escape*. Biochemistry, 2005. **44**(1): p. 72-81.
278. Cho, J.Y., et al., *Defective lysosomal targeting of activated fibroblast growth factor receptor 3 in achondroplasia*. Proc Natl Acad Sci U S A, 2004. **101**(2): p. 609-14.
279. Legendre, J.Y. and F.C. Szoka, Jr., *Cyclic amphipathic peptide-DNA complexes mediate high-efficiency transfection of adherent mammalian cells*. Proc Natl Acad Sci U S A, 1993. **90**(3): p. 893-7.
280. Abes, R., et al., *Arginine-rich cell penetrating peptides: design, structure-activity, and applications to alter pre-mRNA splicing by steric-block oligonucleotides*. J Pept Sci, 2008. **14**(4): p. 455-60.
281. Tu, Y. and J.S. Kim, *A fusogenic segment of glycoprotein H from herpes simplex virus enhances transfection efficiency of cationic liposomes*. J Gene Med, 2008. **10**(6): p. 646-54.
282. Min, S.H., et al., *A composite gene delivery system consisting of polyethylenimine and an amphipathic peptide KALA*. J Gene Med, 2006. **8**(12): p. 1425-34.
283. Parente, R.A., S. Nir, and F.C. Szoka, Jr., *Mechanism of leakage of phospholipid vesicle contents induced by the peptide GALA*. Biochemistry, 1990. **29**(37): p. 8720-8.

284. Derossi, D., et al., *Cell internalization of the third helix of the Antennapedia homeodomain is receptor-independent*. J Biol Chem, 1996. **271**(30): p. 18188-93.
285. Abes, S., et al., *Efficient splicing correction by PNA conjugation to an R6-Penetratin delivery peptide*. Nucleic Acids Res, 2007. **35**(13): p. 4495-502.
286. Lundberg, P., et al., *Delivery of short interfering RNA using endosomolytic cell-penetrating peptides*. FASEB J, 2007. **21**(11): p. 2664-71.
287. Lundberg, P., et al., *Cell membrane translocation of the N-terminal (1-28) part of the prion protein*. Biochem Biophys Res Commun, 2002. **299**(1): p. 85-90.
288. Hatefi, A., Z. Megeed, and H. Ghandehari, *Recombinant polymer-protein fusion: a promising approach towards efficient and targeted gene delivery*. J Gene Med, 2006. **8**(4): p. 468-76.
289. del Pozo-Rodriguez, A., et al., *A proline-rich peptide improves cell transfection of solid lipid nanoparticle-based non-viral vectors*. J Control Release, 2009. **133**(1): p. 52-9.
290. Boussif, O., et al., *A versatile vector for gene and oligonucleotide transfer into cells in culture and in vivo: polyethylenimine*. Proc Natl Acad Sci U S A, 1995. **92**(16): p. 7297-301.
291. Ghosn, B., S.P. Kasturi, and K. Roy, *Enhancing polysaccharide-mediated delivery of nucleic acids through functionalization with secondary and tertiary amines*. Curr Top Med Chem, 2008. **8**(4): p. 331-40.
292. Mellman, I., R. Fuchs, and A. Helenius, *Acidification of the endocytic and exocytic pathways*. Annu Rev Biochem, 1986. **55**: p. 663-700.
293. Walton, C.M., C.H. Wu, and G.Y. Wu, *A DNA delivery system containing listeriolysin O results in enhanced hepatocyte-directed gene expression*. World J Gastroenterol, 1999. **5**(6): p. 465-469.
294. Heffelfinger, S.C., et al., *SK HEP-1: a human cell line of endothelial origin*. In Vitro Cell Dev Biol, 1992. **28A**(2): p. 136-42.
295. Diamond, L., et al., *The WIRL-3 rat liver cell lines and their transformed derivatives*. Cancer Res, 1973. **33**(11): p. 2627-36.

296. Hao, Z., et al., *Potent DNA chain termination activity and selective inhibition of human immunodeficiency virus reverse transcriptase by 2',3'-dideoxyuridine-5'-triphosphate*. Mol Pharmacol, 1990. **37**(2): p. 157-63.
297. Starnes, M.C. and Y.C. Cheng, *Cellular metabolism of 2',3'-dideoxycytidine, a compound active against human immunodeficiency virus in vitro*. J Biol Chem, 1987. **262**(3): p. 988-91.
298. Chen, C.H. and Y.C. Cheng, *Delayed cytotoxicity and selective loss of mitochondrial DNA in cells treated with the anti-human immunodeficiency virus compound 2',3'-dideoxycytidine*. J Biol Chem, 1989. **264**(20): p. 11934-7.
299. Hashiguchi, K. and Q.M. Zhang-Akiyama, *Establishment of human cell lines lacking mitochondrial DNA*. Methods Mol Biol, 2009. **554**: p. 383-91.
300. Lopez-Alonso, J.P., et al., *Carbodiimide EDC induces cross-links that stabilize RNase A C-dimer against dissociation: EDC adducts can affect protein net charge, conformation, and activity*. Bioconjug Chem, 2009. **20**(8): p. 1459-73.
301. Colombo, S., et al., *Orosomucoid (alpha1-acid glycoprotein) plasma concentration and genetic variants: effects on human immunodeficiency virus protease inhibitor clearance and cellular accumulation*. Clin Pharmacol Ther, 2006. **80**(4): p. 307-18.
302. Schwarze, E., H. Tolleshaug, and O. Seglen, *Uptake and degradation of asialo-orosomucoid in hepatocytes from carcinogen-treated rats*. Carcinogenesis, 1985. **6**(5): p. 777-82.
303. Singh, M. and M. Ariatti, *Targeted gene delivery into HepG2 cells using complexes containing DNA, cationized asialoorosomucoid and activated cationic liposomes*. J Control Release, 2003. **92**(3): p. 383-94.
304. Siess, E.A., *Influence of isolation media on the preservation of mitochondrial functions*. Hoppe Seylers Z Physiol Chem, 1983. **364**(3): p. 279-89.
305. Siess, E.A., *Different actions of mono- and disaccharides on rat liver mitochondria*. Hoppe Seylers Z Physiol Chem, 1983. **364**(7): p. 835-8.
306. Witter, R.F. and W. Mink, *Effect of synthetic detergents on the swelling and the ATPase of mitochondria isolated from rat liver*. J Biophys Biochem Cytol, 1958. **4**(1): p. 73-82.

307. Petersons, M. and J.B. Allred, *Buffer-induced rat liver mitochondrial aggregation during differential centrifugation*. *Physiol Chem Phys*, 1981. **13**(5): p. 473-80.
308. Gregg, C., P. Kyryakov, and V.I. Titorenko, *Purification of mitochondria from yeast cells*. *J Vis Exp*, 2009(30).
309. Frezza, C., S. Cipolat, and L. Scorrano, *Organelle isolation: functional mitochondria from mouse liver, muscle and cultured fibroblasts*. *Nat Protoc*, 2007. **2**(2): p. 287-95.
310. Whitehead, P.H. and H.G. Sammons, *A simple technique for the isolation of orosomucoid from normal and pathological sera*. *Biochim Biophys Acta*, 1966. **124**(1): p. 209-11.
311. Stockert, R.J. and F.F. Becker, *Diminished hepatic binding protein for desialylated glycoproteins during chemical hepatocarcinogenesis*. *Cancer Res*, 1980. **40**(10): p. 3632-4.
312. Hui, E., et al., *Synaptotagmin-mediated bending of the target membrane is a critical step in Ca(2+)-regulated fusion*. *Cell*, 2009. **138**(4): p. 709-21.
313. Untergasser, A., et al., *Primer3--new capabilities and interfaces*. *Nucleic Acids Res*, 2012. **40**(15): p. e115.
314. Ye, J., et al., *Primer-BLAST: a tool to design target-specific primers for polymerase chain reaction*. *BMC Bioinformatics*, 2012. **13**: p. 134.
315. Schefe, J.H., et al., *Quantitative real-time RT-PCR data analysis: current concepts and the novel "gene expression's CT difference" formula*. *J Mol Med (Berl)*, 2006. **84**(11): p. 901-10.
316. Li, S.S., et al., *Mapping of human lactate dehydrogenase-A, -B, and -C genes and their related sequences: the gene for LDHC is located with that for LDHA on chromosome 11*. *Cytogenet Cell Genet*, 1988. **48**(1): p. 16-8.
317. Tweten, R.K., *Cholesterol-dependent cytolysins, a family of versatile pore-forming toxins*. *Infect Immun*, 2005. **73**(10): p. 6199-209.
318. Saito, G., G.L. Amidon, and K.D. Lee, *Enhanced cytosolic delivery of plasmid DNA by a sulfhydryl-activatable listeriolysin O/protamine conjugate utilizing cellular reducing potential*. *Gene Ther*, 2003. **10**(1): p. 72-83.

319. Varkouhi, A.K., et al., *Endosomal escape pathways for delivery of biologicals*. J Control Release, 2011. **151**(3): p. 220-8.
320. Decatur, A.L. and D.A. Portnoy, *A PEST-like sequence in listeriolysin O essential for Listeria monocytogenes pathogenicity*. Science, 2000. **290**(5493): p. 992-5.
321. Lorenzi, G.L. and K.D. Lee, *Enhanced plasmid DNA delivery using anionic LPDII by listeriolysin O incorporation*. J Gene Med, 2005. **7**(8): p. 1077-85.
322. Kullberg, M., J.L. Owens, and K. Mann, *Listeriolysin O enhances cytoplasmic delivery by Her-2 targeting liposomes*. J Drug Target, 2010. **18**(4): p. 313-20.
323. Kim, S.C., et al., *Clinical and health care use characteristics of patients newly starting allopurinol, febuxostat, and colchicine for the treatment of gout*. Arthritis Care Res (Hoboken), 2013. **65**(12): p. 2008-14.
324. Dainese, L., A. Cappai, and P. Biglioli, *Recurrent pericardial effusion after cardiac surgery: the use of colchicine after recalcitrant conventional therapy*. J Cardiothorac Surg, 2011. **6**: p. 96.
325. Skoufias, D.A. and L. Wilson, *Mechanism of inhibition of microtubule polymerization by colchicine: inhibitory potencies of unliganded colchicine and tubulin-colchicine complexes*. Biochemistry, 1992. **31**(3): p. 738-46.
326. Piasek, A. and J. Thyberg, *Effects of colchicine on endocytosis and cellular inactivation of horseradish peroxidase in cultured chondrocytes*. J Cell Biol, 1979. **81**(2): p. 426-37.
327. Dupont, F.M., *Effect of temperature on the plasma membrane and tonoplast ATPases of barley roots : comparison of results obtained with acridine orange and quinacrine*. Plant Physiol, 1989. **89**(4): p. 1401-12.
328. Walton, C.M., C.H. Wu, and G.Y. Wu, *A method for purification of listeriolysin O from a hypersecretor strain of Listeria monocytogenes*. Protein Expr Purif, 1999. **15**(2): p. 243-5.
329. Cossart, P., et al., *Listeriolysin O is essential for virulence of Listeria monocytogenes: direct evidence obtained by gene complementation*. Infect Immun, 1989. **57**(11): p. 3629-36.
330. Jacobs, T., et al., *Listeriolysin O: cholesterol inhibits cytolysis but not binding to cellular membranes*. Mol Microbiol, 1998. **28**(6): p. 1081-9.

331. Costabile, M., *Measuring the 50% haemolytic complement (CH50) activity of serum*. J Vis Exp, 2010(37).
332. Boveris, A., et al., *Regulation of mitochondrial respiration by adenosine diphosphate, oxygen, and nitric oxide*. Methods Enzymol, 1999. **301**: p. 188-98.
333. Walther, D.M. and D. Rapaport, *Biogenesis of mitochondrial outer membrane proteins*. Biochim Biophys Acta, 2009. **1793**(1): p. 42-51.
334. Mannella, C.A., *Structure and dynamics of the mitochondrial inner membrane cristae*. Biochim Biophys Acta, 2006. **1763**(5-6): p. 542-8.
335. Green, D.E., D.M. Ziegler, and K.A. Doeg, *Sequence of components in the succinic chain of the mitochondrial electron transport system*. Arch Biochem Biophys, 1959. **85**: p. 280-2.
336. Linnane, A.W. and C.W. Wrigley, *Fragmentation of the Electron Transport Chain of Escherichia Coli. Preparation of a Soluble Formate Dehydrogenase-Cytochrome B1 Complex*. Biochim Biophys Acta, 1963. **77**: p. 408-18.
337. Storey, B.T. and J.T. Bahr, *The respiratory chain of plant mitochondria. I. Electron transport between succinate and oxygen in skunk cabbage mitochondria*. Plant Physiol, 1969. **44**(1): p. 115-25.
338. Jato-Rodriguez, J.J., A.J. Hudson, and K.P. Strickland, *Activities of enzymes of the citric acid cycle and electron transport chain in the skeletal muscle of normal and dystrophic mice (strain 129)*. Enzyme, 1972. **13**(5-6): p. 286-92.
339. Golubev, A.M., *[On the mechanism of electron transport in the oxidation-reduction chain in experimental myocardial infarct]*. Arkh Patol, 1968. **30**(3): p. 39-43.
340. Storey, B.T., *The Respiratory Chain of Plant Mitochondria: XII. Some Aspects of the Energy-linked Reverse Electron Transport from the Cytochromes c to the Cytochromes b in Mung Bean Mitochondria*. Plant Physiol, 1972. **49**(3): p. 314-22.
341. Onishi, T., *Mechanism of electron transport and energy conservation in the site I region of the respiratory chain*. Biochim Biophys Acta, 1973. **301**(2): p. 105-28.

342. Storey, B.T., *The Respiratory Chain of Plant Mitochondria: XI. Electron Transport from Succinate to Endogenous Pyridine Nucleotide in Mung Bean Mitochondria*. Plant Physiol, 1971. **48**(6): p. 694-701.
343. Segal, A.W., *The electron transport chain of the microbicidal oxidase of phagocytic cells and its involvement in the molecular pathology of chronic granulomatous disease*. Biochem Soc Trans, 1989. **17**(3): p. 427-34.
344. Hatefi, Y., *Introduction--preparation and properties of the enzymes and enzymes complexes of the mitochondrial oxidative phosphorylation system*. Methods Enzymol, 1978. **53**: p. 3-4.
345. Wang, D., et al., *Oxygen flux analysis to understand the biological function of sirtuins*. Methods Mol Biol, 2013. **1077**: p. 241-58.
346. Rose, S., et al., *Oxidative stress induces mitochondrial dysfunction in a subset of autism lymphoblastoid cell lines in a well-matched case control cohort*. PLoS One, 2014. **9**(1): p. e85436.
347. Brittain, T. and C. Greenwood, *Kinetic studies on the binding of cyanide to oxygenated cytochrome c oxidase*. Biochem J, 1976. **155**(2): p. 453-5.
348. Greenamyre, J.T., D.S. Higgins, and R.V. Eller, *Quantitative autoradiography of dihydrorotenone binding to complex I of the electron transport chain*. J Neurochem, 1992. **59**(2): p. 746-9.
349. Shchepina, L.A., et al., *Oligomycin, inhibitor of the F₀ part of H⁺-ATP-synthase, suppresses the TNF-induced apoptosis*. Oncogene, 2002. **21**(53): p. 8149-57.
350. Tretter, L., C. Chinopoulos, and V. Adam-Vizi, *Plasma membrane depolarization and disturbed Na⁺ homeostasis induced by the protonophore carbonyl cyanide-*p*-trifluoromethoxyphenyl-hydrazon in isolated nerve terminals*. Mol Pharmacol, 1998. **53**(4): p. 734-41.
351. Potter, V.R. and A.E. Reif, *Inhibition of an electron transport component by antimycin A*. J Biol Chem, 1952. **194**(1): p. 287-97.
352. Koopman, W.J., et al., *Inhibition of complex I of the electron transport chain causes O₂⁻-mediated mitochondrial outgrowth*. Am J Physiol Cell Physiol, 2005. **288**(6): p. C1440-50.

353. Kim, J.S., et al., *Cellular uptake of magnetic nanoparticle is mediated through energy-dependent endocytosis in A549 cells*. J Vet Sci, 2006. **7**(4): p. 321-6.
354. WILLIAM MARTIN and KLAUS V. KOWALLIK (1999). Annotated English translation of Mereschkowsky's 1905 paper 'Über Natur und Ursprung der Chromatophoren im Pflanzenreiche'. European Journal of Phycology.
355. Sagan, L., *On the origin of mitosing cells*. 1967. J NIH Res, 1993. **5**(3): p. 65-72.
356. Lang, B.F., M.W. Gray, and G. Burger, *Mitochondrial genome evolution and the origin of eukaryotes*. Annu Rev Genet, 1999. **33**: p. 351-97.
357. Tarze, A., et al., *GAPDH, a novel regulator of the pro-apoptotic mitochondrial membrane permeabilization*. Oncogene, 2007. **26**(18): p. 2606-20.
358. PETER M . BRUINENBERG, J.P.V.D., J . GIJS KUENEN AND W. ALEXANDER SCHEFFERS, *Critical Parameters in the Isolation of Mitochondria from Candida utilis Grown in Continuous Culture*. Journal of General Microbiology, 1985. **131**, **1035-1 042**.
359. Figueiredo, P.A., et al., *Age-induced morphological, biochemical, and functional alterations in isolated mitochondria from murine skeletal muscle*. J Gerontol A Biol Sci Med Sci, 2008. **63**(4): p. 350-9.
360. Di Lisa, F., et al., *Mitochondrial membrane potential in single living adult rat cardiac myocytes exposed to anoxia or metabolic inhibition*. J Physiol, 1995. **486** (Pt 1): p. 1-13.
361. Karmali, P.P. and D. Simberg, *Interactions of nanoparticles with plasma proteins: implication on clearance and toxicity of drug delivery systems*. Expert Opin Drug Deliv, 2011. **8**(3): p. 343-57.
362. Chudasama, S.L., et al., *Heparin modifies the immunogenicity of positively charged proteins*. Blood, 2010. **116**(26): p. 6046-53.
363. Dobrovolskaia, M.A., et al., *Interaction of colloidal gold nanoparticles with human blood: effects on particle size and analysis of plasma protein binding profiles*. Nanomedicine, 2009. **5**(2): p. 106-17.
364. Buzea, C., Pacheco, II, and K. Robbie, *Nanomaterials and nanoparticles: sources and toxicity*. Biointerphases, 2007. **2**(4): p. MR17-71.

365. Walkey, C.D., et al., *Nanoparticle size and surface chemistry determine serum protein adsorption and macrophage uptake*. J Am Chem Soc, 2012. **134**(4): p. 2139-47.
366. Chambers, E. and S. Mitragotri, *Prolonged circulation of large polymeric nanoparticles by non-covalent adsorption on erythrocytes*. J Control Release, 2004. **100**(1): p. 111-9.
367. Chonn, A., S.C. Semple, and P.R. Cullis, *Association of blood proteins with large unilamellar liposomes in vivo. Relation to circulation lifetimes*. J Biol Chem, 1992. **267**(26): p. 18759-65.
368. Chen, J., et al., *Quantification of extrapulmonary translocation of intratracheal-instilled particles in vivo in rats: effect of lipopolysaccharide*. Toxicology, 2006. **222**(3): p. 195-201.
369. Renwick, L.C., K. Donaldson, and A. Clouter, *Impairment of alveolar macrophage phagocytosis by ultrafine particles*. Toxicol Appl Pharmacol, 2001. **172**(2): p. 119-27.
370. Lundborg, M., et al., *Human alveolar macrophage phagocytic function is impaired by aggregates of ultrafine carbon particles*. Environ Res, 2001. **86**(3): p. 244-53.
371. Fellner, S.K. and L. Parker, *Endothelin-1, superoxide and adeninediphosphate ribose cyclase in shark vascular smooth muscle*. J Exp Biol, 2005. **208**(Pt 6): p. 1045-52.
372. Galie, N., et al., *Ambrisentan for the treatment of pulmonary arterial hypertension: results of the ambrisentan in pulmonary arterial hypertension, randomized, double-blind, placebo-controlled, multicenter, efficacy (ARIES) study 1 and 2*. Circulation, 2008. **117**(23): p. 3010-9.
373. Seo, B. and T.F. Luscher, *ETA and ETB receptors mediate contraction to endothelin-1 in renal artery of aging SHR. Effects of FR139317 and bosentan*. Hypertension, 1995. **25**(4 Pt 1): p. 501-6.
374. Stahler, G. and P. von Hunnius, *Successful treatment of portopulmonary hypertension with bosentan: case report*. Eur J Clin Invest, 2006. **36 Suppl 3**: p. 62-6.

375. Liang, T.J., et al., *Targeted transfection and expression of hepatitis B viral DNA in human hepatoma cells*. J Clin Invest, 1993. **91**(3): p. 1241-6.
376. Haqshenas, G., et al., *A 2a/1b full-length p7 inter-genotypic chimeric genome of hepatitis C virus is infectious in vitro*. Virology, 2007. **360**(1): p. 17-26.